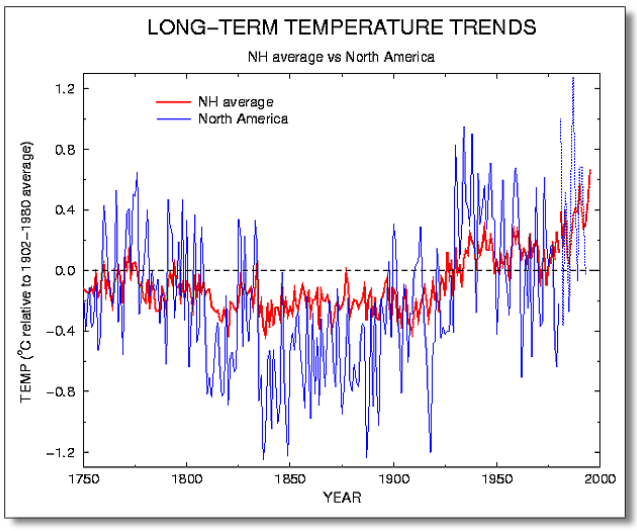

# NOAA Scientific Publications Report

MARCH 28, 2013

## HIGHLIGHTED ARTICLE

Continental-scale temperature variability during the last two millennia

The "coast" is complicated: a model to consistently describe the Nation's coastal population

Habitat availability and heterogeneity and the Indo-Pacific warm pool as predictors of marine species richness in the tropical Indo-Pacific

Passive acoustic tracking of singing humpback whales *(Megaptera novaeangliae)* on a North Atlantic feeding ground

## ADDITIONAL ARTICLES

Model support for forcing of the 8.2 ka event by meltwater from the Hudson Bay ice dome

Use of high-resolution DIDSON sonar to quantify attributes of predation at ecologically relevant space and time scales

Integrating multiple techniques to identify stock boundaries of common bottlenose dolphins *(Tursiops truncatus)*

HadISDH: an updateable land surface specific humidity product for climate monitoring

Probable Maximum Precipitation (PMP) and Climate Change

Insecticide toxicity in Fish

Response to $CO_2$ doubling of the Atlantic hurricane main development region in a high-resolution climate model

The Greenwich photo-heliographic results (1874-1976): initial corrections to the printed publications

Ocean warming effect on surface gravity wave climate change for the end of the 21st century

Biological reference points for nutritional status of Chesapeake Bay Striped Bass

Corrigendum for Nature 494: inertia is speeding fish-stock declines, K. Swing, Correspondence – Corrected numbers for fish on Red List

Global speleothem oxygen isotope measurements since the Last Glacial Maximum

## OTHER REPORTS, BOOK CHAPTERS, & INTERNAL PUBLICATIONS

Assessment of contaminant body burdens and histopathology of fish and shellfish species frequently used for subsistence food by Alaskan Native communities

An assessment of wastewater contaminants detected in the St. Thomas East End Reserves (STEER)

Visual identification of fins from common elasmobranchs in the Northwest Atlantic Ocean

An Atlantic sturgeon population index for ESA management analysis

Tide gauge data rescue

# HIGHLIGHTED ARTICLE

## AUTHORS

78 authors from PAGES 2k Consortium; **E. R. Wahl (NESDIS/NCDC), H. Diaz (NESDIS/NCDC/CIRES)**

## PUBLICATION DATE

Expected: April 2013

## TITLE

*Continental-scale temperature variability during the last two millennia*

## JOURNAL

Nature Geoscience

## SIGNIFICANCE

- This study adds to the considerable scientific evidence that global warming in the 20th century represents a clear change from prior long-term temperature trends.
- Past global climate changes had a strong regional expression. All continental regions experienced a long-term cooling trend followed by recent warming during the 20th century.
- The average reconstructed temperature in 1971-2000 CE, the last 30 year period examined in this study, was likely higher than any time in nearly 1400 years.

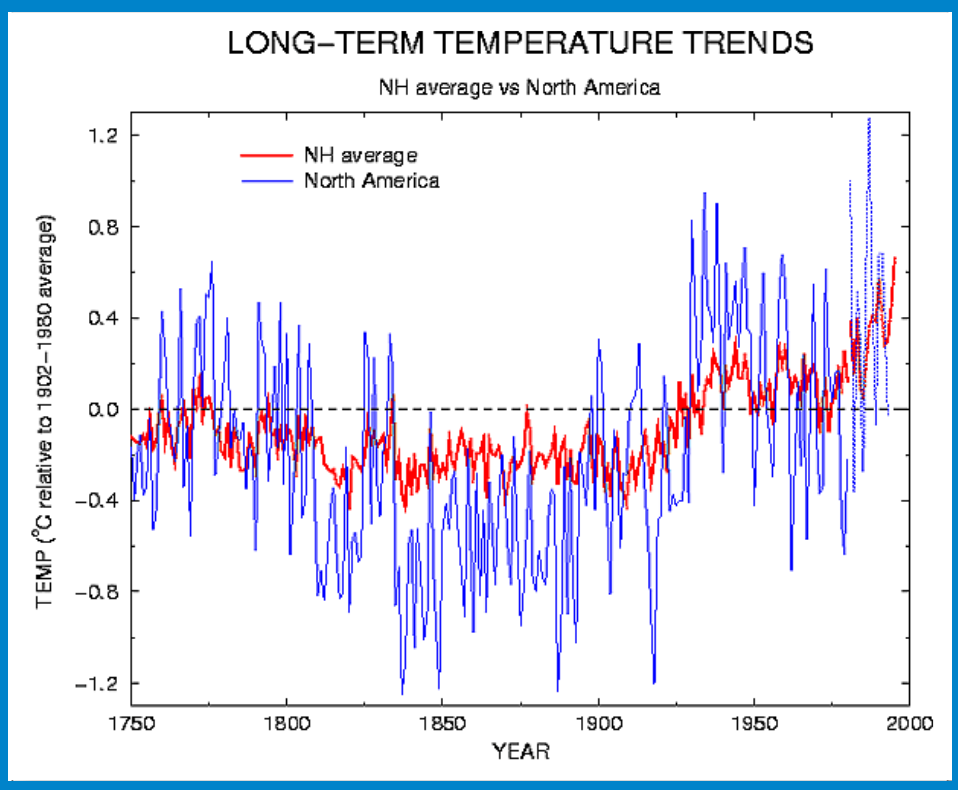


## SUMMARY

The authors reconstructed past temperatures for seven continental-scale regions during the last one to two millennia. The most coherent feature in nearly all of the regional temperature reconstructions is a long-term cooling trend, which ended late in the 19th century. At multi-decadal to centennial scales, temperature variability shows distinctly different regional patterns, with more similarity within each hemisphere than between them. There were no globally synchronous multi-decadal warm or cold intervals that define a worldwide Medieval Warm Period or Little Ice Age, but all reconstructions show generally cold conditions between 1580 and 1880 CE, punctuated in some regions by warm decades during the 18th century. The transition to these colder conditions occurred earlier in the Arctic, Europe and Asia than in North America or the Southern Hemisphere regions. Recent warming reversed the long-term cooling; during the last 30-year period (1971-2000 CE), the area-weighted average reconstructed temperature was likely higher than any time in nearly 1400 years. This study will act as a benchmark for comparisons with climate-model simulations aimed at understanding the cause(s) of last-millennium global cooling, and the extent to which externally forced and unforced variability can explain temperature fluctuations and trends at the continental scale.

VISIT THE SCIENTIFIC PUBLICATIONS REPORT ARCHIVE

# HIGHLIGHTED ARTICLE

## AUTHORS

**B. Ache, K. Crossett, P. Pacheco, J. Adkins,** and **P. Wiley (NOS/Management and Budget-Special Projects Office)**

## PUBLICATION DATE

Expected: Fall 2013 or early 2014

## TITLE

*The "coast" is complicated: a model to consistently describe the Nation's coastal population*

## JOURNAL

Estuaries and Coasts

## SIGNIFICANCE

- Researchers and coastal management/planning officials require consistent and accurate reports of U.S. coastal population statistics.
- The authors' model retains counties as the geographic unit to delineate the coast, but distinguishes between different populations within those counties: 1) the population that most directly affects the coast and 2) the population most directly affected by the coast.
- If accepted by the larger coastal management community, this model will increase consistency in national and regional level reporting of population and other demographic statistics, and it also might be used to consistently report complementary economic production statistics.

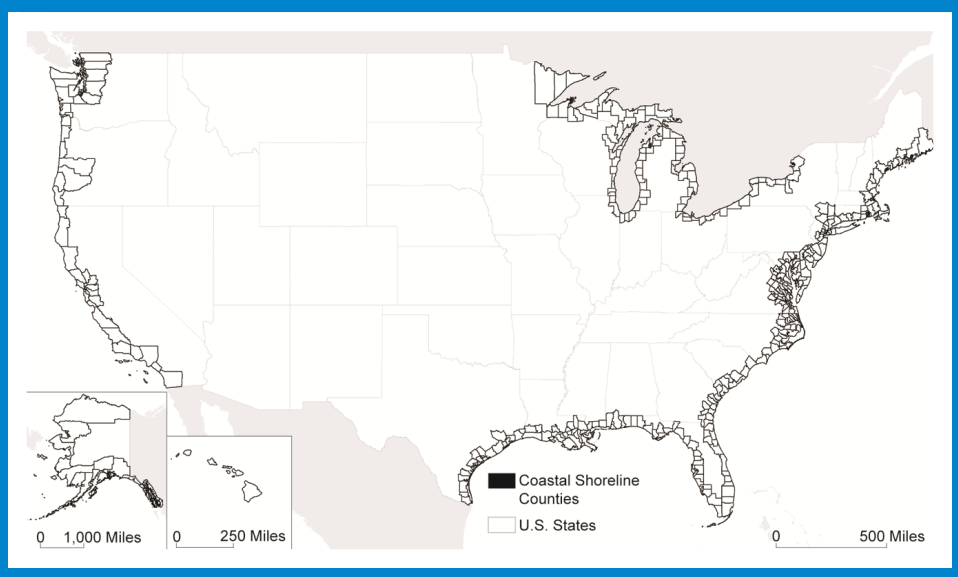


## SUMMARY

No single delineation of "the coast" provides all of the demographic statistics needed to address the full range of policy and management issues. Presently, a variety of U.S. coastal population statistics are being used, but these data are sometimes applied inappropriately, adding confusion to policy discussions and public understanding of coastal issues. For example, statistics on the population in coastal watersheds can be useful when discussing estuarine water quality, because people upstream can affect water quality downstream. These same population statistics, however, may be misleading if used when discussing coastal hazards such as tsunamis or hurricane storm surges. Additionally, even when there is general agreement about a particular framework for population reporting, (e.g., shoreline-adjacent counties), slightly different county suites have been used; at least three Federal agencies – the U.S. Census, the Federal Emergency Management Agency, and NOAA have used different lists of shoreline-adjacent counties for the purposes of reporting coastal population. Thus, an increasing number of researchers are calling for consistency in reporting U.S. coastal population statistics. The authors propose a simple model for generating and applying coastal population statistics at the national and regional level. This model builds on the long precedent of using counties as the geographic unit to delineate the coast for the purposes of reporting population. The proposed model includes two major components: 1) "The population that most directly affects the coast," represented by the U.S. population that resides in a standard suite of Coastal Watershed Counties where land use and water quality changes most directly impact coastal ecosystems; and 2) "The population most directly affected by the coast," represented by the U.S. population that resides in a standard suite of Coastal Shoreline Counties that are directly adjacent to the open ocean, major estuaries, and the Great Lakes, which due to their proximity to these waters, bear a great proportion of the full range of effects from coastal hazards and host the majority of economic production associated with coastal and ocean resources.

VISIT THE SCIENTIFIC PUBLICATIONS REPORT ARCHIVE

# HIGHLIGHTED ARTICLE

## AUTHORS

J. C. Sanciangco, K. E. Carpenter, P. **J. Etnoyer (NOS/NCCOS),** and F. Moretzsohn

## PUBLICATION DATE

February 15, 2013

## TITLE

*Habitat availability and heterogeneity and the Indo-Pacific warm pool as predictors of marine species richness in the tropical Indo-Pacific*

## JOURNAL

PLoS One

## SIGNIFICANCE

- Habitat availability, habitat heterogeneity, and surface temperature are the best predictors of marine species richness for shallow tropical water environments at a global scale.
- The authors' conclusions suggest that marine protected areas for tropical shallow water environments should be large and heterogeneous, and guarded against climate change.

Indo-Pacific Reef

## SUMMARY

Range overlap patterns were observed in a dataset of 10,446 expert-derived marine species distribution maps, including 8,295 coastal fishes, 1,212 invertebrates (crustaceans and molluscs), 820 reef-building corals, 50 seagrasses and 69 mangroves. Distributions of tropical Indo-Pacific shore fishes revealed a concentration of species richness in the northern apex and central region of the Coral Triangle epicenter of marine biodiversity. This pattern was supported by distributions of invertebrates and habitat-forming primary producers. Habitat availability, heterogeneity and sea surface temperatures were highly correlated with species richness across spatial grains ranging from 23,000 to 5,100,000 km2 with and without correction for autocorrelation. The consistent retention of habitat variables in our predictive models supports the area of refuge hypothesis which posits reduced extinction rates in the Coral Triangle. This does not preclude support for a center of origin hypothesis that suggests increased speciation in the region may contribute to species richness. In addition, consistent retention of sea surface temperatures in models suggests that available kinetic energy may also be an important factor in shaping patterns of marine species richness. Kinetic energy may hasten rates of both extinction and speciation. The position of the Indo-Pacific Warm Pool on the east of the Coral Triangle in central Oceania and a pattern of increasing species richness from this region into the central and northern parts of the Coral Triangle suggests peripheral speciation with enhanced survival in the cooler parts of the Coral Triangle that also have highly concentrated available habitat. These results indicate that conservation of habitat availability and heterogeneity is important to reduce extinction and that changes in sea surface temperatures may influence the evolutionary potential of the region.

## RESOURCE LINK

*http://www.plosone.org/article/info%3Adoi%2F10.1371%2Fjournal.pone.0056245*

VISIT THE SCIENTIFIC PUBLICATIONS REPORT ARCHIVE

# HIGHLIGHTED ARTICLE

## AUTHORS

**J.E. Stanistreet, D. Risch,** and **S.M. Van Parijs (NMFS/NEFSC)**

## PUBLICATION DATE

Expected: TBD

## TITLE

*Passive acoustic tracking of singing humpback whales* (Megaptera novaeangliae) *on a North Atlantic feeding ground*

## JOURNAL

PLoS One

## SIGNIFICANCE

- The authors' results provide a first description of the movements of singers on a feeding ground, and demonstrate the utility of passive acoustic tracking for studying the fine-scale movements of whales within the behavioral context of their calls.
- These methods have further applications for conservation and management purposes, particularly by enhancing our ability to estimate whale densities using passive acoustic monitoring.

Humpback Whale Breach

## SUMMARY

Passive acoustic tracking provides an unobtrusive method of studying the movement of sound-producing animals in the marine environment where traditional tracking methods may be costly or infeasible. We used passive acoustic tracking to characterize the fine-scale movements of singing humpback whales (Megaptera novaeangliae) on a North Atlantic feeding ground. Male humpback whales produce complex songs in association with breeding behavior, a phenomenon that is well documented on tropical breeding grounds but also occurs at higher latitudes. Acoustic recordings were made throughout 2009 using an array of autonomous recording units deployed in the Stellwagen Bank National Marine Sanctuary. Song was recorded during spring and fall, and individual singing whales were localized and tracked throughout the array using a correlation sum estimation method on the time-synchronized recordings. Tracks were constructed for forty-three song sessions, and a high level of variation in movement patterns occurred in both the spring and fall seasons, ranging from slow meandering to faster directional movement. Tracks were 30 min to 8 h in duration, and singers traveled distances ranging from 0.9 to 20.1 km. Mean swimming speed was 2.06 ± 0.98 km/h. Patterns and rates of movement indicated that most singers were actively swimming. In one case, two singers were tracked simultaneously, revealing a potential reaction by one singer to the presence of the second.

VISIT THE SCIENTIFIC PUBLICATIONS REPORT ARCHIVE

# ADDITIONAL ARTICLE

## AUTHORS

**A. Wagner,** C. Morrill, B. L. Otto-Bliesner, N. Rosenbloom, and K. R. Watkins **(NESDIS/NCDC/CIRES)**

## PUBLICATION DATE

Expected: Spring 2013

## TITLE

*Model support for forcing of the 8.2 ka event by meltwater from the Hudson Bay ice dome*

## JOURNAL

Climate Dynamics

## SIGNIFICANCE

- The ocean circulation in the North Atlantic appears to be less sensitive to freshwater inputs from melting ice sheets than was previously thought.
- The 8.2 ka event is the most recent analogue to the expected future changes in Atlantic Ocean circulation. By documenting the climate response to this circulation change, we can both better predict future climate impacts and also test the skill of models that are being used to make climate projections.

## SUMMARY

Previous model experiments of the 8.2 ka event forced by the drainage of Lake Agassiz often do not produce climate anomalies as long as those inferred from proxies. In addition to the Agassiz forcing, there is new evidence for significant amounts of freshwater entering the ocean at 8.2 ka from the disintegration of the Laurentide ice sheet (LIS). We use the Community Climate System Model version 3 (CCSM3) to test the contribution of this additional meltwater flux. Similar to previous model experiments, we find that the estimated freshwater forcing from Lake Agassiz is capable of sustaining ocean and climate anomalies for only two to three decades, much shorter than the event duration of ~150 years in proxies. Using new estimates of the LIS freshwater flux (~0.13 Sv for 100 years) from the collapse of the Hudson Bay ice dome in addition to the Agassiz drainage, the CCSM3 generates climate anomalies with a magnitude and duration that match within error those from proxies. This result is insensitive to the duration of freshwater release, a major uncertainty, if the total volume remains the same. An analysis of the modeled North Atlantic freshwater budget indicates that the Agassiz drainage is rapidly transported out of the North Atlantic while the LIS contribution generates longer-lasting freshwater anomalies that are also subject to recirculation by the subtropical gyre back into the North Atlantic. Thus, the meltwater flux originating from the LIS appears to be more important than the Agassiz drainage in generating 8.2 ka climate anomalies and is one way to reconcile some model-data discrepancies.

# ADDITIONAL ARTICLE

## AUTHORS

V. E. Price, P. J. Auster, and **L. Kracker (NOS/NCCOS)**

## PUBLICATION DATE

February 2013

## TITLE

*Use of high-resolution DIDSON sonar to quantify attributes of predation at ecologically relevant space and time scales*

## JOURNAL

Marine Technology Society Journal

## SIGNIFICANCE

- High resolution images from Dual-Frequency Identification Sonar (DIDSON) can be used to observe predator-prey interactions at ecologically relevant space and time scales often missed by traditional methods.
- Developing effective and consistent data acquisition and analysis techniques from DIDSON will allow for incorporation of variation in predation rates and intensity across habitats into population models so that spatially explicit demographic processes can be incorporated.

## SUMMARY

Predator-prey interactions of large vagile fishes are difficult to study in the ocean due to limitations in the space and time requirements for observations. Small-scale direct underwater observations by divers (ca. <10 m radius) and large-scale hydroacoustic surveys (10 s m2 to 100 s km2) are traditional approaches for surveying fish. However, large piscivorous predators identify and attack prey at the scale of meters to tens of meters. Dual-Frequency Identification Sonar (or DIDSON) is a high-resolution acoustic camera operating in the MHz range that provides detailed continuous video- like imaging of objects up to a range of 30 m. This technology can be used to observe predator-prey interactions at ecologically relevant space and time scales often missed by traditional methods. Here we establish an approach for quantifying predation related behaviors from DIDSON records. Metrics related to predator and prey group size, prey responses to predation, predation rate, predator strategies, and the nonrandom use of landscape features by both predator and prey are described. In addition, relationships between patterns in these attributes are tested and issues regarding sampling strategies for future studies are discussed. We suggest that approaches combining direct visual observation and acoustic sampling at multiple scales are required to quantify variation in these relationships across underwater landscapes.

VISIT THE SCIENTIFIC PUBLICATIONS REPORT ARCHIVE

# ADDITIONAL ARTICLE

## AUTHORS

B. C. Balmer, R. S. Wells, **L. H. Schwacke,** J. H. Schwacke, B. Danielson, R. C. George, **S. M. Lane,** W. A. McLellan, D. A. Pabst, K. Sparks, **T. R. Speakman,** F. I. Townsend, and **E. S. Zolman (NOS/NCCOS)**

## PUBLICATION DATE

Expected: Unknown

## TITLE

*Integrating multiple techniques to identify stock boundaries of common bottlenose dolphins* (Tursiops truncatus)

## JOURNAL

Aquatic Conservation: Marine and Freshwater Ecosystems

## SIGNIFICANCE

- Satellite-linked telemetry works best for initial identification of overall dolphin ranges and for gaining insight into stock boundaries.
- Attaching both a satellite-linked and radio transmitter to individual dolphins would identify fine-scale ranging patterns and permit visual observations to assess animal and tag condition for the life of the tag.
- Photo-identification surveys could then be used to identify long-term ranging patterns and determine abundance estimates to assist with stock assessment.

## SUMMARY

Photo-identification surveys, vessel-based radio telemetry, automated radio telemetry systems (ARTS), and satellite-linked telemetry are sampling techniques that have been used to determine common bottlenose dolphin ranging patterns and provide detailed insight into stock boundaries. The results of near simultaneous use of these sampling techniques are compared using data from a case study of bottlenose dolphins within the estuaries of southern Georgia. Satellite-linked and radio telemetry were determined to be useful sampling techniques for identification of short-term ranging patterns. Satellite-linked telemetry had the second lowest cost per location ($122) and identified dolphin ranging patterns within and outside of the study area boundaries. Vessel-based radio telemetry was more costly ($195 per location) and had relatively limited tracking coverage. However, this sampling technique permitted visual observations of animal and tag condition. The combination of vessel- based radio telemetry and ARTS, which had the lowest cost per location ($34), was an effective method for determining ranging patterns of tagged individuals within and outside of the study area. Photo-identification surveys, relative to satellite-linked and radio telemetry, were not as efficient for determination of targeted individuals' short-term ranging patterns and had the highest cost per location of the 4 sampling techniques ($292). However, photo-identification is more effective than any other technique for compiling data on large numbers of individuals within a designated study area. Photo-identification surveys are essential for long-term monitoring and provide additional insight into dolphin stock structure that cannot be determined through telemetry alone.

VISIT THE SCIENTIFIC PUBLICATIONS REPORT ARCHIVE

# ADDITIONAL ARTICLE

## AUTHORS

K. M. Willett, **C. N. Williams Jr. (NESDIS/NCDC),** R. J. H. Dunn, **P. W. Thorne (Cooperative Institute for Climate and Satellites-North Carolina);** S. Bell, M. de Podesta, P. D. Jones, and D. E. Parker

## PUBLICATION DATE

Expected: March 2013

## TITLE

*HadISDH: an updateable land surface specific humidity product for climate monitoring*

## JOURNAL

Climate of the Past

## SIGNIFICANCE

- HadISDH is in good agreement with existing land surface humidity products in periods of overlap.
- Widespread moistening is shown over the 1973-2011 period.
- The largest moistening signals are over the tropics with drying over the subtropics, supporting other evidence of an intensified hydrological cycle over recent years.

## SUMMARY

Presented herein is HadISDH: an annually-updated near-global land-surface specific humidity product providing monthly means from 1973 onwards over large scale grids. HadISDH is an update to the land component of HadCRUH, utilizing the global high resolution land surface station product HadISD as a basis. HadISD, in turn, uses an updated version of NOAA's Integrated Surface Database. Intensive automated quality control has been undertaken at the synoptic level, as part of HadISD processing. The data have been subsequently run through the pairwise homogenization algorithm developed for NCDC's GHCN Monthly temperature product. Uncertainty estimates including station uncertainty and sampling uncertainty are provided at the gridbox spatial scale and monthly time scale. HadISDH is in good agreement with existing land surface humidity products in periods of overlap. Widespread moistening is shown over the 1973-2011 period. The largest moistening signals are over the tropics with drying over the subtropics, supporting other evidence of an intensified hydrological cycle over recent years. Moistening is detectable with high (95%) confidence over large-scale averages for the globe, Northern Hemisphere and tropics with trends of 0.095 (0.086 to 0.105) g kg-1 per decade, 0.091 (0.080 to 0.103) g kg-1 per decade and 0.147 (0.133 to 0.162) g kg-1 per decade respectively. No change (0.008 [-0.011 to 0.028] g kg-1 per decade) is detectable in the Southern Hemisphere. When globally averaged, 1998 was the moistest year since records began in 1973, closely followed by 2010, two strong El Niño years.

# ADDITIONAL ARTICLE

## AUTHORS

**K. E. Kunkel (CICS-NC), T. R. Karl (NESDIS/NCDC), D. R. Easterling (NESDIS/NCDC),** K. Redmond, J. Young, **X. Yin (NESDIS/NCDC),** and P. Hennon **(CICS-NC)**

## PUBLICATION DATE

Expected: April 2013

## TITLE

*Probable maximum precipitation (PMP) and climate change*

## JOURNAL

Geophysical Research Letters

## SIGNIFICANCE

- Climate change effects on Probable Maximum Precipitation (PMP) were analyzed using both climate model simulations and conceptual models of relevant meteorological systems.
- PMP values are likely to increase in the future in response to increasing levels of greenhouse gases and higher atmospheric moisture content.

## SUMMARY

PMP is defined as the greatest accumulation of precipitation for a given duration meteorologically possible for an area. Climate change effects on PMP are analyzed, in particular, maximization of moisture and persistent upward motion, using both climate model simulations and conceptual models of relevant meteorological systems. Climate model simulations indicate a substantial future increase in mean and maximum water vapor concentrations. For the RCP8.5 scenario, the changes in maximum values for the continental United States are approximately 20-30% by 2071-2100. The magnitudes of the maximum water vapor changes follow temperature changes with an approximate Clausius-Clapeyron relationship. Model-simulated changes in maximum vertical and horizontal winds are too small to offset water vapor changes. Thus, our conclusion is that the most scientifically sound projection is that PMP values will increase in the future due to higher levels of atmospheric moisture content and consequent higher levels of moisture transport into storms.

# ADDITIONAL ARTICLE

## AUTHORS

**M.H. Fulton, P.B. Key,** and **M.E. DeLorenzo (NOS/NCCOS)**

## PUBLICATION DATE

Expected: TBD

## TITLE

*Insecticide toxicity in fish*

## JOURNAL

Fish Physiology

## SIGNIFICANCE

- The insecticides that pose the greatest risk to fish have changed over time. The organochlorine compounds which are now largely banned, remain a concern due to their persistence in sediments and potential for bioaccumulation. Pyrethroids and other modern insecticides such as the phenylpyrazole, fipronil, are highly toxic to invertebrate species, and this may decrease food availability for fish.
- Continued development of less toxic insecticides and improved regulation of existing compounds, along with run-off mitigating techniques such as buffers, will decrease the risk of insecticides to fish.
- Understanding how different insecticides affect fish health and survival will help us manage and protect fishery resources.

## SUMMARY

Insecticides can contaminate surface waters as a result of spray drift, runoff, or intentional or accidental misapplication. If insecticide concentrations are high enough, fish kills will result, and at lower concentrations insecticides have been shown to impair fish growth, behavior, reproduction, and immune function. The insecticides that pose the greatest risk to fish have changed over time. Of the more recently developed insecticide classes (pyrethroids, neonicotinoids, and phenylpyrazoles), only the pyrethroids are considered highly toxic to fish. The use of pyrethroid insecticides continues to increase as they are being used to replace organophosphate compounds and carbamates, particularly in non- agricultural applications. Insufficient monitoring data are available to fully describe pyrethroid exposure to fish. Furthermore, pyrethroids and other modern insecticides such as the phenylpyrazole, fipronil, are highly toxic to invertebrate species, and this may decrease food availability for fish.

# ADDITIONAL ARTICLE

## AUTHORS

T. Doi, **G. A. Vecchi, A. J. Rosati,** and **T. L. Delworth (OAR/GFDL)**

## PUBLICATION DATE

Expected: May 2013

## TITLE

*Response to $CO_2$ doubling of the Atlantic hurricane main development region in a high-resolution climate model*

## JOURNAL

Journal of Climate

## SIGNIFICANCE

- The authors simulated the response of sea surface temperature (SST) in the Atlantic Hurricane Main Development Region (MDR) to a doubling of $CO_2$, using a cutting-edge global high-resolution coupled model developed at GFDL (CM2.5).
- The skillful representation of Atlantic interannual variability with this model enables the exploration of the response of interannual variability to increasing $CO_2$ – in addition to exploring changes in the average conditions in the Atlantic.
- This change in the interannual variability of SST will be one of the factors in projecting the risk of extremes in Atlantic Hurricanes, and for drought (or flood) in the Sahel and South America in a future climate.

## SUMMARY

This study reveals an increase of approximately 25% in the amplitude of interannual variations of SST in the Atlantic MDR, in response to $CO_2$ doubling. The seasonal timing of the peak in interannual SST variations moves from northern hemisphere spring to early summer, moving that peak variability closer to the North Atlantic hurricane season. A statistical refinement allows estimation of the impact of $CO_2$ changes on Atlantic hurricane frequency. The average number of hurricanes is found to decrease in response to increasing $CO_2$, (consistent with previous studies); however, the frequency of hurricanes in the most active years is as high or higher, because of the enhanced year-to-year variability in Atlantic MDR SSTs and its alignment with the hurricane season. The combined impact of natural climate variations, changes in average conditions, and changes in variability is key to the response of climate extremes to increasing greenhouse gases.

VISIT THE SCIENTIFIC PUBLICATIONS REPORT ARCHIVE

# ADDITIONAL ARTICLE

## AUTHORS

**E. H. Erwin, H. E. Coffey, W. F. Denig,** D.M. Willis, R. Henwood, and M.N. Wild **(NESDIS/NGDC)**

## PUBLICATION DATE

Expected: September 2013

## TITLE

*The Greenwich photo-heliographic results (1874 – 1976): initial corrections to the printed publications*

## JOURNAL

Solar Physics

## SIGNIFICANCE

- A new sunspot and faculae digital dataset for the interval 1874-1955 has been prepared under the auspices of the NOAA National Geophysical Data Center (NGDC).
- The authors correct errors associated with the systematic recordings of sunspots and related solar data produced by the Royal Observatory, Greenwich (1874-1976). The resulting digital dataset is important for maintaining an historical environmental database.

## SUMMARY

The new sunspot and faculae digital dataset for the interval 1874-1955 contains measurements of the positions and areas of both sunspots and faculae published initially by the Royal Observatory, Greenwich, and subsequently by the Royal Greenwich Observatory (RGO), under the title Greenwich Photo-heliographic Results (GPR), 1874-1976. The authors used Quality control procedures based on logical consistency to identify errors in the RGO publications. Examples of identifiable errors include North versus South errors in specifying heliographic latitude, errors in specifying heliographic (Carrington) longitude, errors in dates and times, errors in sunspot group numbers, arithmetical errors in the summation process, and omission of solar ephemerides. Although the number of errors in the RGO publications is remarkably small, the authors provide an initial table of necessary corrections for the interval 1874-1917. This paper is the third in a three-part series that identifies errors in the historical sunspot records and provides recommendations for maintaining an accurate digital database. As noted in the preceding companion papers, the existence of two independently prepared digital datasets, which both contain information on sunspot positions and areas, makes it possible to outline a preliminary strategy for the development of a more accurate digital dataset. Further work is in progress to generate an extremely reliable sunspot digital dataset, based on the long programme of solar observations supported first by the Royal Observatory, Greenwich, and then by the Royal Greenwich Observatory.

VISIT THE SCIENTIFIC PUBLICATIONS REPORT ARCHIVE

# ADDITIONAL ARTICLE

## AUTHORS

Y. Fan, **I. M. Held, S.-J. Lin,** and X. Wang **(OAR/GFDL)**

## PUBLICATION DATE

Early Online Release: March 2013

## TITLE

*Ocean warming effect on surface gravity wave climate change for the end of the 21st century*

## JOURNAL

Journal of Climate

## SIGNIFICANCE

- Change in the global wind-wave climate is one of the main drivers in the assessment of the effects of climate change on coastal erosion and risks to coastal population and ecosystems.
- The authors provide global dynamic wave projections for the remainder of this century.

## SUMMARY

The authors investigated surface wind (U10) and significant wave height (Hs) response to global warming using a coupled atmosphere-wave model by perturbing the sea surface temperatures with anomalies generated by WGCM CMIP-3 coupled models that use the IPCC/AR4/A1B scenario late in the 21st century. Several consistent changes were observed across all four realizations for the seasonal means: robust increase of U10 and Hs in the Southern Ocean for both the austral summer and winter due to the poleward shift of the jet stream; a dipole pattern of the U10 and Hs with increases in the northeast sector and decreases at the mid-latitude during the boreal winter in the North Atlantic due to the more frequent occurrence of the positive phases of NAO; and strong decrease of U10 and Hs at the tropical western Pacific Ocean during the austral summer, which might be caused by the joint effect of the weakening of the Walker circulation and the large hurricane frequency decrease in the South Pacific. Changes of the 99th percentile U10 and Hs are twice as strong as changes in the seasonal means, and the maximum changes are mainly dominated by the changes in hurricanes. Robust strong decreases of U10 and Hs in the South Pacific are due to the large hurricane frequency decrease, while the results in the Northern Hemisphere basins differ among the models. An additional sensitivity experiment suggests that the qualitative response of U10 and Hs is not affected by using SST anomalies only and maintaining the radiative forcing unchanged (using 1980 values) as in this study.

## RESOURCE LINK

*http://journals.ametsoc.org/doi/pdf/10.1175/JCLI-D-12-00410.1*

# ADDITIONAL ARTICLE

## AUTHORS

**J. Jacobs,** R. Harrell, J. Uphoff, **H. Townsend,** and K. Hartman **(NOS/NCCOS)**

## PUBLICATION DATE

Expected: March 2013

## TITLE

*Biological reference points for nutritional status of Chesapeake Bay Striped Bass*

## JOURNAL

North American Journal of Fisheries Management

## SIGNIFICANCE

- Tissue moisture serves as a robust, easy to determine indicator of striped bass nutritional status.
- This effort developed a tool for describing the nutritional health of striped bass in response to management needs for appropriate indicators for ecosystem approaches to fisheries management.
- The techniques and reference values are being implemented by state resource management agencies in 2013 and will serve as an annual indicator of health and foraging success.

## SUMMARY

The assessment of the nutritional status of fish is a central requirement of fisheries management. However, there has been little consensus on the appropriate indicator to use, and even less effort in defining biological thresholds and reference points. With current efforts to manage fisheries in an ecosystem context, environmental effects and trophic relationships need to be considered and appropriate indicators developed. To address this concern, we compiled five different studies where multiple indicators of nutritional status were applied to Striped Bass Morone saxatilis spanning age classes, geographical origin, and environment (cultured and wild). Proximate composition analysis was used to compare measured lipid concentration in the anterior dorsal muscle against selected indicators including Fulton's condition factor, relative weight, percent moisture, and an index of visceral body fat. Results suggest that weight- at-length indices are less sensitive than proximate analysis and poorly related to lipid concentration. However, models developed for both moisture and the body fat index (BFI) adequately represent tissue lipids and offer clear thresholds of lipid depletion. We propose the use of the proportion of Striped Bass with anterior dorsal muscle composed of greater than 80% moisture, or classified as having no observable visceral body fat, as a working protocol for poor-condition thresholds for ecosystem approaches to Chesapeake Bay Striped Bass management. Further, we propose an interim target condition based on historical data of 75% of individuals containing less than 80% moisture as a management goal.

VISIT THE SCIENTIFIC PUBLICATIONS REPORT ARCHIVE

# ADDITIONAL ARTICLE

## AUTHORS

**B. B. Collette (NMFS/NSL),** B. Polidoro, and K. Carpenter

## PUBLICATION DATE

May 6, 2013

## TITLE

*Corrigendum for Nature 494: Inertia is speeding fish-stock declines, K. Swing, Correspondence – Corrected numbers for fish on Red List*

## JOURNAL

Nature

## SIGNIFICANCE

- The authors respond to a recent publication by K. Swing and assert that many more species of marine fishes are on the IUCN Red List than Swing recorded, 4,337, rather than 'fewer than 100' as reported by Swing (2013).

## SUMMARY

The authors assert that K. Swing provided inaccurate numbers for marine fish species on the International Union for Conservation of Nature (IUCN) Red List of Threatened Species. They state that Swing also mistakenly conflates the scientific process of species assessment for the Red List with the separate political process of IUCN member voting (Swing 2013). About one-quarter, or 4,337, of some 17,000 species of marine fish are on the IUCN Red List (not fewer than 100 species out of 25,000, as Swing reported). Of those, 416 species have been placed in a threatened category (Critically Endangered, Endangered, or Vulnerable) and 1,180 species were classed as Data Deficient. The IUCN Tuna and Billfish Specialist Group has assessed all 10 species of billfish and 51 species of tuna and mackerel through a series of regional workshops, unhindered by the "IUCN's worldwide voting procedures". Seven species meet the IUCN threshold for a threatened category (Collette et al. 2011). The sale of billfish has since been banned in the continental United States. The IUCN Marine Biodiversity Unit's Global Marine Species Assessment programme is now evaluating all remaining marine fish, and aims to finish within five years.

## RESOURCE LINK

*http://www.nature.com/nature/journal/v495/n7439/full/495047a.html*

# ADDITIONAL ARTICLE

## AUTHORS

**A. Shah (NESDIS/NCDC/CIRES), C. Morrill (NESDIS/NCDC/CIRES), E. Gille (NESDIS/NCDC/CIRES), W. Gross (NESDIS/NCDC), D. M. Anderson (NESDIS/NCDC), B. Bauer (NESDIS/NCDC), R. Buckner (NESDIS/NCDC),** and **M. Hartman (NESDIS/NCDC/CIRES)**

## PUBLICATION DATE

Expected: Spring 2013

## TITLE

*Global speleothem oxygen isotope measurements since the Last Glacial Maximum*

## JOURNAL

Dataset Papers in Geoscience

## SIGNIFICANCE

- Thirty-five sites (sixty cores with over 27,000 measurements) located around the world provide data on the climate of the last 21,000 years.
- Using data contributed to the World Data Center for Paleoclimatology, we have created data files for individual sites, as well as composite data sets of annual to millennial resolution.

## SUMMARY

Data is obtained from oxygen isotope (δ18O) measurements provide evidence of water variability and change. Compared to paleoclimate proxies from sedimentary archives, the age uncertainty is unusually small, around +/- 100 years for the last 21,000 year interval. These individual files also often contain the chronology information about the sites. The data are useful in understanding hydrologic variability at local and regional scales, such as the Asian summer monsoon and the Intertropical Convergence Zone (as discussed in the underlying source publications), should also be useful in understanding large-scale aspects of hydrologic change since the Last Glacial Maximum.

This dataset paper documents a new compilation of speleothem d18O measurements, which are among the highest quality of any paleoclimate proxy archive in terms of their accuracy, precision and resolution. One important application of this dataset is direct model-data comparisons that may help to test and to improve the representation of the hydrologic cycle in the models being used to generate future climate projections.

## RESOURCE LINK

*http://www.hindawi.com/dpis/geosciences/2013/548048/*

## AUTHORS

**A. D. Apeti, S. I. Hartwell, M. Myers,** J. Hetrick, and J. Davenport **(NOS/NCCOS)**

## PUBLICATION DATE

Expected: May 2013

## TITLE

*Assessment of contaminant body burdens and histopathology of fish and shellfish species frequently used for subsistence food by Alaskan Native communities*

## SIGNIFICANCE

- Our results from contaminant body burden and histopathological characterization of the soft-shell clams, cockles, chum and sockeye salmon collected from traditional subsistence harvest areas in Alaska showed that the fish and shellfish were healthy and non-contaminated.
- Chemistry and histopathology data from this study represent useful information for concerned Native community members and coastal resource managers in Alaska. The data from this study were georeferenced and incorporated into the NS&T data portal and are available to the public.

## SUMMARY

Subsistence food items may constitute a health concern in rural Alaska because community members often rely on fish and wildlife resources not routinely monitored for persistent bioaccumulative contaminants and pathogens. Subsistence activities are a large part of the traditional culture, as well as a means of providing protein in the diets for Tribal members. In response to the growing concerns among Native communities, contaminant body burden and histopathological condition of chum and sockeye salmon (Oncorhynchus keta and Oncorhynchus nerka) and the shellfish cockles and softshell clams (Clinocardium nuttallii and Mya arenaria) were assessed. In the Spring of 2010, the fish and shellfish were collected from traditional subsistence harvest areas in the vicinity of Nanwalek, Port Graham, and Seldovia, AK, and were analyzed for trace metals and residues of organic contaminants routinely monitored by the NOAA National Status & Trends Program (NS&T). Additionally, the fish and shellfish were histologically characterized for the presence, prevalence and severity of tissue pathology, disease, and parasite infection. The fish and shellfish sampled showed low tissue contamination, and pathologic effects of the parasites and diseases were absent or minimal. Taken together, the results showed that the fish and shellfish were healthy and pose no safety concern for consumption. This study provides reliable chemistry and histopathology information for local resource managers and Alaska Native people regarding subsistence fish and shellfish use and management needs.

## AUTHORS

**T. Pait (NOS/NCCOS)**

## PUBLICATION DATE

Expected: April 2013

## TITLE

*An assessment of wastewater contaminants detected in the St. Thomas East End Reserves (STEER)*

## SIGNIFICANCE

- This study was a collaborative effort that analyzed wastewater contaminants within the St. Thomas East End Reserves of the U.S. Virgin Islands. Only one contaminant exceeded water quality guidelines.

## SUMMARY

This report is the second from a project to assess land-based sources of pollution and effects in the St. Thomas East End Reserves (STEER) in St. Thomas, USVI, and is the result of a collaborative effort between NOAA's National Centers for Coastal Ocean Science, the USVI Department of Planning and Natural Resources, the University of the Virgin Islands, and The Nature Conservancy. This document summarizes the results from the deployment of passive water samplers in the STEER in February 2012, specifically Polar Organic Chemical Integrative Samplers (POCIS). The POCIS were deployed in the STEER at five locations. In addition to the February 2012 deployment, the results from an earlier POCIS deployment in May 2010 in Turpentine Gut, a perennial stream which drains to the STEER, are also reported here. A total of 26 wastewater contaminants were detected at least once during the February 2012 deployment at the five sites in the STEER. Detections were high enough to estimate ambient water concentrations for nine wastewater contaminants using USGS experimentally derived POCIS sampling rates. From the May 2010 deployment in Turpentine Gut, 31 wastewater contaminants were detected, and ambient water concentrations could be estimated for 17 of those compounds. Ambient water concentrations were estimated for a number wastewater contaminants including the detergent metabolite 4-tert-octylphenol, phthalate ester plasticizers DEHP and diethyl phthalate, bromoform a byproduct of water chlorination, personal care products including menthol, indole, n,n-diethyltoluamide (DEET ), along with the animal/plant sterol cholesterol, and the plant sterol beta-sitosterol. Only DEHP appeared to have exceeded a water quality guidelines.

## AUTHORS

D. L. Abercrombie, D. D. Chapman, **S. J. B. Gulak,** and **J. K. Carlson (NMFS/SEFSC)**

## PUBLICATION DATE

March 2013

## TITLE

*Visual identification of fins from common elasmobranchs in the Northwest Atlantic Ocean*

## SIGNIFICANCE

- Five shark species were recently listed under Appendix II of the Convention on International Trade in Endangered Species (CITES).
- Successful implementation of these proposals will require the accurate identification of shark fins.

## SUMMARY

Scientists have designed an easy-to-use field guide based on morphological characteristics of shark fins (i.e. fin color, distinct markings, fin shape). This guide will be used by wildlife inspectors, customs personnel, researchers, and fishers to identify detached, dried, unprocessed dorsal and pectoral fins from sharks that are common in the U.S. Atlantic Ocean, including the Gulf of Mexico. The format of the guide allows for rapid and, for many species, unambiguous identification using key characteristics of the fin, such as shape, color and texture. The guide includes photographs of dorsal and pectoral fins, along with information on the general distribution if species, a brief fin description, and a list of similar species (if applicable) that may be confused for fins of the species in question. While designed for the NW Atlantic species, the guide is broad based and applicable to species that occur in other oceans.

## AUTHORS

**J. Kocik, C. Lipsky, T. Miller, P. Rago,** and **G. Shepherd**
**(NMFS/NEFSC)**

## PUBLICATION DATE

Expected: 29 March 2013

## TITLE

# *An Atlantic sturgeon population index for ESA management analysis*

## SIGNIFICANCE

- Derived interim estimates provide an alternative perspective of Atlantic sturgeon abundance, suggesting abundance may be higher than index estimates used in the original listing decision.
- However, the estimates and error bounds for the five units is wide and the geographic extent is expansive.
- Most ESA listings are initially controversial, and this was no exception. Threats, rather than abundance, were a key factor in listing.

## SUMMARY

The listing of Atlantic sturgeon under the Endangered Species Act in 2012 identified four Distinct Population Segments as endangered and one as threatened. We developed an index of population abundance for Atlantic sturgeon in the Northeast to aid managers in their efforts to evaluate potential threats to Atlantic sturgeon stocks. The population index is based on fishery bycatch estimates, data from USFWS's Atlantic Coast Sturgeon Tagging Database, and estimates of life history parameters from the literature. Estimates of total bycatch are based on observed trips monitored by the Northeast Fisheries Observer Program. We evaluated the influence of uncertainty in the model inputs using a risk analysis model that uses a parametric bootstrapping approach. Our estimate of the sampling distribution of ocean abundance has a mean of 417,934 fish and a 95% confidence interval of 165,381 to 744,597. These estimates define the population of sturgeon in the spatial domain monitored by the Northeast Fisheries Observer Program, but do not include populations that may reside year-round in rivers and estuaries. Our estimates of ocean abundance are consistent with annual swept-area estimates for nearshore areas derived using the Northeast Area Monitoring and Assessment Program data collected between 2007 and 2012.

## AUTHORS

**P. C. Caldwell (NESDIS/NODC)**

## PUBLICATION DATE

February 2013

## TITLE

*Tide gauge data rescue*

## SIGNIFICANCE

- Extending the length of tide gauge time series for enhancing research on global sea level change.

## SUMMARY

Historical, non-digitized tide gauge records are of potential great value to the oceanographic research community for extension of existing sea level time series as far back as possible in order to understand more completely the time scales of sea level change, and in particular, sea level rise associated with climate change. At the 12th session of the Global Sea Level Observing System (GLOSS) Group of Experts (GE), the topic of rescue of tide gauge data in non-computer form (charts, tabulations, etc.) was discussed. The GLOSS GE acknowledges that a large amount of historic data remain in paper form and noted that there had been recent findings in non-oceanographic facilities such as the United States National Archives and Records Administration and the archives of the French territorial divisions. To learn more of the potential global holdings of tide gauge records, a questionnaire was developed and sent to national focal points for GLOSS as well as national hydrographic agencies identified via the International Hydrographic Organization. The questionnaire sought specific details on locations, time spans, sampling frequencies, and media type, volume, and quality. The responses were compiled in an inventory of the Committee for Data in Science and Technology Data-at-Risk Task Group, which seeks to assess the availability and quality of historical records from a wide spectrum of scientific and technological fields, with the longer term goal of identifying funding sources and means for the transfer of the old records into computer-ready form. This paper describes the accomplishments of the 2012 GLOSS questionnaire.

# Correspondence

## Corrected numbers for fish on Red List

Kelly Swing gives inaccurate numbers for marine fish species on the International Union for Conservation of Nature (IUCN) Red List of Threatened Species. He also mistakenly conflates the scientific process of species assessment for the Red List with the separate political process of IUCN member voting (*Nature* **494,** 314; 2013).

About one-quarter, or 4,337, of some 17,000 species of marine fish are on the IUCN Red List (not fewer than 100 species out of 25,000, as Swing writes). Of those, 416 species have been placed in a threatened category (Critically Endangered, Endangered or Vulnerable) and 1,180 species were classed as Data Deficient.

The IUCN Tuna and Billfish Specialist Group has assessed all 10 species of billfish and 51 species of tuna and mackerel through a series of regional workshops, unhindered by the "IUCN's worldwide voting procedures". Seven species meet the IUCN threshold for a threatened category (B. B. Collette *et al. Science* **333,** 291–292; 2011). The sale of billfish has since been banned in the continental United States.

The IUCN Marine Biodiversity Unit's Global Marine Species Assessment programme is now evaluating all remaining marine fish, and aims to finish within 5 years (http://sci.odu.edu/gmsa).

**Bruce B. Collette** *National Marine Fisheries Service, Washington DC, USA.*
*collettb@si.edu*
**Beth Polidoro** *Arizona State University, Phoenix, USA.*
**Kent Carpenter** *Old Dominion University, Norfolk, Virginia, USA.*

## Regulating stem-cell therapies worldwide

Japan's drive to regulate experimental stem-cell treatments is a welcome step (*Nature* **494,** 5; 2013). However, it could be hard to define universally applicable criteria that ensure the safety and effectiveness of such treatments worldwide.

There is a risk that the social and economic circumstances of patients and researchers might blur or compromise crucial criteria, such as evidence-based support (including adequate preclinical and clinical testing), ethical review and no-fee experimental treatment.

Stem-cell therapies are all too often unsupported by scientific evidence, but many patients are prepared to accept the risks. And nations with inadequate health-care resources may expect patients to pay for experimental treatments.

Proliferation of experimental stem-cell therapies may even be indirectly encouraged in countries such as China, where ultra-light regulation through official notification (see www.moh.gov.cn) has uncertain regulatory value.

**Margaret Sleeboom-Faulkner** *University of Sussex, Brighton, UK.*
*m.sleeboom-faulkner@sussex.ac.uk*

## Order health systems in developing world

Governments and policy-makers are aiming to improve health markets in developing countries as they take up the challenge of last year's United Nations resolution to move towards universal health coverage (see go.nature.com/acsmss). We caution that they must do more than simply legislate their way to a more orderly health system.

We have highlighted the risks associated with unregulated health-care services and products in developing countries (*Nature* **487,** 163–165; 2012). We now wish to draw governments' attention to improvements proposed at a conference on securing international agreements on future health markets.

A small group of health policy-makers, entrepreneurs, academics and funders met in Bellagio, Italy, at the end of last year. Among their recommendations were that countries should establish systems for collecting better basic health-market data for incorporation into local policy and management processes, and that they should organize funds to promote sound regulatory practice (see go.nature.com/npsdvg).

The group called for a major effort by all market players to test innovative regulatory approaches and business models to improve access to safe and effective health services in the developing world.

**David H. Peters** *Johns Hopkins Bloomberg School of Public Health, Baltimore, Maryland, USA.*
*dpeters@jhsph.edu*
**Gerald Bloom** *University of Sussex, Brighton, UK.*

## Modelling genetics within ecosystems

Safeguarding genetic diversity is one of the Convention on Biological Diversity's main targets, because genetics underpins ecosystems. General models of whole ecosystems (D. Purves *et al. Nature* **493,** 295–297; 2013) therefore need to incorporate genetic data if they are to represent natural systems and guide conservation policy.

Yet it is important to understand that species diversity and genetic diversity do not always correlate; that the interplay between phylodiversity and functional diversity can be highly complex and regulated by interactions between cornerstone species; and that ecosystem resilience is tied to evolutionary history and genetic diversity. An ecosystem's full genetic potential, as represented by ancient lineages and maximally diverse taxa and key species, must be realized.

**Niall McCann, Pablo Orozco ter Wengel, David Stanton** *Cardiff University, Cardiff, UK.*
*mccannnp@cardiff.ac.uk*

**Drew Purves *et al.* reply:** It could be useful to incorporate genetics into general ecosystem models (GEMs), along with complexities such as stoichiometry or long-range migrations. Genetically based GEMs could interface with the increasing amounts of genetic data available to capture the effects of individual-scale adaptation, although this can be approximated without explicit genetics (for example, traits mutate in the Madingley model we describe in our Comment). However, such complexities bring greater computational demands and increased model freedom, which might lead to the model producing almost any output unless properly constrained with data.

## Evaluate gender equality in journals

The European Association of Science Editors established a gender policy committee last year to develop a set of standards for adoption by scientific journals. As co-chairs of the committee, our first step is to invite science editors to contribute to a survey of gender-equality policies in their journals (see go.nature.com/wor7ks; survey closes on 10 April).

In this survey, we ask editors for their views on considering sex and gender in experimental design and data analysis, and on presenting data that are broken down by sex. Information is also requested on gender balance and its promotion among editorial staff, editorial boards and peer reviewers.

Our hope is that all journals will eventually follow *Nature*'s example in promoting gender equality in science (see www.nature.com/women).

**Shirin Heidari** Journal of the International AIDS Society, *Geneva, Switzerland.*
*shirin.heidari@iasociety.org*
**Tom Babor** *University of Connecticut School of Medicine, Farmington, Connecticut, USA.*



© 2013 Macmillan Publishers Limited. All rights reserved

VISIT THE SCIENTIFIC PUBLICATIONS REPORT ARCHIVE

PAPER

# Use of High-Resolution DIDSON Sonar to Quantify Attributes of Predation at Ecologically Relevant Space and Time Scales


AUTHORS

**Victoria E. Price**
Department of Marine Sciences and National Undersea Research Technology and Education Center, University of Connecticut

**Peter J. Auster**
Department of Marine Sciences at the University of Connecticut and Sea Research Foundation, Mystic Aquarium, Groton, Connecticut

**Laura Kracker**
NOAA National Centers for Coastal Ocean Science, Charleston, South Carolina



ABSTRACT

Predator-prey interactions of large vagile fishes are difficult to study in the ocean due to limitations in the space and time requirements for observations. Small-scale direct underwater observations by divers (ca. <10 m radius) and large-scale hydroacoustic surveys (10 s $m^2$ to 100 s $km^2$) are traditional approaches for surveying fish. However, large piscivorous predators identify and attack prey at the scale of meters to tens of meters. Dual-Frequency Identification Sonar (or DIDSON) is a high-resolution acoustic camera operating in the MHz range that provides detailed continuous video-like imaging of objects up to a range of 30 m. This technology can be used to observe predator-prey interactions at ecologically relevant space and time scales often missed by traditional methods. Here we establish an approach for quantifying predation-related behaviors from DIDSON records. Metrics related to predator and prey group size, prey responses to predation, predation rate, predator strategies, and the nonrandom use of landscape features by both predator and prey are described. In addition, relationships between patterns in these attributes are tested and issues regarding sampling strategies for future studies are discussed. We suggest that approaches combining direct visual observation and acoustic sampling at multiple scales are required to quantify variation in these relationships across underwater landscapes.


Keywords: predator, prey, behavior, reef, hydroacoustics


## Introduction

Predation plays a critical role in the structure of reef fish communities (Tupper & Boutilier, 1997; Carr et al., 2002; Hixon & Beets, 2003). In addition to the direct effects on mortality of prey populations, predators also affect the distribution and behavior of co-occurring predators and prey species (Cosner et al., 1999). Predator-prey interactions are generally thought of most frequently in terms of direct mortality of prey and observed in the field using indirect methods such as stomach content sampling (e.g., Lindquist et al., 1994). Acoustic telemetry of muscle contraction rates (e.g., related to swimming speed) and stomach temperature have also been employed to infer patterns of feeding (Oswald, 1978; Sepulveda et al., 2004). Such indirect approaches are employed without regard to the more complex behavioral interactions between competing predators as well as between predators and prey, and their surrounding habitat that ultimately mediate predation success (but see Crowder et al., 1997). However, indirect methods cannot identify other important variables that influence predation dynamics and the impacts they have on population and community structure (Dill et al., 2003) such as predator group composition, effects of predator abundance, variation in the functional roles of species, interactions with landscape features, distribution and behavior of prey, and indirect species interactions (between predators as well as between predator and prey). The nature of these interactions makes them difficult to observe in any direct fashion at ecologically relevant space and time scales.

Variation in prey density has been shown to modify the relationship between prey survival and refuge availability through density-dependent predation mortality (Lannin, 2011). There are several mechanisms that mediate this phenomenon. Predator abundance can affect species richness of prey fish communities by forcing competition for refuge as well as altering species distributions (Cosner et al.,




VISIT THE SCIENTIFIC PUBLICATIONS REPORT ARCHIVE

1999). Anderson (2001) found that increasing habitat complexity produced a pattern of density-dependent prey mortality that had a stabilizing effect on prey fish populations. However, these patterns have an implicit assumption of homogenous distribution of predators and prey. A shortage of prey refugia has also been shown to cause short-term density dependent mortality due to predation (Johnson, 2006). If prey use particular seafloor features for refuge, predators may then occur at a higher density around these features (Kracker et al., 2008; Auster et al., 2009, 2011, 2013). Cosner et al. (1999) suggests that predation rates are therefore density dependent for both predator and prey as competition between predators increases.

The importance of intra- and interspecific interactions that facilitate predation, such as herding and confusing prey for other group members to attack or ambush (e.g., Hobson, 1968; Strand, 1988; Parrish, 1993; Auster et al., 2013), is unknown in most ecological settings in the ocean. However, where studies have been conducted, the act of facilitation between predator species (*sensu* Dill, 2003) appears to be common. For example, pelagic predators drive schools of prey to the surface, which increases prey availability to sea birds and has important population level effects (Au & Pitman, 1986; Ribic et al,. 1997; Safina, 1990; Clua & Grosvalet, 2001; Robinson & Tetley, 2007). Auster et al. (2013) observed predation by single and mixed-species groups of piscivores at subtropical reefs off the southeast United States and eastern Gulf of Mexico, where only 11% of 379 predation events involved only a single piscivore. All other events involved facilitation of predation by monospecific and mixed species groups of midwater and demersal predators. Most complex were events where midwater predators forced prey species to retreat to the seafloor, resulting in ephemeral high density patches of prey, which were then attacked by single and mixed species groups of demersal piscivores (67% of 274 events off the southeast United States and 28% of 105 events in the northeast Gulf of Mexico). Other studies of the interactions of multiple predators on a single prey species demonstrated that prey risk either decreased due to interactions between the predators themselves or increased because of conflicting prey responses to multiple predators (Sih et al., 1998). Clearly greater understanding of the outcomes of such interactions is critical to the development of a mechanistic understanding behind variations in local predator and prey populations as well as community structure. Such data can provide the foundation for improving the effectiveness of conservation and management strategies for reef fish communities.

To observe predation events at suitable space and time scales, new observational techniques are needed. Data collected by direct underwater observations by divers provide high-resolution "snapshots" of species composition and predator-prey interactions in a specific area but are limited in space and time (e.g., ca. <10 m horizontal radius, <1 h observation time). Hydroacoustic approaches can be used to expand observations in both space and time; for example, to investigate schooling behavior in response to predation (Gerlatto et al., 2006; Brierly & Cox, 2010) and examine the spatial distribution of prey species (Mayer et al., 2002). Ship-mounted split beam sonar systems are commonly used to assess large-scale patterns of fish distribution and abundance (e.g., 10 s $m^2$ to 100 s $km^2$) but lack the spatiotemporal resolution necessary to capture individual predation events as they occur. The scale at which high-resolution sonar imaging operates falls between the spatiotemporal resolution of these two approaches by expanding the range of visible diver observations, especially in turbid waters, and by providing detailed imagery of predation events at single sites within the context of the marine landscape surveyed using hydroacoustics.

DIDSON (Dual-Frequency Identification Sonar, SoundMetrics Corp.) is a high-frequency (i.e., MHz range) sonar camera that produces video-like images at a rapid rate allowing the movement and behavior of individual animals to be observed and quantified. Recent applications of DIDSON sonar include fish counts (e.g., salmonids passing particular areas in a river) and size estimates (Boswell, 2007; Maxwell & Gove, 2007). Work has also been done using DIDSON to perform abundance estimates of fishes in turbid waters, such as mangrove channels, where diver observations are not practical or possible (Frias-Torres & Luo, 2009). Behavioral studies using DIDSON to investigate the spawning of chum salmon (Tiffan et al., 2010) and avoidance by fishes of trawl gear (Rakowitz et al., 2012) illustrate the potential to investigate behavior on a scale useful for predation studies.

The DIDSON sonar used in this study ensonifies a region ranging from 1 to 30 m from the transducer. This allows for the collection of data at ecologically relevant space and time scales, capturing the fine-grain characteristics of predation. Because the use of DIDSON for behavioral observations is still exploratory, there is a need to first develop metrics and approaches to quantify attributes of predator-prey



VISIT THE SCIENTIFIC PUBLICATIONS REPORT ARCHIVE

interactions from sonar records. Here we report on the development of a set of metrics and related analytical approaches for using DIDSON imagery to assess attributes of piscivory in reef fish communities. Our intent is to develop an approach for using this state-of the art tool to ultimately gain a more thorough understanding of the role of predation processes in reef fish communities.

## Materials and Methods

### DIDSON System Characteristics

We used a DIDSON standard model 300M in this study. It is a high-resolution sonar unit that operates at a 1.1- or 1.8-MHz frequency, producing video-like images (Figures 1a and 1b). For this study the system was set to 1.8 MHz with a 2- to 11-m horizontal range. The sensor produces 96 beams with a 28.8° × 12° field of view. Data were collected continuously at a rate of 8 frames $s^{-1}$ with data files parsed into 12-min segments. The subsea sonar unit was mounted in a weighted frame affixed with a metal fin to orient into the current. The system was deployed shipside via power and data cable (the vessel was stationary using dynamic positioning) and rested on the sea floor facing along the edge of a reef (Figure 1c).

### Study Site

Anchor Ledge (31°37.7′N, 80° 34.6′W; depth 25 m) is located approximately 20 miles off the coast of Georgia. It is part of a large network of subtropical sandstone reef habitat representing approximately 5% of the continental shelf off the southeast United States (Powles & Barans, 1980; Parker et al., 1983). Emergent ledges in this region are up to 3 m in height surrounded by sand plains and exposed flat hard substratum. Hard substratum is dominated by suspension feeding organisms such as coral and sponge (Kendall et al., 2007). This structurally complex environment provides shelter and prey resources for a diversity of fishes, subsequently mediates their distribution, and affects spatial patterns of predator-prey interactions (Figure 1d; Sedberry & Van Dolah, 1984). Common midwater piscivores at these reefs include bar jack *Carangoides ruber*, blue runner *Caranx crysos*, greater amberjack *Seriola dumerili*, great barracuda *Sphyraena barracuda*, and Spanish mackerel *Scomberomorus maculatus*. Demersal piscivores include black sea bass *Centropristis striata*, bank sea bass *Centropristis ocyurus*, scamp *Mycteroperca phenax* and gag grouper *Mycteroperca microlepis*. Both groups prey upon highly abundant round scad *Decapterus punctatus*, mackerel scad *Decapterus macarellus,* and juvenile tomtate *Haemulon aurolineatum* (Auster et al., 2009, 2013).

**FIGURE 1**

(a and b) Example still frames of DIDSON imagery from 17 June 2009 illustrating a group of predators interacting with aggregations of prey. Note herding of prey at center of image b. (c) Deployment of DIDSON shipside via power and data cable. (d) Example of typical ledge with greater amberjack and prey.

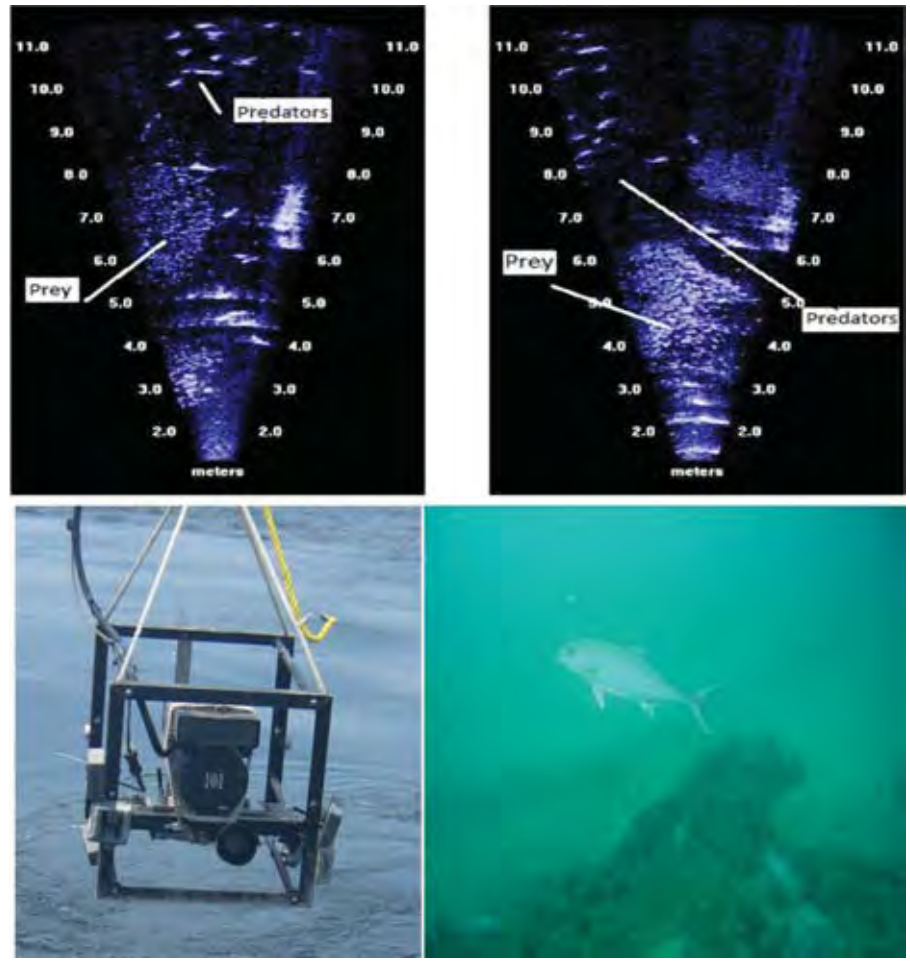


### Attributes of Predation and Analysis

Initial review of DIDSON records from this study revealed discrete



VISIT THE SCIENTIFIC PUBLICATIONS REPORT ARCHIVE

predation events with quantifiable behavioral attributes. Earlier work based on direct observation by divers (Auster et al., 2009) used discrete predation events as sample units and this approach is continued here for analysis. Small and large fish were present and moving within and through the ensonified volume in most records; however, this by itself does not indicate predation related behaviors. Because it is impossible to verify if the actual consumption of prey occurred, criteria were established to determine if a predation-*related* event (PRE) occurred (Figure 2). Both predator and prey needed to be present in the field of view for a PRE to occur, and we assumed that predator reaction to prey was evident by a rapid change in predator trajectory. Likewise, response by prey was evident in a rapid change in prey trajectory. It is important to recognize that these images are a two-dimensional representation of three-dimensional phenomena and that elements of each event may be occurring outside the ensonified region. However, we assumed that the individuals and interactions in the field of view are representative of each event and scaled appropriately in both space and time. If multiple attacks by two different groups of predators were observed, then they were considered separate events. Alternatively, two attacks by the same group were considered a single event.

Image files were initially reviewed using DIDSON Control and Display software (SoundMetrics Corp., V5.25.16). Records for each PRE were delineated based on the file time code and then individual frames in jpeg format extracted at three points (Figure 3): when the largest number of individuals were present in the field of view (referred to as Image 1_max), just prior to the PRE (referred to as Image 2_pre), and at the moment predators reacted to prey (i.e., at the time of a rapid change in predator trajectory; referred to as Image 3_react).

Sixteen metrics (13 measures of continuous data and 3 categorical classifications) were developed *a priori* to describe each event (Table 1). However, one measure based on continuous data was eliminated from the present study and four were ultimately treated as categorical data. Measures of predator length were eliminated due to large numbers of small individuals with variation affected by image resolution and animal orientation. Rather than using predator length as a continuous measure, predators were binned into 20-cm size classes instead. Number of prey groups and number of predator groups varied little and were classified by abundance category.

For counts and areal measurements, image files were digitized using Image J software (version 1.45s; Abramoff et al., 2004), which converted the DIDSON screen captures to 8-bit jpeg format with the low and high contrast threshold set to 30 and 255, respectively, enhancing the contrast between fish and background. These values were determined through an iterative process to eliminate background reflectance and facilitate counts and measurements. Predator and prey group area measurements as well as areal extent of prey response measurements (using Image1_max) were made in Image J based on an intercalibration of a known length acquired from an image. That is, a 1-m measured distance normal to the transducer at a 6-m range was translated to 57.4 pixels using the Image J Set

**FIGURE 2**

Decision diagram to determine if a predation-related event occurred. Reaction to prey was determined by a rapid change in predator trajectory. Response by prey was determined by a rapid change in prey trajectory.

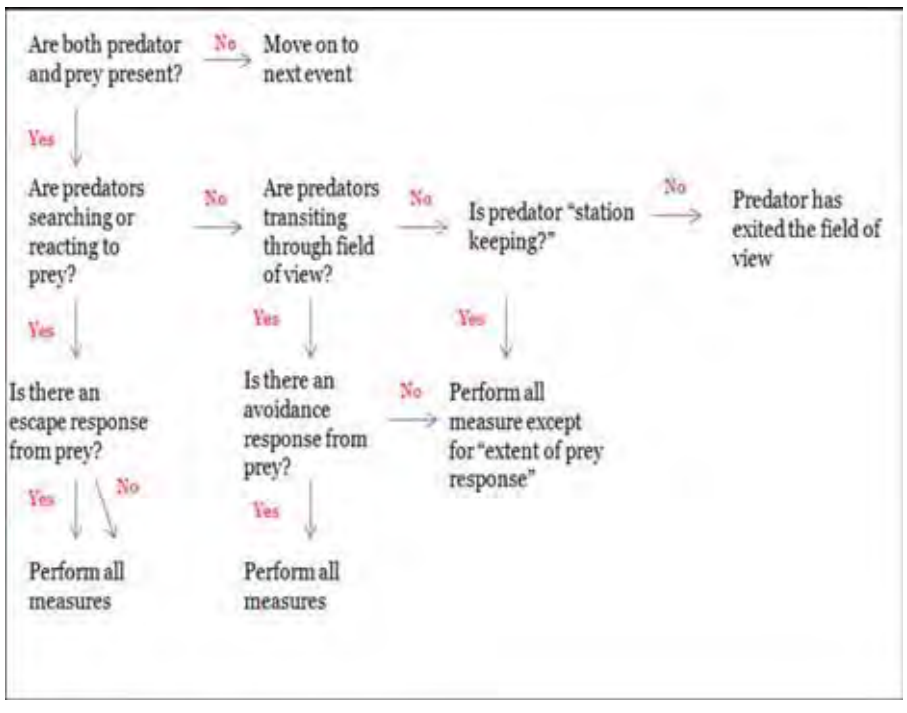




VISIT THE SCIENTIFIC PUBLICATIONS REPORT ARCHIVE

**FIGURE 3**

Example frame grabs from a single PRE used for analysis as described: just prior to the PRE (top), during the event (center), and just after the event (bottom).

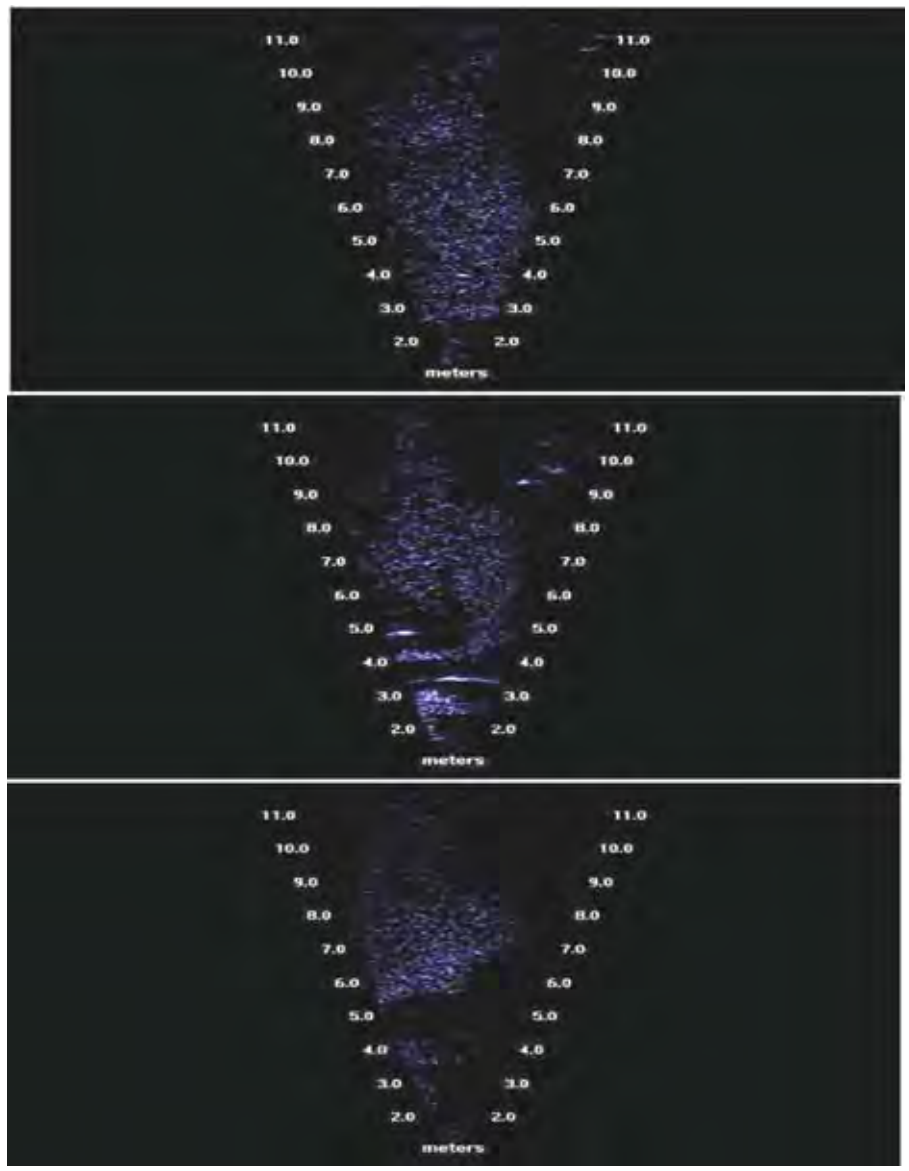


Scale tool. While there is a decrease in resolution with increasing distance from the transducer, measurements taken at 6 m did not differ by more than 2 cm across the 1- to 12-m range.

Density of predator and prey schools were measured using the particle counting tool for objects over 5 cm in Image1_max. The areal extent of prey response was measured as the difference in prey school area just prior to and during the PRE by comparing Image2_pre and Image3_react (Figure 4). The number of total attacks by all predator schools per event was measured, as well as the predation rate for each event (i.e. the number of attacks/duration of the PRE). The duration of events (in seconds) was also recorded, as well as by the total PRE rate per file (i.e., the number of events per 12-min file—admittedly an arbitrary sample unit time based on software configuration).

Categorical data include sizes of predators in each PRE, which were binned by 20-cm size classes. Predator trajectory through the field of view was classified to assess predator orientation to the long axis of the reef. Classes are either along the reef axis (parallel to) or across (intersecting) the reef from an off reef position. Predator behavior was classified based on shape of aggregations and orientation within or outside of prey schools. The formation of predators relative to prey schools were classed as: single individuals, a distinctly linear formation of multiple individuals, or as a circular-like group (or polygon) with individuals three or more deep. Furthermore, predators initiated PREs either within or adjacent to aggregations of prey. Therefore, inclusive categories are circular/along (CA), circular/integrated (CI), linear/along (LA), linear/integrated (LI), singular/along (SA), and singular/integrated (SI) (Figures 5a and 5b). Behavior classifications based on movements in relation to prey and habitat elements were made by viewing original records using DIDSON software.

To assess the relationships between metrics, a correlation matrix based on the Pearson's R statistic was computed. The *a priori* threshold for significance was $p < 0.05$. To better visualize and contrast relationships between pairs of metrics and to assess the degree of linearity in these relationships, a regression matrix was produced with a scatterplot of data points and a linear regression forced through the origin. As each variable has an independent distribution, the right side of the matrix plots $y$ on $x$ and the left side plots $x$ on $y$, hence each side of the matrix is not a mirror image.



VISIT THE SCIENTIFIC PUBLICATIONS REPORT ARCHIVE

**TABLE 1**

Description of continuous and categorical metrics.

| Metric | Description |
|---|---|
| *Measures with continuous data* | |
| Predator length | Size of individual predators; changed to categorical |
| Number of prey groups | Number of schools of prey (presented as numerical classes) |
| Number of predator groups | Number of schools of predators (presented as numerical classes) |
| Predator group size | The number of individuals in a school of predators |
| Predator group density | Number of individuals/area of group |
| Prey group size | Number of individuals in a school of prey fish |
| Prey group area | Area of prey group |
| Prey group density | Number of individuals/area of group |
| Areal extent of prey response | Measurement of change in prey group area during predation-related event |
| Number of attacks event$^{-1}$ | The number of times all predator schools attacked a prey school |
| Predation rate | Number of attacks min$^{-1}$ within each event |
| Duration of event | Time elapsed from first reaction to prey to end of reaction to prey |
| Global predation rate | Number of attacks per 12-min file |
| *Categorical data* | |
| Size class of predators | The average size of predators in the school; 20 cm increments |
| Formation of predators relative to prey school | Circular/along (CA), circular/integrated (CI), linear/along (LA), linear/integrated (LI), singular/along (SA), and singular/integrated (SI) |
| Trajectory of predators across field of view | Across or along field of view |

To determine if patterns of predation are patchy (clumped) over time, a two-term local quadrat variance (TTLQV) analysis was performed. The TTLQV was originally developed to quantify patterns of spatial patchiness from quadrat data, but in this case we used temporal period in lieu of quadrats to assess patchiness in time. Here global predation rate based on each 12-min file was the sample unit. The two-term local quadrat variance method blocks sample units at a consistent scale (here set at 10%). The mean square difference between neighboring blocks is then calculated to determine the variance across a range of distances (i.e., in this case time) between blocks (Rosenberg & Anderson, 2011).

Because this was an exploratory effort to assess approaches for future research, we also performed a *post hoc* power analysis to determine approximate sample sizes needed for future studies, assuming future data exhibit similar statistical distributions. Here we specified the range of numerical differences between sample means (i.e., 1–5) based on a power level of 0.8 and significance level of $p < 0.05$ for a two-sample $t$ test. Sample size requirements were calculated based on the standard deviation for each metric.

## Results

A total of 192 min of sonar data (parsed in sixteen 12-min record files) were recorded at Anchor Ledge from 1051 to 1336 EST on 17 June 2009. Analyses of sonar imagery yielded a total of 111 PREs. Descriptive statistics for each metric based on continuous data are summarized in Table 2. Only one measure, global predation rate, had a normal distribution based on the Anderson-Darling test for normality ($p > 0.05$). All others were non-normal ($p < 0.05$). Note that normally distributed data have a skewness of 0 and a kurtosis of 3. All metrics here have high skewness (a measure of asymmetry) and a wide range of kurtosis (a measure of peaked versus flat distribution).

Typically, predator group size was small (<20 individuals; Figure 6), and groups had relatively low density (Figure 7). The majority of PREs (68%) consisted of a single predator group and a single prey group; however, there were 15 events with multiple predator groups and a single prey group. Seventy-three percent of predator groups moved through the field of view along the reef axis. Fifty percent of predators were between 20 and 39 cm in length and groups always contained similarly sized individuals. Five percent of predators were over 100 cm in length, and



VISIT THE SCIENTIFIC PUBLICATIONS REPORT ARCHIVE

## FIGURE 4

Example of measurement of extent of prey response; comparison in area pre (top) and during (bottom) an event. Inset windows are from Image J software.

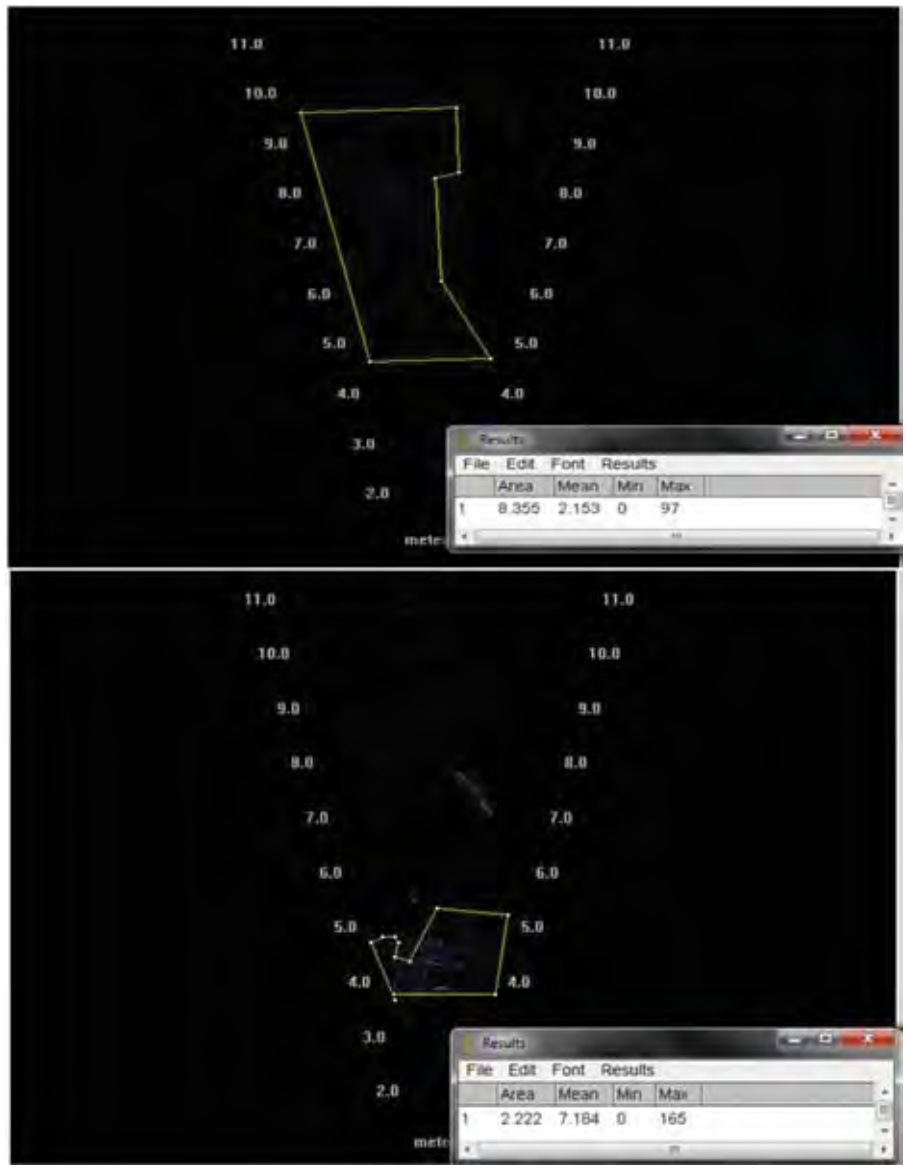


these individuals were always solitary (Figure 8). Ninety percent of events were under 1 min in duration (Figure 9). Table 3 contrasts the relationships in metrics based on continuous data with only 12 statistically significant paired contrasts. Interestingly, the relationship between predator group size (mean 10.4 individuals, *SD* = 16.8) and extent of prey response (mean 2.99 $m^2$, *SD* = 2.16) was not significant ($p = 0.99$, $r^2 = 0.1197$). A significant negative relationship was found between prey group area and predator group size ($p = 0.018$, $r^2 = 0.0514$) as well as predation rate and extent of prey response ($p = 0.04$, $r^2 = 0.070$). There was a positive relationship between the number of attacks per event and predator group size ($p < 0.001$, $r^2 = 0.1420$) as well as event duration and predator group size ($p < 0.001$, $r^2 = 0.2990$). As expected prey group area, density and the extent of prey response were strongly correlated ($p < 0.05$, $r^2 = 0.4060, 0.1341, 0.2460$, respectively), as well as the duration of event, number of attacks, and predation rate ($p < 0.01$, $r^2 = 0.4104, 0.0500, 0.0110$, respectively). The regression matrix (Figure 10) illustrates that even with significant *r* values few pairs exhibited a linear relationship, suggesting some form of polynomial relationship is required.

Predation rate and prey group size varied over time (Figure 11); with a pattern of higher activity in the morning and afternoon, and with a minimum at midday. The relationship between predation rate and prey group size was marginally significant ($p = -0.0713$, $r^2 = 0.0020$). The two-term local quadrat variance analysis of global predation rate revealed that variance was highest over time at a scale of three blocked sample units (30% of the total sample time or 57.6 min). As blocks represent a radius when used in a spatial context, the peak values are doubled to calculate the degree of patchiness. In a temporal context therefore time is doubled, indicating patchiness in predation events at roughly 120 min (Figure 12). Over the entire observation period, mean predation rate was 0.485 events $min^{-1}$, ranging from 0.0 to 1.25 events $min^{-1}$.

The *post hoc* power analysis revealed that sample size requirements varied widely in order to detect differences between samples at a 95% confidence level (power coefficient = 0.80). Detecting differences between sample means of three or more will require observation of a reasonable number of predation events for most metrics (i.e., less than 500 events per site; Table 4). Prey group size had such a large standard deviation (i.e., 89.09) that sample sizes in excess of 4,900 events would be required



VISIT THE SCIENTIFIC PUBLICATIONS REPORT ARCHIVE

**FIGURE 5**

(a) Example of a predator group classified as "circular/along" to prey group (outlined in yellow); a second predator group is present close to the transducer (outlined in red). (b) Illustration of categories for predator group orientation to prey. (Color versions of figures available online at: http://www.ingentaconnect.com/content/mts/mts/2013/00000047/00000001.)

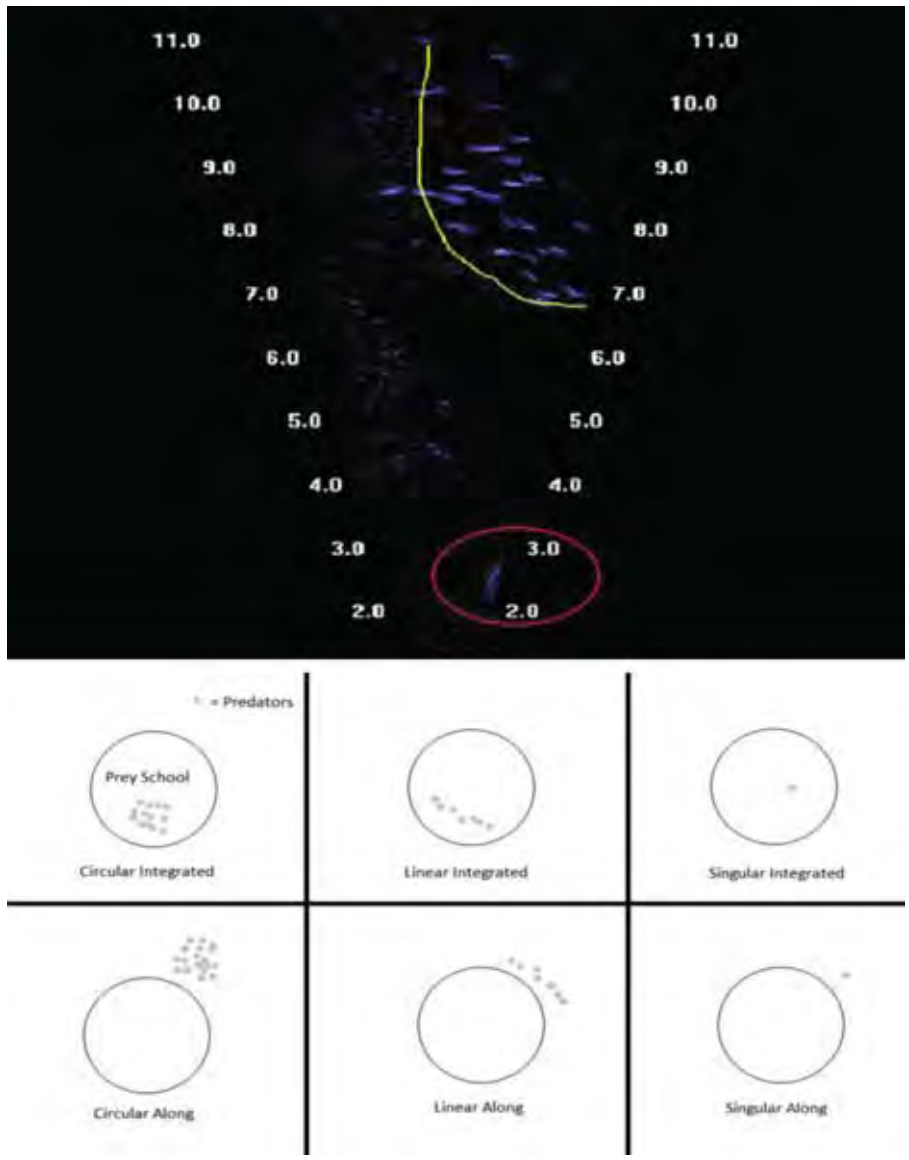


to detect significant differences between mean values that, in the present case, are around 150 individuals.

## Discussion

Here we demonstrated that analyses of DIDSON records can be used to produce quantitative measures to describe multiple attributes of predator-prey interactions of large vagile fishes. This study was conducted explicitly to establish approaches for processing DIDSON records, and based on these results, we are now in a position to implement studies to answer important ecological questions. DIDSON records enable a powerful approach for collecting data over long periods within and between sites irrespective of bottom time, depth and visibility, which typically impose severe limitations for direct visual data collection by divers or remote video cameras alone. Understanding variation in predator and prey abundance, behavior and rate of interactions within and between sites will allow tests of hypotheses related to facilitation and interference between predators, variation in prey response, and the role of variation in structural habitat and oceanographic settings. Based on the limited data sets produced from this work, it is clear that relatively large sample sizes (ca. $n$ = 500) will be needed to test for differences across treatments. If 3 h of observation yields approximately 100 PREs, then a 15-h deployment per station could produce sufficient sample sizes for most metrics to conduct appropriate statistical contrasts. Such a time period, while long by traditional visual sampling approaches, covers normal day (or night) periods inclusive of crepuscular periods over much of the globe and can capture variability at particular sample sites. The metrics derived from DIDSON imaging support, in general, diver observations related to the range in numbers and sizes of predators, coordinated group behaviors, and patchy prey distribution localized to ledge features (Auster et al., 2009, 2013).

The lack of statistical significance in many of the relationships between paired metrics raises many questions for further investigation regarding whether this pattern is due to limitations based on the region ensonified with a single DIDSON or a true lack of a relationship. The metrics that one would expect to be strongly correlated (e.g,. density and area, duration and number of attacks) were indeed so, suggesting that the sample region was not the limiting factor. While one



VISIT THE SCIENTIFIC PUBLICATIONS REPORT ARCHIVE

## TABLE 2

Descriptive statistics of continuous metrics.

| Variable | Mean | SD | Minimum | Q1 | Median | Q3 | Maximum | Skewness | Kurtosis |
|---|---|---|---|---|---|---|---|---|---|
| Predator group size (count) | 10.47 | 16.89 | 1 | 1 | 3 | 12.5 | 81 | 2.48 | 5.81 |
| Predator group density ($m^{-2}$) | 4.579 | 5.617 | 0.043 | 2.211 | 3.887 | 5.398 | 55.556 | 7.17 | 63.69 |
| Prey group size (count) | 155.84 | 89.09 | 24 | 95.5 | 136 | 199.5 | 501 | 1.66 | 3.65 |
| Prey group area ($m^2$) | 7.1 | 4.46 | 0.897 | 4.353 | 5.833 | 9.325 | 24.29 | 1.36 | 2.08 |
| Prey group density ($m^{-2}$) | 28.72 | 21.94 | 2.27 | 14.43 | 22.52 | 34.58 | 134.75 | 2.52 | 8.94 |
| Extent of prey response ($m^2$) | 2.944 | 2.146 | 0.013 | 1.426 | 2.445 | 3.854 | 14.85 | 2.01 | 7.81 |
| Attacks per event | 1.5138 | 1.0239 | 1 | 1 | 1 | 2 | 7 | 2.68 | 8.78 |
| Predation rate (events $s^{-1}$) | 0.1428 | 0.3209 | 0.0147 | 0.0436 | 0.0667 | 0.125 | 3 | 7.19 | 60.06 |
| Duration of event (s) | 25.94 | 20.62 | 2 | 9 | 19 | 39.5 | 90 | 1.08 | 0.56 |

would assume that a greater abundance of predators would elicit a larger areal response of prey (i.e., extent of prey response), it may be that prey actively engage in risk assessment when foraging and do not always view predators as an immediate threat (Ferrari et al., 2010). That is, the area of prey reaction is the same for small and large groups. An alternative explanation is that activities of both predator and prey groups may be occurring outside the ensonified region as well as in acoustic shadows cast by landscape features. It is important to emphasize that the DIDSON beam has a fairly narrow swath of about 28° horizontally and 12° vertically. While we assumed that behaviors observed in the ensonified region were representative of the sampling site and that variation in metrics addressed this problem, these space and time issues have yet to be fully resolved, especially when addressing limitations on accurately measuring absolute group size and dimensions. Development of sampling methods to address spatial variation in the ensonified region may produce a more refined picture of these dynamic interactions. For example, placing a single DIDSON on a pan-tilt unit and conducting either timed samples over a range of pre-set positions or periodic sweeps of a larger volume can increase overall sample volume both horizontally and

## FIGURE 6

Distribution of predator group size. Predator schools were predominantly under 20 individuals in size, although groups ranged from 1 to 100+ individuals.

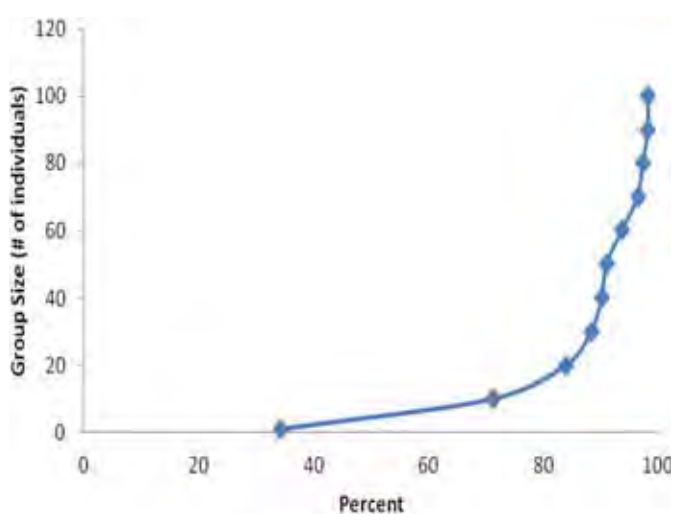


## FIGURE 7

Distribution of predator group density. Schools were generally loosely packed.

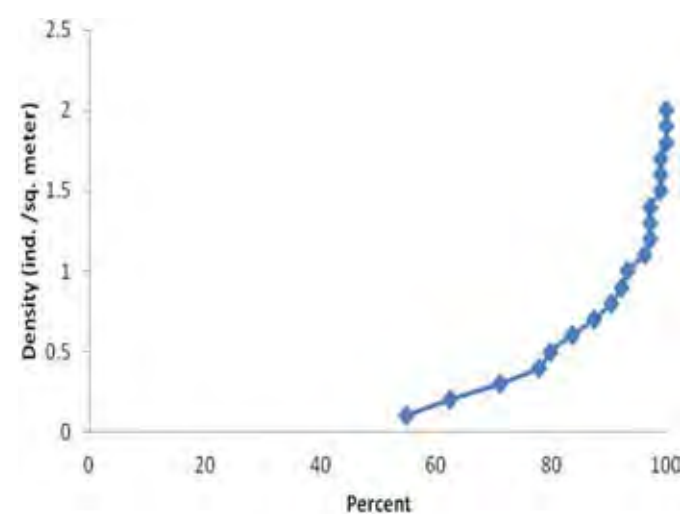




VISIT THE SCIENTIFIC PUBLICATIONS REPORT ARCHIVE

**FIGURE 8**

Frequency of predator size classes. Larger predators were generally solitary; smaller predators were the most common and occurred in larger groups.

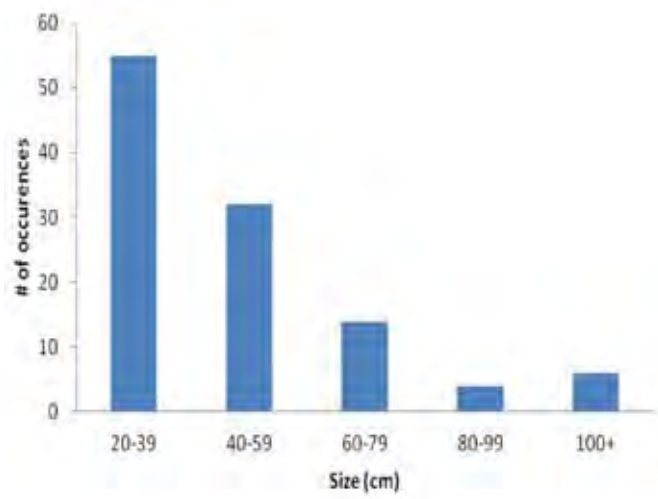


**FIGURE 9**

Distribution of PRE duration. Events were typically under 1 min in duration.

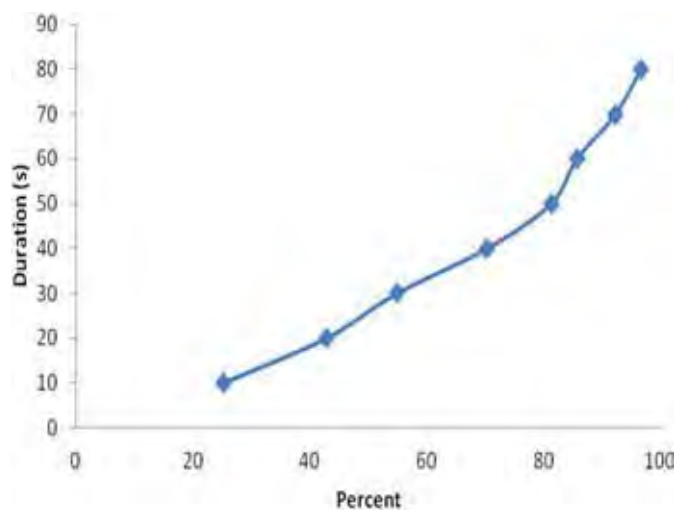


vertically. An arrangement of multiple sensors for simultaneous observations within and between habitat features also would resolve the issue of the optimal volume required for sampling (and perhaps reduce the number of samples required for comparisons).

Interesting relationships that were found to be statistically significant also prompt the need for further explanation. The negative relationship between predation rate and the extent of prey response as well as positive relationships between predator group size, duration of the event, and number of attacks per event may lend clues about prey group response to the intensity of attacks as well as dynamics within the predator group.

Resolving the issue of measures of prey response to predators has long been of interest to ecologists. The use of DIDSON may allow us to better address this problem, encompassing both predation behavior, as well as how prey species assess risk (e.g., behavior modifications in response to predation risk, deemed "risk effects"; Heithaus, 2008). Clemente et al. (2011) observed that areas closed to fishing positively affected predator assemblages, enhancing the intensity of predatory interactions compared to unprotected areas. Testing whether such patterns emerge in multiple regions and ecological settings as well as under different management scenarios would be a particularly useful application of this technology.

Increasing awareness of the utility of these types of sonar systems for studies of behavioral ecology will yield concomitant advances in analytical approaches. For example, Boswell et al. (2008) developed methods for autonomous analysis of large data sets from DIDSON records in order to measure fish size, biomass, swimming speed and direction. Mueller et al. (2010) used Echoview software (Myriax Echoview and Eonfusion, Hobart, Tasmania, Australia) to quantify species-specific tailbeat frequencies of two salmonids in a river in Alaska. Such approaches can then be used in sonar studies of migration behaviors addressing issues such as timing of upstream movements and patterns of habitat use. Automated approaches for quantifying the metrics we described here would greatly facilitate future studies given the predicted sample sizes required for comparisons. Concrete species identification remains elusive with acoustic work; however, the high-resolution imagery provided by DIDSON can lend information on body morphology, flexion, swimming behavior, and tail beat frequencies. These attributes, combined with the



VISIT THE SCIENTIFIC PUBLICATIONS REPORT ARCHIVE

VISIT THE SCIENTIFIC PUBLICATIONS REPORT ARCHIVE

**TABLE 3**

Correlation matrix of continuous metrics (Pearson's *r* value is top number).

| | Predator Group Size | Predator Group Density | Prey Group Size | Prey Group Area | Prey Group Density | Extent of Prey Response | #Attacks/Event | Predation Rate (events/s) |
|---|---|---|---|---|---|---|---|---|
| Predator group size | **** | | | | | | | |
| Predator group density | –0.0990, $p = 0.306$ | **** | | | | | | |
| Prey group size | –0.105, $p = 0.277$ | –0.047, $p = 0.629$ | **** | | | | | |
| Prey group area | –0.226, $\boldsymbol{p = 0.018}$ | 0.080, $p = 0.404$ | 0.489, $\boldsymbol{p < 0.001}$ | **** | | | | |
| Prey group density | 0.182, $p = 0.058$ | –0.078, $p = 0.419$ | 0.265, $\boldsymbol{p = 0.005}$ | –0.495, $\boldsymbol{p < 0.001}$ | **** | | | |
| Extent of prey Response | –0.125, $p = 0.194$ | 0.093, $p$=0.335 | 0.338, $\boldsymbol{p < 0.001}$ | 0.636, $\boldsymbol{p < 0.001}$ | –0.366, $\boldsymbol{p < 0.001}$ | **** | | |
| #Attacks/Event | 0.376, $\boldsymbol{p < 0.001}$ | 0.061, $p = 0.527$ | 0.033, $p = 0.733$ | –0.099, $p = 0.305$ | 0.045, $p = 0.641$ | 0.075, $p = 0.437$ | **** | |
| Predation Rate (events/s) | –0.123, $p = 0.137$ | 0.130, $p = 0.134$ | –0.071, $p = 0.869$ | 0.101, $p = 0.635$ | –0.093, $p = 0.487$ | –0.097, $\boldsymbol{p = 0.0400}$ | –0.093, $p = 0.288$ | **** |
| Duration of event (s) | 0.547, $\boldsymbol{p < 0.001}$ | –0.086, $p = 0.373$ | 0.044, $p = 0.652$ | 0.124, $p = 0.198$ | 0.098, $p = 0.313$ | 0.022, $p = 0.822$ | 0.643, $\boldsymbol{p < 0.001}$ | –0.224, $\boldsymbol{p = 0.019}$ |

## FIGURE 10

Regression matrix plot of paired metrics with continuous data plotting both *x* on *y* and *y* on *x*. A general lack of linearity suggests there may be a polynomial model that may be more descriptive of these relationships. Pred. GS = predator group size; Pred. GD = predator group density; Prey GS = prey group size; Prey GA = prey group area; Prey GD = prey group density; EPR = extent of prey response; Att/Ev = number of attacks/event; PredRate = global predation rate; DurEvent = duration of event.

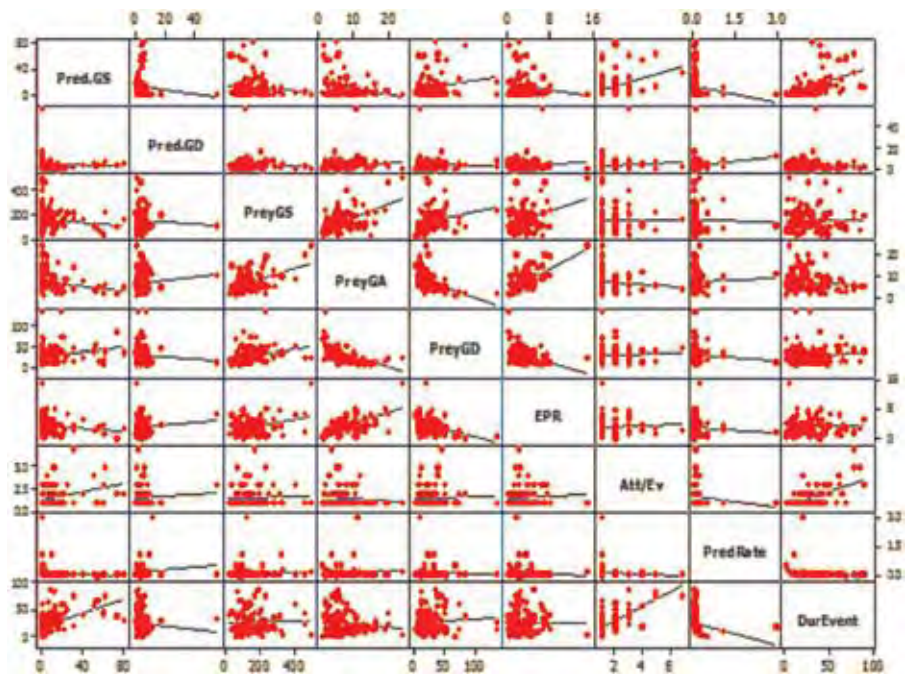


knowledge of species typically present in the area, may allow for the development of techniques to identify fish at least to species groups (such as jack, grouper, and sea bass).

Split-beam hydroacoustics provide a snapshot of fish distribution over a large spatial scale. However, key to understanding processes that result in this spatial variation are the real-time interactions that occur at the level of individual animals. DIDSON allows for the collection of continuous behavior data at a specific location over a long temporal period. Characterizing predation at multiple sites will allow statistical comparisons between sites and increase understanding of variation in species interactions as a whole. Developing effective and consistent data acquisition and analysis techniques for use of sonar records from DIDSON will allow for incorporation of variation in predation rates and predation intensity across habitats into population models so that spatially explicit demographic processes can be incorporated.

## FIGURE 11

Variability over time for both the number of prey (left axis) and predation rate (right axis), ranging from midmorning to midafternoon (*x* axis is local EDT).

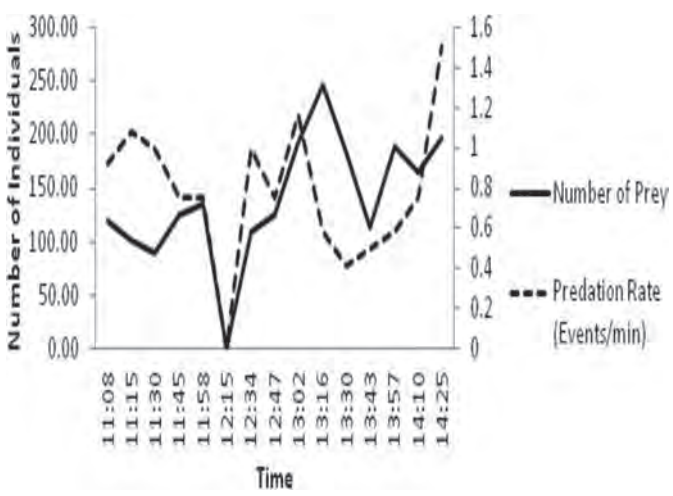


## FIGURE 12

Result of two-term local quadrat variance analysis indicating that variance in predation rate is highest at a scale of 3 block units equivalent to approximately 120 min.

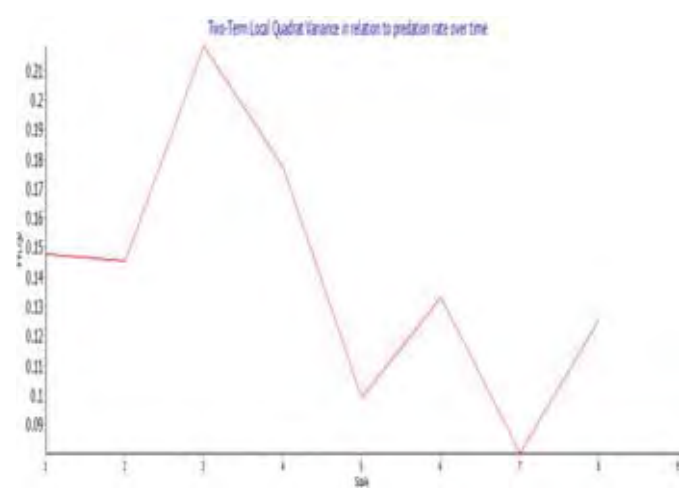



VISIT THE SCIENTIFIC PUBLICATIONS REPORT ARCHIVE

**TABLE 4**

Sample size requirements for a power level of 0.8 and alpha < 0.05.

| Metric | Sample Size |
|---|---|
| Predator group size | 856 |
| Predator group density | 858 |
| Prey group size | 859 |
| Prey group area | 859 |
| Prey group density | 859 |
| Extent of prey response | 854 |
| Attacks/event | 856 |
| Predation rate | 860 |
| Duration of event | 854 |

The knowledge gained from these approaches can then provide a more complete foundation for effective management and conservation strategies.

## Acknowledgments

The authors thank Frank Bohlen and Chris Taylor for advice during the course of this study and for comments on earlier drafts of this paper. The officers and crew of the NOAA Ship Nancy Foster made time in the field pleasant and productive. Support from Gray's Reef National Marine Sanctuary, especially from Greg McFall and Sarah Fangman, made this work possible. Scholarships from the Manasquan River Marlin and Tuna Club to the lead author are gratefully acknowledged. The opinions expressed herein are those of the authors and do not necessarily reflect the opinions of NOAA or its subagencies.

## Corresponding Author:

Victoria E. Price
Department of Marine Sciences and National Undersea Research Technology and Education Center, University of Connecticut, Groton, CT 06340
Email: Victoria.Price@noaa.gov

## References

**Abramoff**, M.D., Magalhaes, P.J., & Ram, S.J. 2004. Image processing with ImageJ. Biophoto Int. 11(7):36-42.

**Anderson**, T.W. 2001. Predator responses, prey refuges, and density-dependent mortality of a marine fish. Ecology. 82(1):245-57. http://dx.doi.org/10.1890/0012-9658(2001)082[0245:PRPRAD]2.0.CO;2.

**Au**, D., & Pitmann, R. Seabird interactions with dolphins and tuna in the eastern tropical Pacific. The Condor. 88:304-3 I 7.

**Auster**, P.J, Godfrey, J., Watson, A., Paquette, A., & McFall, G. 2009. Behavior or prey links midwater and demersal piscivorous reef fishes. Neotrop Ichthyol. 7(1):109-12. http://dx.doi.org/10.1590/S1679-62252009000100014.

**Auster**, P.J, Kracker, L., Price, V., Heupel, E., McFall, G., & Grenda, D. 2013. Behavior webs of piscivores at subtropical live-bottom reefs. Bull Mar Sci. 89:early view.

**Barans**, C.A., Arendt, M.D., Moore, T., & Schmidt, D. 2005. Remote video revisited: A visual technique for conducting long term monitoring of reef fishes on the continental shelf. Mar Technol Soc J. 39(2):110-8. http://dx.doi.org/10.4031/002533205787443917.

**Brierly**, A., & Cox, M. 2010. Shapes of krill swarms and dish schools emerge as aggregation members avoid predators and access oxygen. Curr Biol. 20:1758-62. http://dx.doi.org/10.1016/j.cub.2010.08.041.

**Boswell**, K., Wilson, M., & Wilson, C. 2007. Hydroacoustics as a tool for assessing fish biomass and size distribution associated with discrete shallow water estuarine habitats in Louisiana. Estuar Coast. 30(4):607-17.

**Boswell**, K., Wilson, M., & Cowan, J. 2008. A semi-automated approach to estimate fish size, abundance, and behavior from Dual-Frequency Identification Sonar (DIDSON) data. N Am J Fish Manage. 28:799-807. http://dx.doi.org/10.1577/M07-116.1.

**Carr**, M., Anderson, T., & Hixon, M. 2002. Biodiversity, population regulation, and the stability of coral-reef fish communities. P Natl A Sci. 99:11241-5. http://dx.doi.org/10.1073/pnas.162653499.

**Clua**, E., & Grosvalet, F. 2001. Mixed-species feeding aggregation of dolphins, large tunas and seabirds in the Azores. Aquat Living Resour. 14:11-8. http://dx.doi.org/10.1016/S0990-7440(00)01097-4.

**Cosner**, C., DeAngelis, D., Ault, J., & Olson, B. 1999. Effects of spatial grouping on the functional response of predators. Theor Popul Biol. 56:65-75. http://dx.doi.org/10.1006/tpbi.1999.1414.

**Crowder**, L.B., Squires, D.B., & Rice, J.A. 1997. Nonadditive effects of terrestrial and aquatic predators on juvenile estuarine fish. Ecology. 78:1796-804. http://dx.doi.org/10.1890/0012-9658(1997)078[1796:NEOTAA]2.0.CO;2.

**Dill**, L., Heithaus, R., & Walters, C. 2003. Behaviorally mediated indirect interactions in marine communities and their conservation implications. Ecology. 84(5):1151-7. http://dx.doi.org/10.1890/0012-9658(2003)084[1151:BMIIIM]2.0.CO;2.

**Ferrari**, M., Elvidge, C., Jackson, C., Chivers, D., & Brown, G. 2010. The responses of prey



VISIT THE SCIENTIFIC PUBLICATIONS REPORT ARCHIVE

fish to temporal variation in predation risk: Sensory habituation or risk assessment? Behav Ecol. 21:532-6. http://dx.doi.org/10.1093/beheco/arq023.

**Frias-Torres**, S., & Luo, J. 2009. Using Dual-Frequency Identification Sonar to detect juvenile goliath grouper *Epinephelus itajara* in mangrove habitat. Endangered Spec Res. 7:237-42. http://dx.doi.org/10.3354/esr00138.

**Gerlatto**, F., Bertrand, S., Bez, N., & Gutierrez, M. 2006. Waves of agitation inside anchovy schools observed with multibeam sonar: A way to transmit information in response to predation. ICES J Mar Sci. 63:1405-17. http://dx.doi.org/10.1016/j.icesjms.2006.04.023.

**Heithaus**, M., Frid, A., Wirsing, A., & Worm, B. 2008. Predicting ecological consequences of marine top predator declines. Trends Ecol Evol. 23(4):202-10. http://dx.doi.org/10.1016/j.tree.2008.01.003.

**Hixon**, M., & Beets, J. 2003. Predation, prey refuges, and the structures of coral-reef fish assemblages. Ecol Monogr. 63(1): 77-101. http://dx.doi.org/10.2307/2937124.

**Hobson**, E.S. 1968. Predatory behavior of some shore fishes in the Gulf of California. Res Rpt US Fish Wildl Serv. 73:1-92.

**Johnson**, D.W. 2006. Predation, habitat complexity, and variation in density-dependent mortality of temperate reef fishes. Ecology. 87:1179-88. http://dx.doi.org/10.1890/0012-9658(2006)87[1179:PHCAVI]2.0.CO;2.

**Kracker**, L., Kendall, M., & McFall, G. 2008. Benthic features as a determinant for fish biomass in Gray's Reef National Marine Sanctuary. Mar Geod. 31: 267-80. http://dx.doi.org/10.1080/01490410802466611.

**Kendall**, M., Bauer, L., & Jeffrey, C. 2007. Characterization of the benthos, marine debris and bottom fish at Gray's Reef National Marine Sanctuary. NOAA Tech Mem NOS NCCOS 50. 82p. + Appendices. Maryland, USA: NOAA, Silver Spring.

**Lannin**, R., & Hovel, K. 2011. Variable prey density modifies the effects of seagrass habitat structure on predator-prey interactions. Mar Ecol-Prog Ser. 442:59-70.http://dx.doi.org/10.3354/meps09393.

**Lindquist**, D. G., Cahoon, L.B., Clavijo, I.E., Posey, M.H., Bolden, S.K., Pike, L.A., … Cardullo, P.A. 1994. Reef fish stomach contents and prey abundance on reef and sand substrata associated with adjacent artificial and natural reefs in Onslow Bay, North Carolina. Bull Mar Sci. 55:482-7.

**Mayer**, L., Li, Y., & Melvin, G. 2002. 3D visualization for pelagic fisheries research and assessment. ICES J Mar Sci. 59:216-25. http://dx.doi.org/10.1006/jmsc.2001.1125.

**Maxwell**, S., & Gove, N. 2007. Assessing Dual-Frequency Identification Sonar's fish-counting accuracy, precision, and turbid river range capability. Acoust Soc Am. 122(6):3364-77. http://dx.doi.org/10.1121/1.2799500.

**Mueller**, A., Burwen, D., Boswell, K., & Mulligan, T. 2010. Tail-Beat patterns in Dual-Frequency Identification Sonar echograms and potential use for species identification and bioenergetics studies. Trans Am Fish Soc. 139:900-10. http://dx.doi.org/10.1577/T09-089.1.

**Oswald**, R.L. 1978. The use of telemetry to study light synchronization with feeding and gill ventilation rates in *Salmo trutta*. J Fish Biol. 13:729-39. http://dx.doi.org/10.1111/j.1095-8649.1978.tb03487.x.

**Parker**, R., Colby, D., & Willis, T. 1983. Estimated amount of reef habitat on a portion of the U.S. South Atlantic and Gulf of Mexico continental shelf. Bull Mar Sci. 33: 935-40.

**Parrish**, J.K. 1993. Comparison of the hunting behavior of four piscine predators attacking schooling prey. Ethology. 95:233-46. http://dx.doi.org/10.1111/j.1439-0310.1993.tb00473.x.

**Powles**, H., & Barans, C. 1980. Groundfish monitoring in sponge-coral areas off the South-eastern United States. Mar Fish Rev. 42: 21-35.

**Rakowitz**, G., Tušer, M., Říha, M., Jůza, T., Balk, H., & Kubečka, J. 2012. Use of high-frequency imaging sonar (DIDSON) to observe fish behaviour towards a surface trawl. Fish Res. 123-(124):37-48. http://dx.doi.org/10.1016/j.fishres.2011.11.018.

**Ribic**, C., Ainley, D., & Spear, L. 1997. Seabird associations in Pacific equatorial waters. Ibis. 139:482-87.

**Robinson**, K., & Tetley, M. 2007. Behavioural observations of foraging minke whales (*Balaenoptera acutorostrata*) in the outer Moray Firth, north-east Scotland. J Mar Biol Assoc UK. 87:85-6. http://dx.doi.org/10.1017/S0025315407054161.

**Rosenberg**, M., & Anderson, C. 2011. PASSaGE: Pattern Analysis, Spatial Statistics and Geographic Exegesis. Version 2. Methods Ecol Evol. 2(3):229-32. http://dx.doi.org/10.1111/j.2041-210X.2010.00081.x.

**Safina**, C. 1990. Bluefish mediation of foraging competition between Roseate and Common turns. Ecology. 71(5):1804-09. http://dx.doi.org/10.2307/1937588.

**Sedberry**, G., & Van Dolah, R. 1984. Demersal fish assemblages associated with hard bottom habitat in the South Atlantic Bight of the U.S.A. Environ Biol Fish. 11:241-58. http://dx.doi.org/10.1007/BF00001372.

**Sih**, A., Englund, G., & Wooster, D. 1998. Effects of multiple predators on prey. TREE. 13(9):350-5. http://dx.doi.org/10.1016/S0169-5347(98)01437-2.

**Sepulveda**, C.A., Kohin, S., Chan, C., Vetter, R., & Graham, J.B. 2004. Movement patterns, depth preferences, and stomach temperatures of free-swimming juvenile mako sharks, *Isurus oxyrinchus*, in the Southern California Bight. Mar Biol. 145:191-9. http://dx.doi.org/10.1007/s00227-004-1356-0.

**Strand**, S. 1988. Following behavior: interspecific foraging associations among Gulf of California reef fishes. Copeia. 1988:351-7. http://dx.doi.org/10.2307/1445875.

**Tiffan**, K., Haskell, C., & Kock, T. 2010. Quantifying the behavioral response of spawning chum salmon to elevated discharges from Bonneville Dam, Columbia River, USA. River Res Appl. 26:81-101.

**Tupper**, M., & Boutilier, R. 1997. Effects of habitat on settlement, growth, predation risk and survival of a temperate reef fish. Mar Ecol-Prog Ser. 151: 225-36. http://dx.doi.org/10.3354/meps151225.



VISIT THE SCIENTIFIC PUBLICATIONS REPORT ARCHIVE

OPEN ACCESS Freely available online

PLOS | ONE

# Habitat Availability and Heterogeneity and the Indo-Pacific Warm Pool as Predictors of Marine Species Richness in the Tropical Indo-Pacific

**Jonnell C. Sanciangco[1,2]*, Kent E. Carpenter[1,2], Peter J. Etnoyer[3], Fabio Moretzsohn[4]**

**1** Marine Biodiversity Unit/Global Marine Species Assessment, Global Species Programme, International Union for Conservation of Nature, Gland, Switzerland, **2** Department of Biological Sciences, Old Dominion University, Norfolk, Virginia, United States of America, **3** NOAA Center for Coastal Environmental Health and Biomolecular Research, Charleston, South Carolina, United States of America, **4** Harte Research Institute for Gulf of Mexico Studies, Texas A&M University-Corpus Christi, Corpus Christi, Texas, United States of America

## Abstract

Range overlap patterns were observed in a dataset of 10,446 expert-derived marine species distribution maps, including 8,295 coastal fishes, 1,212 invertebrates (crustaceans and molluscs), 820 reef-building corals, 50 seagrasses, and 69 mangroves. Distributions of tropical Indo-Pacific shore fishes revealed a concentration of species richness in the northern apex and central region of the Coral Triangle epicenter of marine biodiversity. This pattern was supported by distributions of invertebrates and habitat-forming primary producers. Habitat availability, heterogeneity, and sea surface temperatures were highly correlated with species richness across spatial grains ranging from 23,000 to 5,100,000 $km^2$ with and without correction for autocorrelation. The consistent retention of habitat variables in our predictive models supports the area of refuge hypothesis which posits reduced extinction rates in the Coral Triangle. This does not preclude support for a center of origin hypothesis that suggests increased speciation in the region may contribute to species richness. In addition, consistent retention of sea surface temperatures in models suggests that available kinetic energy may also be an important factor in shaping patterns of marine species richness. Kinetic energy may hasten rates of both extinction and speciation. The position of the Indo-Pacific Warm Pool to the east of the Coral Triangle in central Oceania and a pattern of increasing species richness from this region into the central and northern parts of the Coral Triangle suggests peripheral speciation with enhanced survival in the cooler parts of the Coral Triangle that also have highly concentrated available habitat. These results indicate that conservation of habitat availability and heterogeneity is important to reduce extinction of marine species and that changes in sea surface temperatures may influence the evolutionary potential of the region.

**Citation:** Sanciangco JC, Carpenter KE, Etnoyer PJ, Moretzsohn F (2013) Habitat Availability and Heterogeneity and the Indo-Pacific Warm Pool as Predictors of Marine Species Richness in the Tropical Indo-Pacific. PLoS ONE 8(2): e56245. doi:10.1371/journal.pone.0056245

**Editor:** Diego Fontaneto, Consiglio Nazionale delle Ricerche (CNR), Italy

**Received** October 5, 2012; **Accepted** January 7, 2013; **Published** February 15, 2013

This is an open-access article, free of all copyright, and may be freely reproduced, distributed, transmitted, modified, built upon, or otherwise used by anyone for any lawful purpose. The work is made available under the Creative Commons CC0 public domain dedication.

**Funding:** This research was generously supported by core funding from the Tom Haas and the New Hampshire Charitable Foundation, and the Thomas W. Haas Foundation. The funders had no role in study design, data collection and analysis, decision to publish, or preparation of the manuscript.

**Competing Interests:** The authors have declared that no competing interests exist.

* E-mail: jsanc005@odu.edu

## Introduction

Persistent questions remain regarding the origins of the uneven distribution of marine species richness across the tropical Indo-Pacific [1], despite numerous relevant ecological and biogeographical studies and an urgent need to improve conservation effort [2]. In particular, explanations for the Coral Triangle epicenter of marine biodiversity [3] have received more attention in the literature than any other topic in marine biogeography [4]. This area encompasses much of Indonesia, Malaysia, the Philippines, Papua New Guinea, the Solomon Islands, Timor L'Este, and Brunei. It is also referred to as the East Indies Triangle [5–7], the Indo-Malay-Philippine Archipelago [8,9], and a variety of other names [1]. The term Indo-Australian Archipelago (e.g. [10,11]) is also used frequently, though the Coral Triangle does not include Australia [3] and does include geological elements beyond Indonesia [12].

The tropical Indian and Pacific Oceans encompass about two thirds of the earth's equatorial circumference and include two distinct marine zoogeographic regions [13,14], the Eastern Tropical Pacific and the Indo-West Pacific. Their shore biotas are effectively separated by a pelagic eastern Pacific barrier, a vast expanse of open ocean that lacks shallow island stepping stones for dispersal [13,15]. The Eastern Tropical Pacific has limited shelf area and coral reef development. Species in this region have primary biogeographic affinities in the Caribbean except perhaps for some reef-building corals [16]. The tropical Indo-West Pacific is the most biologically diverse marine region worldwide, and is also the largest marine biogeographic realm, extending longitudinally more than halfway around the world and through more than 60° of latitude [17] with several distinct provinces [14]. It is a tropical and subtropical region extending from the Indian Ocean (including the Red Sea and Persian Gulf) eastward to the central Pacific Ocean through Polynesia to Easter Island [13,18]. The extent of shallow water area and the length of coastline in the Indo-Pacific is a result of a complex geological history in the region [19] that resulted in separate successive biodiversity hotspots (areas of exceptional species richness) that coincided with areas of tectonic collision [20–25]. This tectonic activity both created and maintained extensive and complex shallow-water habitat at



VISIT THE SCIENTIFIC PUBLICATIONS REPORT ARCHIVE

different periods. The current biodiversity hotspot is the Coral Triangle where the Eurasian, Philippine, Pacific, and Australian plates collide and effectively closed off the Indo-Pacific equatorial seaway [26]. This constricted ocean circulation in the western Pacific and initiated the formation of the Indo-Pacific Warm Pool in the late Miocene [27]. This warmest open ocean area continues to influence global climate. The western part of the Coral Triangle [3] spatially coincides with the main part of the area of consistent peak temperatures above 29°C of the Indo-Pacific Warm Pool [28–30].

The observation that peaks in marine species richness throughout geologic time follow changing concentrations of available habitat is an extension of the area of refuge hypothesis, one of the numerous hypotheses invoked to explain the current epicenter of marine biodiversity in the Coral Triangle [1,8,31]. The area of refuge hypothesis [32] suggests that species richness mainly depends on the extent of shallow-water (photic and mesophotic) habitat available over geologic time to consistently provide niches and effectively reduce rates of extinction. This hypothesis also relates to positive species-area relationships, a long-standing paradigm in ecology [33]. The Coral Triangle currently has the greatest concentration of tropical shallow water habitat on Earth, encompassing highly diverse and extensive areas of coral reefs, mangroves, seagrass beds, estuaries, and soft-sediment habitats [6,9,34,35]. The Coral Triangle also has the longest coastline in the Indo-Pacific [26,36] and extensive shallow water area that contributes geographic complexity which ultimately leads to species diversification [25]. The extent and diversity of habitat appears to correspond closely with species-area and species-habitat diversity relationships for this region [1].

In addition to area of refuge, other hypotheses used to explain the current epicenter of marine biodiversity can be summarized as: 1) center of origin [17,22,37–43]; 2) area of overlap of Indian and Pacific Ocean biotas [6,44]; 3) area of accumulation of peripherally-originating species [45,46]; 4) tectonic integration of biotas [9,47]; and, 5) available energy [48]. The available energy hypothesis suggests that more energy can support more species (less partitioning of available energy) or higher temperatures promote faster population turnover rates and hence faster rates of speciation and extinction. Evidence exists to support many of these proposed hypotheses suggesting a combination of factors promote species richness in the Coral Triangle [6,8,9,20,35,49–51].

A neutral hypothesis has also been tested relating to the mid-domain effect [52,53]. This effect states that the geometric factor of range size causes species to randomly accumulate at the center of a bounded domain. Although the Coral Triangle epicenter of diversity is at the approximate center of an Indo-Pacific domain, non-random predictors such as habitat area influence on species richness are more important than the mid-domain effect in shaping diversity gradients in the region [42,52,53]. More generally, a review of a large number of published studies [54] concluded "observed patterns of species richness are not consistent with the mid-domain hypothesis." Despite the potential utility of a mid-domain model in describing species richness gradients, there are other potential null models and the choices and underlying assumptions of each of these models are still a subject of considerable debate [55,56]. The mid-domain effect was not tested in a global analysis of marine biodiversity patterns because of the subjective nature of mid-domain delineation [57]. The same constraint confounds its inclusion in an Indo-Pacific study. It is questionable to test a single mid-domain across two distinct regions such as the tropical eastern Pacific and tropical Indo-West Pacific because of the intervening east Pacific barrier. Separate mid-domains or an inclusive mid-domain for the provinces within the tropical Indo-West Pacific is also questionable. Due to these numerous constraints and the fact that mid-domains are not generally supported [54], a mid-domain model was not considered in our hypothesis-testing. Instead, we focused on hypotheses relating to habitat availability and available energy as these were best supported in a global study of species richness [57].

The area of refuge hypothesis was primarily formulated as an alternative to the well-established center of origin hypothesis which heavily relies on assumptions about dispersal [32] that presumably gave rise to the diminishing pattern of species richness with distance from the epicenter (Figure 1A). The area of refuge hypothesis is also founded in a long-held axiom in ecology, that larger areas hold more species than smaller areas [33]. Stehli and Wells (1971) [37], in the first depiction of the bull's-eye pattern of species richness of coral genera in the Indo-West Pacific, invoked a center of origin hypothesis but also suggested that available area of coral habitat was important but that it "cannot yet be quantified." In what is now called the area of refuge hypothesis [8,9,31], McCoy and Heck (1976) [32] first suggested that species-area relationships and extent of area available for refuge from extinction are responsible for tropical marine biogeographic pattern. They also invoke an eclectic approach in which the center of diversity in the Indo-West Pacific is accumulating species and that the extensive shoreline in this area allows for isolation and diversification of species. However, explicit in the area of refuge hypothesis as originally described by McCoy and Heck (1976) [32] is that the Coral Triangle has served as an area of lower extinction than the rate of either migration into or origination of species in the area over time. This basic concept is supported by other studies [11,42,58]. Evidence is accumulating that area of refuge, in terms of extensive and varied habitat, is an important factor in explaining species richness in the Indo-West Pacific [10,53]. Many taxa also show lowered extinction risk that correlates with the extensive and diverse habitats of the Coral Triangle [42,59,60].

One component of the area of refuge hypothesis is habitat heterogeneity, which has long been considered important in shaping species diversity patterns [61,62,63]. A varied and complex habitat provides many different ways of exploiting environmental resources potentially catering to many species and promoting speciation when niches are not exploited by existing species. However, the accuracy of measuring the influence of habitat heterogeneity can depend on the index used, the spatial scale, and whether a 'keystone structure' has been identified that accurately reflects the species represented in the study [64–66]. For example, in a terrestrial system at small scales insect diversity may be dependent on presence of keystone vegetation types but at larger scales wetland presence may be the keystone structure [65]. There are many different keystone structures and grid sizes (scales) to choose from when testing predictors of species richness across the entire Indo-Pacific. In addition, alternative habitat variables may have different responses at varying scales. Coastline length has been proposed as a predictor of species richness [25,32,36,57], and therefore can be hypothesized as a keystone structure to measure habitat availability and heterogeneity. In addition, available habitat in terms of extent and gradients of continental shelf area, reef area, seagrass bed area, and mangrove area can potentially influence species richness across the tropical Indo-Pacific [6,67–69]. In previous explicit tests of species richness across the Indo-Pacific, available habitat and habitat heterogeneity have been lumped as either a conglomerate proxy in the form of coastline length [57] or different shallow area indices [53]. Here for the first time, we test the marine species richness predictive value of coastal length, available shelf area, and two different indices based on relative amounts of soft bottom, coral reef,



VISIT THE SCIENTIFIC PUBLICATIONS REPORT ARCHIVE

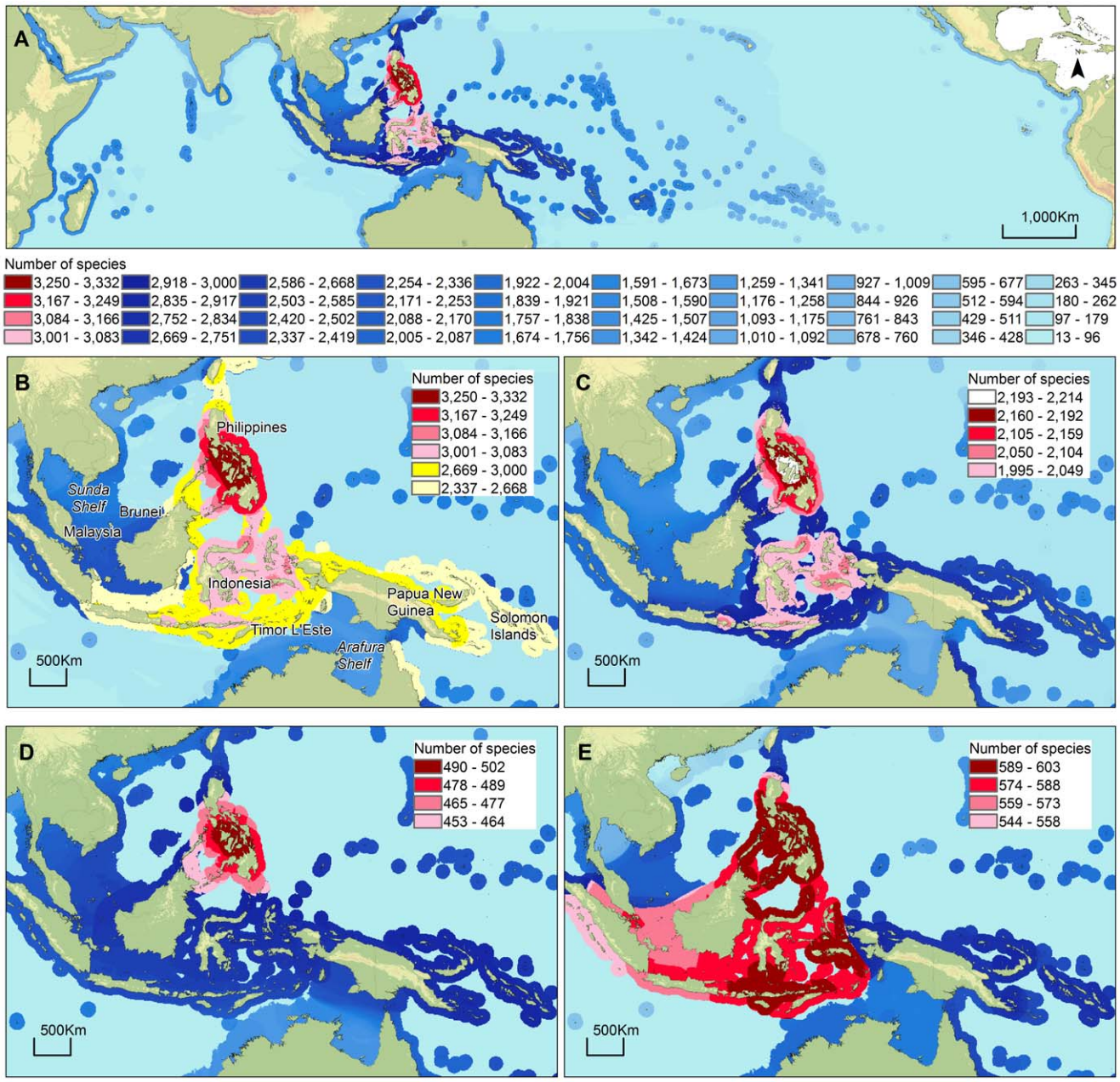


**Figure 1. Patterns of species richness from range overlap raster data from 10,446 species.** Each change in color represents an increase or decrease of 82 species (40 total classes or a 2.5% change per class). (A) Pattern of species distribution in the entire Indo-Pacific region. The top 10% for the highest species richness is found in the Coral Triangle (marked in red, pink, and yellow in panel B, with decreasing increments of species richness indicated by lighter shades), and the remaining decreasing increments of total species richness are indicated by lighter shades of blue, (B) The top 10% (shades of red), 20% (dark yellow) and 30% (light yellow) of concentration of species is in the Coral Triangle, with Philippines as the epicenter, (C) All fishes showing the top 1% of species richness (white); (D) Molluscs and crustaceans showing the top 10% of species richness (shades of red); (E) Habitat-forming species (corals, seagrasses, and mangroves) showing the top 10% of species richness (shades of red).
doi:10.1371/journal.pone.0056245.g001

seagrass beds, and mangrove swamps, in addition to available energy in the form of sea surface temperatures and net primary productivity.

It has long been established that there are latitudinal gradients in species richness with highest species richness in the tropics linked to multiple potential factors [61] although there are many exceptions to this gradient such as a subtropical peak in some oceanic tuna and shark species [57]. Explanations of this latitudinal gradient are that available kinetic energy [70] or patterns of primary productivity [66,71,72] influence rates of evolution. In the marine realm, sea surface temperature (SST) is most consistently linked to patterns of species richness on a global basis [57]. However, this pattern is weak within the tropics [71] and the energy hypothesis is specifically considered of insignificant predictive value for species richness in the tropical Indo-Pacific [53]. Indeed, in Rosen's (1988) [31] review of biogeography of reef corals that largely addressed the concentration of species in the Coral Triangle, none of the 13 hypotheses he considered invoked



VISIT THE SCIENTIFIC PUBLICATIONS REPORT ARCHIVE

an energy hypothesis. Frasier and Currie (1996) [48] went on to state "The most striking case that appears to contradict the species richness-energy hypothesis is that of coral reef organisms." However, in their test of this statement they concluded that the best predictor of species richness was mean annual ocean temperature [48], but they did not directly address the relationship of SST to the position of the Indo-Pacific Warm Pool. Alternative hypotheses to explain marine species richness patterns such as the predictive value of environmental stress and stability have also been tested but only available habitat and available energy have consistent significant predictive value for marine species richness [48,57]. In the present study, we reduced climate-related environmental effects influenced by latitudinal gradients by limiting the range of analysis to the tropics [66]. However, we retained average SST as a measure of available energy in our analyses because of its marked longitudinal variation in the Indo-Pacific as a result of the Indo-Pacific Warm Pool. Net primary productivity (NPP) was also retained as a predictor variable in our study as a possible factor related to the available energy hypothesis. Moreover, the nature, form, and structure of data quantifying taxonomic diversity and its ecological or evolutionary correlates change across scales [66]. Thus, we examined the effect on predictability of species richness relating to choice of scale, available energy, net primary productivity, available habitat, and habitat heterogeneity in the tropical Indo-Pacific.

## Methods

A number of different methods have been used to examine causes of the uneven distribution of marine species across the Indo-Pacific [1]. Recently, these include theoretical constructs based on existing studies [11,21,22,41]; area cladograms [7,73]; phylogenetic analyses and molecular clocks [25,42,60]; phylogeography (recently reviewed by Carpenter et al. 2011 [4]); and spatial analyses of distribution data [9,10,53,57,74–77]. Of those that used distribution data, Bellwood et al. (2005) [53] and Tittensor et al. (2010) [57] tested explicit alternative hypotheses and took into consideration autocorrelation, which violates one of the key assumptions in statistical analysis, that residuals are independent and identically distributed [78]. Bellwood et al. (2005) [53] tested hypotheses relating to the tropical Indo-Pacific but a large part of the data was based on a limited representation of reef fishes that shows an observed pattern of peak species richness very different from more complete studies [67]. The scope of the Tittensor et al. (2010) [57] study was global and used a large data set that includes cold-water species, and therefore, perhaps not a good test of patterns of species richness specifically for the tropical Indo-Pacific, although their fish distributions no doubt included a large proportion of tropical Indo-Pacific species.

### Spatial Range

The study range covers the entire Indian Ocean (including Red Sea and Persian Gulf) and the entire Pacific Ocean between 30°N and 30°S. All data layers were projected onto the World Cylindrical Equal Area coordinate system centered at 130° longitude.

### Grids and Grain Size

The study area was divided into equal grids of different horizontal resolutions (spatial grain) and the commonly-used Universal Transverse Mercator (UTM) grid to test the grid choice effects on relationships between predictors and species richness. Different orientations of centroid location were tested and found to have minimal effects (Text S1, Figures S1, S2, S3, S4, S5, and S6, Tables S1, S2) so therefore only the standard UTM centroid position results are presented here. The UTM is a grid-based system composed of 60 different zones globally. Although UTM grids are predisposed to distortion and area, the latitudinal range was limited to the tropics in this study, thereby limiting the effect of area distortion. Thus, each UTM grid measures about 617,000 $km^2$/grid cell, except for the grids located along upper and lower edges of the study area which cover less area. To compare the effect of area distortion, we used, five different equal area grids: small (23,000 $km^2$/grid cell), medium (92,000 $km^2$/grid cell), large (368,000 $km^2$/grid cell), extra large (1,470,000 $km^2$/grid cell), and largest (5,100,000 $km^2$/grid cell). The use of different grid sizes was not to test for the best possible grain but to test at which grain the predictors are likely to operate [79]. Some of the grids fall along the coastal areas and include land. This produces variable effective grid size in terms of available shallow water habitat and is a fundamental flaw with grids that has been dealt with in several ways, one of which is to combine adjacent grids [80–84]. Grid cells that contained nearly all land (these contained 85 to 99% of land) were removed from the analysis while others were combined with adjacent grid cells (about 6–10% in each grid size) to obtain water areas approximately equal to a single grid cell with 100% water (Figure S7; [82,85]).

### Species Distribution Range Maps

The aim of this study was to test for effects of available nearshore habitat on species diversity, and therefore, relates to pelagic, benthic, or demersal species found primarily over continental or island shelves. The total number of species maps produced in this study was 10,446 (Table S3) of which 8,295 were coastal fishes, 1,212 are invertebrates (crustaceans and molluscs), and 939 habitat-forming species comprising of 820 reef-building corals, 50 seagrasses, and 69 mangroves. The set or range maps for coastal fishes (fishes that regularly occur over continental shelf), reef-building corals, seagrasses, and mangroves was comprehensive for these groups with the exception of those few species whose taxonomic validity or occurrence data was questionable. Generalized distribution range maps for these species were obtained from numerous expert-derived sources (Text S2) rather than relying on online databases that potentially suffer from a large proportion of inaccuracies [86]. These generalized species distribution maps were based on expert-verified occurrence localities that are used to bound extent of occurrence, or range, polygons. As such, they were not expected to relate to alpha diversity at highly local scales that were also influenced by habitat specificity, localized limitations to dispersal, and many other factors. Species distribution shapefiles were produced from standardized basemaps using ArcView 3.3 (Environmental Systems Research Institute, Redlands, CA). Two different types of basemaps were used, one for visualization of patterns of species richness and one for analyses relating species richness to independent variables (Figure S8). This study focuses on nearshore species, and therefore, the approximate maximum limit of continental and island shelves of 200 m isobath [87] was used for each species in analyses. However, this 200 m isobath sometimes occurs close to shore and in these areas, visualization of biodiversity patterns was difficult on the scale of the Indo-Pacific. Therefore, a biodiversity visualization basemap was created that consisted of a 100 km shoreline buffer if the 200 m depth contour was less than 100 km from shore or a 200 m depth contour limit if this occurred more than 100 km from shore. However, for pelagic species that occur over continental or island shelves and far from shore, extent of occurrence included open ocean inter-shelf areas within the species range. For analyses of



VISIT THE SCIENTIFIC PUBLICATIONS REPORT ARCHIVE

species richness versus independent variables, each visualization basemap was cut to include only the area within the 200 m depth contour. All species distribution maps were converted into rasters of 10 km by 10 km cell size. The overlay raster tool in ArcGIS 9.3 (Environmental Systems Research Institute, Redlands, CA) was used to combine all the rasterized species distribution maps. This tool assigns a value for each cell that corresponds to the number of overlapping species ranges at the cell location, which was used to estimate species richness. The cell values of the combined rasterized maps were then classified into 40 classes of equal interval to show that each class corresponds to 2.5% of species composition.

## Habitat Availability and Heterogeneity

Using a Geographic Information System (GIS), we calculated the amount of continental shelf or shallow water area (SW) ($km^2$) from a 200 m bathymetry layer processed from ETOPO1 (National Geophysics Data Center) raster data [88]. Land areas were erased from marine habitat data layers using World Vector Shoreline data. This is a standard product of the U.S. Defense Mapping Agency and is a digital data file at a nominal scale of 1:250,000, containing the shorelines, international boundaries and country names of the world [89]. We also used the World Vector Shoreline data to generate the coastline length (km) by converting this to a line using conversion tools in ArcGIS 9.3. Coastline length (CL) was used here as a proxy for available nearshore habitat. To account for cases where grids contained no CL (offshore continental shelf area grid cells most common in small and medium size grids), 0.5 was added to all values of CL as a dummy variable.

We used coral reef, seagrass, and mangrove habitat GIS layers derived largely from atlases [90–92] provided by UNEP World Conservation Monitoring Centre to evaluate habitat heterogeneity. These map layers are high-resolution maps typically prepared from remotely-sensed data but in some cases mapped entirely from field observations. From these layers, we developed two indices – a habitat diversity index using area (HDIa) and a habitat diversity index using number of patches (HDIn). We calculated the habitat diversity indices using a modification of the Shannon-Weiner diversity index [93]. These indices essentially measure entropy and they will be highest when each habitat occupies the same amount of area in a grid cell. The HDIa was calculated from the values of the total area for each habitat including coral reefs (we assume that all hard bottom habitats in the tropics will have a varying degree of coral-reef biota associated with it), seagrass beds, mangrove forest, and soft-bottom areas for each grid. For HDIn, we substituted the measure of area with the number of patches of individual polygons of coral reefs, seagrasses, mangroves, and soft-bottom polygons within the 200 m bathymetry layers per grid cell. Coral reef, seagrass bed, and mangrove forest were composed of multiple independent polygons (i.e., patches) while the patches for soft-bottom 200 m bathymetry were a result of converting raster file (ETOPO1) into vector in ArcGIS 9.3. The number of patches of a particular habitat type may affect a variety of ecological process and often serves as an index of spatial heterogeneity [94]. The Shannon-Weiner Information Theory formula [93] was given as:

$$H = -\sum p_i \ln p_i$$

or

$$H = -\sum \left(\frac{n_i}{N}\right) \ln\left(\frac{n_i}{N}\right)$$

where $n_i$ = area (or number of patches) for each habitat and $N$ = total habitat area (or total number of patches).

## Sea Surface Temperature and Net Primary Productivity

The SST layer was developed from the monthly long-term SST data derived from the National Oceanic and Atmospheric Administration Optimum Interpolation dataset. This product was constructed from two intermediate climatologies to produce a 1° resolution dataset with a 1961–1990 base period [95]. The NPP layer was generated from the standard monthly products available in monthly files. These products used the Vertically Generalized Productivity Model [96] as the standard algorithm, which estimates the productivity using a temperature-dependent description of chlorophyll-specific efficiency. Monthly NPP rasters from 2002–2010 were downloaded and then geoprocessed to get the average value. Both SST and NPP raster layers were converted into point vector shapefiles, which captured the values to be used in overlaying with different grid sizes. In a few cases (28 out of 1,390 cells for the smallest grid size and 3 out of 570 cells for the medium grid size), SST values were not available for certain grid cells and an estimated value was obtained by averaging values from neighboring cells.

## Statistical Analysis

Range overlap maps and environmental layers were combined to form grid matrices with the corresponding values of species richness, habitat availability (i.e. shallow water area, coastal length), two habitat heterogeneity indices (i.e. calculated from area and number of patches of coral reefs, seagrass beds, mangrove forest, and soft-bottom), SST and NPP in each cell. Statistical analyses were performed to test the relationship between the environmental variables versus four different species richness subgroups: combined all species, all fish species, all habitat-forming species (corals, mangroves, and seagrasses), and all invertebrate species. We modeled the influences of habitat area and heterogeneity to each subgroup using both a generalized linear model (GLM) and a spatial linear model (SLM) to account for spatial autocorrelation [78]. If autocorrelation is present, then a non-spatial GLM is not correct and will give biased estimates. We performed GLM using maximum likelihood estimation. Species richness is often considered as a form of count data, and therefore, the response variable $y$ is fitted as a Poisson variable. Using the log of $y$ we fit the GLM as below:

$$y = \beta_o + \beta_1 * CL + \beta_2 * SW + \beta_3 * HDIa + \beta_4 * HDIn$$

where $\beta_o$, $\beta_1$, $\beta_2$, $\beta_3$, and $\beta_4$ are the parameter estimates. For SLM, we used maximum likelihood estimation of spatial simultaneous autoregressive error model in the form:

$$y = X\beta + \lambda W\mu + \varepsilon$$

where $\beta$ is the vector of coefficient for intercept and explanatory variable $X$; $\lambda$ is the spatial autoregression coefficient; $W$ is the spatial weights; $\mu$ is the spatially-dependent error term; and $\varepsilon$ is the error vector. Likewise, the Poisson response variable $y$ was also fitted as a log function.



VISIT THE SCIENTIFIC PUBLICATIONS REPORT ARCHIVE

We performed SLM with spatial distance weights derived from five nearest-neighbor cells. We used five and not eight nearest neighbors since most of the cells (especially in small grids) are isolated creating coastal and island effects. The presence of isolated cells will create a bias in spatial weight distance calculation. To normalize the data, all variables (dependent and independent) were log-transformed. Pearson correlation coefficients were generated for all between-variable comparisons. We tested individual habitat predictors versus each subgroup using single-predictor models. Then we used multiple-predictors model to test the effects of the combination of different habitats in each subgroup. The effects of multiple predictors were further explained by identifying the minimal-adequate model using backwards elimination method. Model fit was assessed using t-values (GLM) and z-values (SLM) for both single and multiple-predictor relationships. In GLM, adjusted $R^2$ values were used as a guide to model selection by evaluating the amount of variation explained. Since an equivalent $R^2$ does not exist in spatial analysis with a logistic regression, we used pseudo-$R^2$ [97] to evaluate the goodness-of-fit in SLM models. We calculated Akaike Information Criterion (AIC) to measure information content of models. Spatial autocorrelation was tested on model residuals using Moran's $I$ [98]. GLM analyses were performed using the open-source language R (R Core Development Team). SLM analyses were performed using the spdep package [99] in R statistical software.

## Results

### Species Richness

Species richness across the Indo-Pacific showed the expected pattern of highest richness in the Coral Triangle (Figure 1A). The central Philippines had the highest 2.5% of species richness, and the highest 10% was found in most of the Philippines and eastern Indonesia (Figure 1B). About 34% of all species in this study occurred in the north and central part of the Coral Triangle. The highest 30% of species richness radiated from this epicenter north to southern Japan, south to south-central Indonesia and the northeast tip of Australia, west to southern Sumatra and east to the easternmost Solomon Islands and species richness continued to diminish with distance from this epicenter (Figure 1A, 1B). Separate analysis for shore fishes, molluscs and crustaceans, and the habitat-forming primary producer species (corals, mangroves, and seagrasses) each showed a similar peak of species richness in the Coral Triangle (Figure 1C–E). The pattern of species richness of shore fishes (Figure 1C) was most similar to the combined analysis (Figure 1B), since fish species constituted the bulk of the species in the analysis, with a peak in the central Philippines. Molluscs and crustaceans appeared more concentrated in the northern part of the Coral Triangle (mostly around the Philippines) than shore fishes (Figure 1C, 1D). The highest 10% of species richness of corals, mangroves, and seagrasses was widely distributed throughout the Coral Triangle, with the highest 2.5% in the northern and central part (Figure 1E). The areas of least species richness in the combined analysis were in the eastern Pacific and along parts of the northern coasts of the Indian Ocean (Figure 1A). The low species richness in the open ocean represented the pelagic species found in coastal waters and was not representative of the total biodiversity of the open ocean.

### Habitat Availability and Heterogeneity

Greatest shallow water area (SW) and longest coastline (CL) per unit area (Figure 2A–F, 3A) were mostly concentrated in the Coral Triangle; however, these two habitat predictors were not evenly distributed within the Coral Triangle (Figures 2, 3A and Figure S9). As expected, the greatest concentration of shallow water area was over the Sunda and Arafura shelves, which are the two largest tropical shelf habitats in the world in terms of total area (Figure 2). These two large tropical shelf areas were reflected in all grid sizes (Figure 2A–E) except the largest grain size that shows a more diffuse concentration of shallow water around the Arafura Shelf (Figure 2F). The cells with the longest coastline mostly complemented rather than coincided with the large shallow water areas of the Sunda and Arafura shelves (Figures 2, 3A and Figure S9) in the Coral Triangle. The location of high coastline concentration generally was found in the Philippines and eastern Indonesia (Figures 3A and Figure S9), but with peaks outside the Coral Triangle at some grain sizes (Figure S9A–C). A peak in coastline length was located in the central Philippines at the UTM grain size (Figure 3A). The cells with the highest values of heterogeneity indices were prevalent in different locations dependent on the type of index used. The cells with high HDIa index values were concentrated mostly around oceanic island areas such as the central Pacific Ocean (Figure 3 and Figure S10). HDIn values were highest at widespread locations across the Indo-Pacific with generally high values found in the Coral Triangle and in areas north and east of the Coral Triangle that had the highest 30% of species richness in the Indo-Pacific (Figures 1B, 3 and Figure S11).

### SST and NPP

Average SST values were highest (over approximately 29°C) around and east of the Solomon Islands and northern Australia and were also high (over approximately 28°C) in eastern central Indonesia, western Sumatra and northwestern Madagascar (Figure 3D and Figure S12). Species richness correlated significantly with latitude ($r = 0.440$, $p<0.001$ for smallest grid size; $r = 0.486$, $p<0.001$ for UTM grid sizes) with peaks in species richness to the north of peaks in SST (Figure 4A, 4B). The longitudinal peak in SST of the Indo-Pacific Warm Pool corresponded closely with the eastern range of the peak in species richness (highest 10% to 30% of species richness; Figure 3B) and these two variables were significantly correlated longitudinally ($r = 0.317$, $p<0.001$ at smallest grid size; $r = 0.377$, $p<0.001$ at UTM grid size), although they did not closely co-vary elsewhere throughout their longitudinal range (Figure 4C, 4D). NPP values were highest in western South America, eastern China, between Australia and New Guinea, southern Borneo, and between Oman and India (Figure 3E and Figure S13).

### Predictors of Species Richness

Predictor variables were consistently highly correlated with one another at all scales, with some notable exceptions (Table 1). SW and CL had strong positive correlations with each other, with HDIn, and with NPP. SW had significant negative correlations with HDIa (except at the largest grid size) and CL was variably correlated with HDIa. SW and CL were insignificantly or negatively correlated with SST. NPP was most consistently negatively correlated with HDIa, insignificantly correlated with HDIn, and negatively or insignificantly correlated with SST except a moderate significant positive correlation at the medium grid size.

Species richness of all taxonomic sets was significantly correlated with most environmental variables at all scales in single predictor GLM and SLM with the exception of insignificant correlations with SST at the smallest grid sizes, insignificant correlations with NPP at nearly all grid sizes, and HDIa and some other variables at the larger grain sizes (Table 2). CL most consistently explained the highest amount of variation with respect to species richness in both single predictor GLM and SLM except



VISIT THE SCIENTIFIC PUBLICATIONS REPORT ARCHIVE

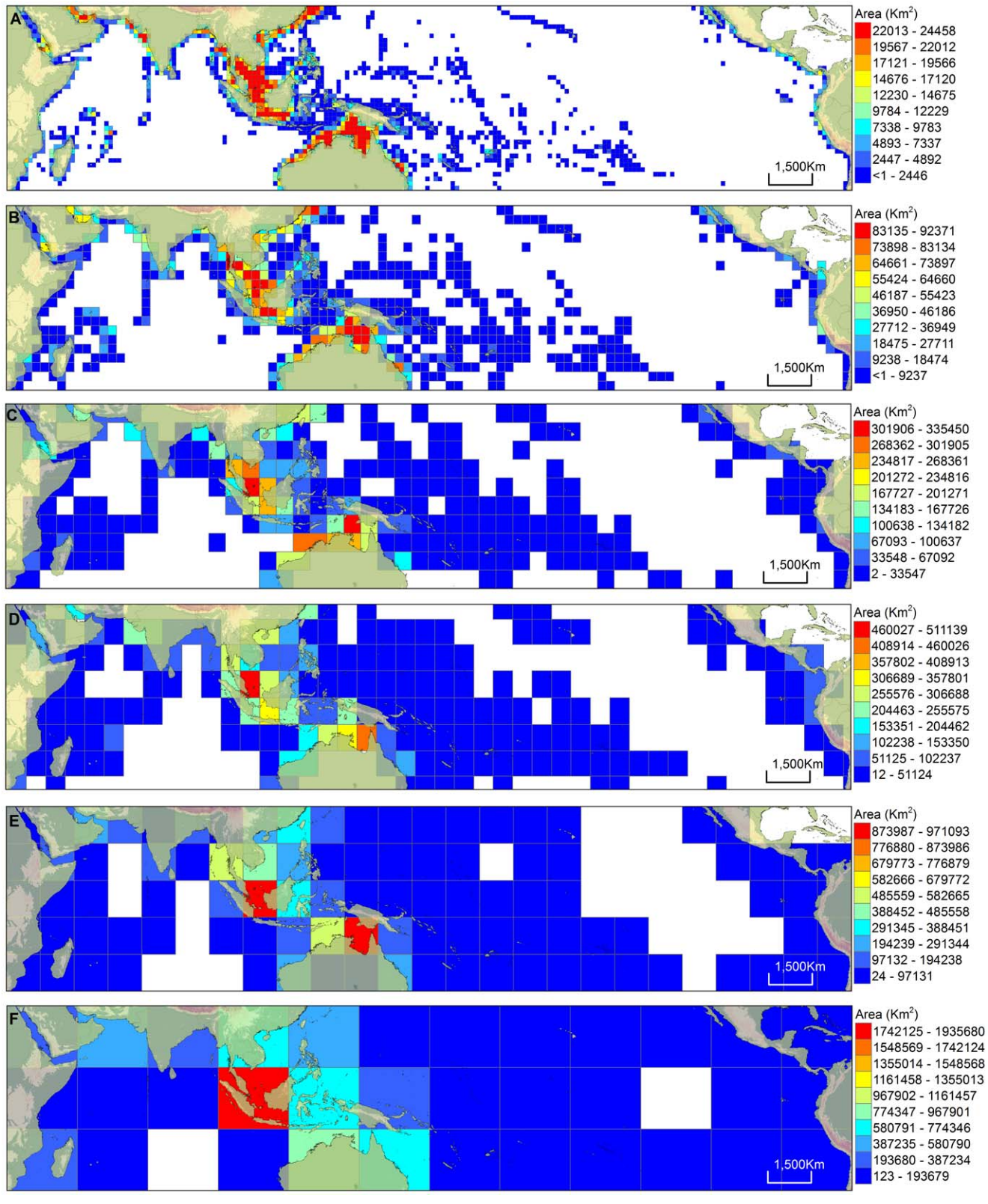


**Figure 2. Distribution pattern of shallow water area extent in the Indo-Pacific at different grid scales.** The grids were classified into 10 equal interval classes based on the amount of shallow water area recorded in each cell such that cells in red have the largest amount of shallow water area, and cells in blue have the lowest amount of shallow water area. Cells with zero values are not displayed. (A) Small grid, (B) Medium grid, (C) Large grid, (d) UTM grid, (E) Extra large grid, (F) Largest grid.
doi:10.1371/journal.pone.0056245.g002



VISIT THE SCIENTIFIC PUBLICATIONS REPORT ARCHIVE

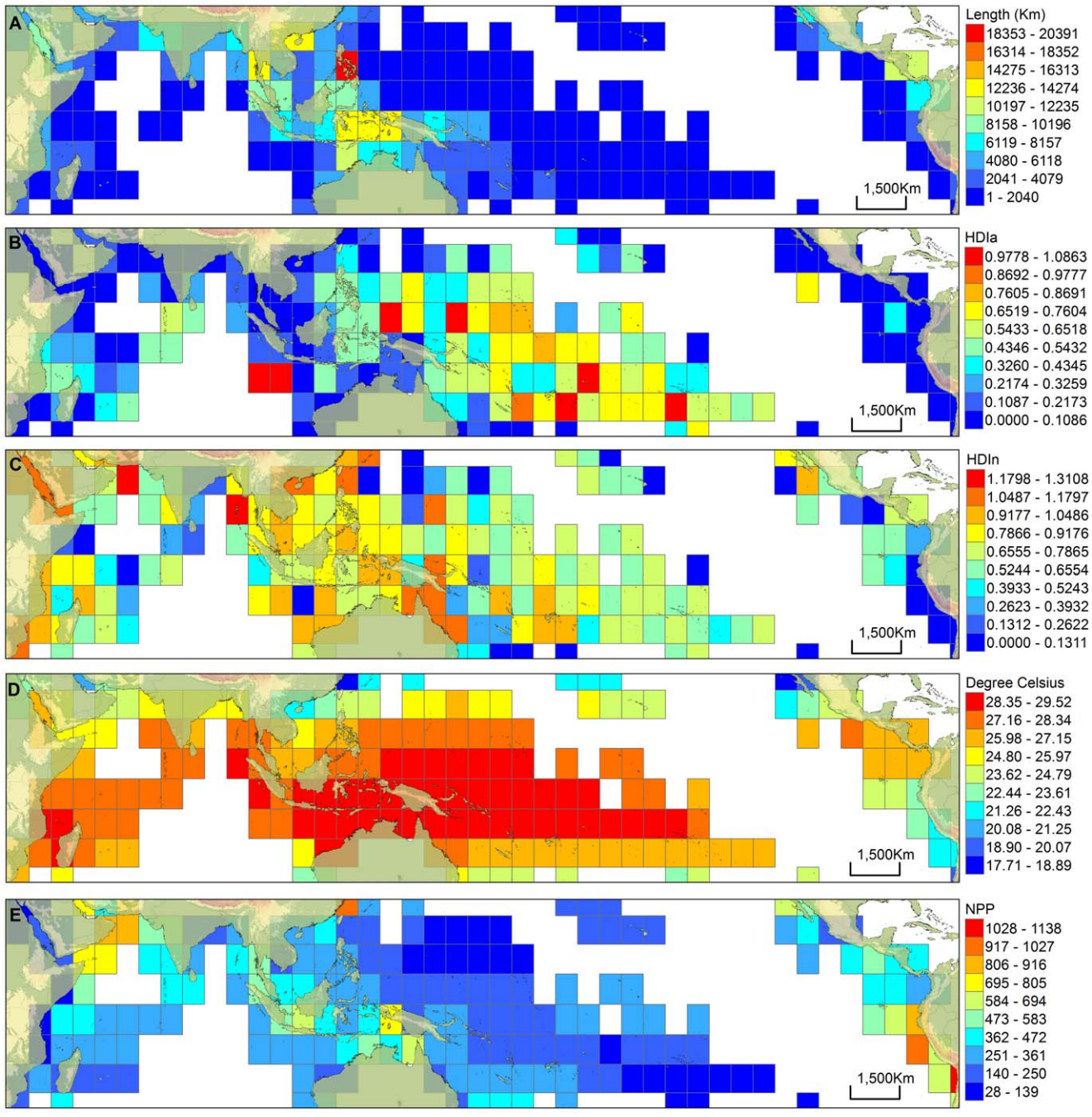


**Figure 3. Distribution pattern of the different parameters in the Indo-Pacific using UTM grid.** The grids were classified (equal interval) into 10 classes based on the amount of shallow water area recorded in each cell such that cells in red have the largest parameter value, and cells in blue have the lowest parameter value. Cells with zero values are not displayed. (A) Extent of coastline (km), (B) Habitat heterogeneity index using area (HDIa), (C) Habitat heterogeneity index using number (HDIn), (D) Sea surface temperature (SST), (E) Net primary productivity (NPP).
doi:10.1371/journal.pone.0056245.g003

SW explained most variation at the smallest grain size, and HDIn was prominent at larger grain sizes for invertebrates and habitat-forming species (Table S4).

Multiple regression results were similar to single predictor results in that many environmental variables were significant and retained in models (Table 3). GLM and SLM results for different taxonomic sets at different grain sizes were also similar in retaining specific environmental variables in models with the notable exception that HDIn, SST, and NPP variables mostly excluded from models at the two smallest grain sizes in the SLM. Moran's $I$ indicated significant autocorrelation at all grains sizes except the largest grain size. As expected with increasing grains size and decreasing sample sizes, $R^2$ and pseudo-$R^2$ increased (less variation to explain) and AIC values decreased with larger grain sizes (less entropy to account for). However, when comparing equal grain sizes between GLM and SLM the correction for significant autocorrelation always improved the model (higher pseudo-$R^2$ versus $R^2$ and lower AIC). CL was consistently retained in all SLM



VISIT THE SCIENTIFIC PUBLICATIONS REPORT ARCHIVE

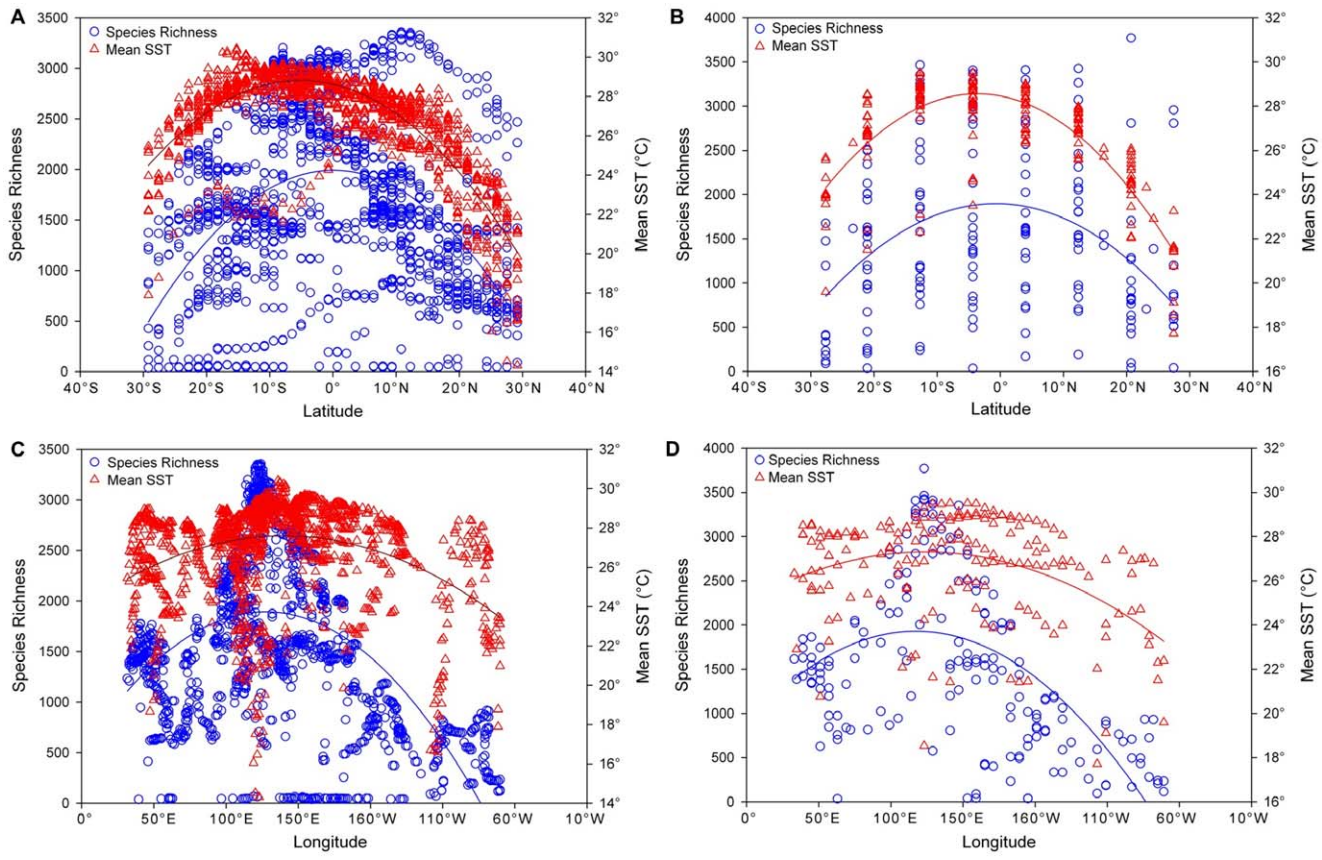


**Figure 4. Species richness and mean SST versus latitude or longitude at different grid scales.** (A) Latitude at small grid, (B) Latitude at UTM grid, (C) Longitude at small grid, (D) Longitude at UTM grid. Latitudinal peaks of species richness (blue circle) are shown along the 10–20° north and latitudinal peaks in mean SST values (°C) (red triangle) are along the 10–20° south. Longitudinal peaks of species richness (blue circle) are located in the 120° east while longitudinal peaks in mean SST values (°C) (red triangle) are found along the 130–150° east.
doi:10.1371/journal.pone.0056245.g004

for all taxonomic sets at all grain sizes except in the largest grain size. In SLM across all taxa most consistently retained were SW at smallest and largest grain sizes, HDIa at smallest grain size and variably in large grain sizes, HDIn and SST mostly at all grain sizes except small and medium, and NPP negatively correlated and variably retained at larger grain sizes.

## Discussion and Conclusions

Range overlap (Figure 1A) of 10,446 expert-based generalized distributions of fishes, invertebrates (molluscs and crustaceans), and habitat-forming species (corals, seagrasses, and mangroves) recovered the classic pattern of decreasing species richness with distance from the Coral Triangle [1]. The highest concentration of species richness within the Coral Triangle, i.e., in the Philippines and eastern Indonesia, was similar to what has been proposed by Veron et al. (2009) [3] based on corals. However, the peak in biodiversity in this region comprises more than corals and coral reefs. Other important habitat-forming biota such as seagrasses and mangroves peak in species richness in this region (Figure 1E) and also substantially support many species [100–101] and form complex ecosystems in conjunction with coral reefs [102]. Therefore, in addition to the Philippines, eastern Sabah, eastern Indonesia, Timor L'Este, New Guinea, and Solomon Island delineation [3], we recommend that western Indonesia, western Sabah, Brunei, Singapore, and peninsular Malaysia should also be considered as part of the Coral Triangle (red and pink areas in Figure 1E).

The pattern of species richness in this study (Figure 1A) is dominated by the preponderance of shore fishes, so generalizations from our results are strongest for shore fishes because the data are nearly complete for this group. However, the pattern of species richness in the more limited subset of macroinvertebrates (Figure 1D) is consistent with what is observed in shore fishes (Figure 1C). The peak in diversity of invertebrates is more concentrated in the northern apex of the Coral Triangle than shore fishes. A part of this may be due to a higher density of sampling effort for invertebrates in the compared to elsewhere in the Coral Triangle [74]. The tighter pattern of peak range overlap may also be related to the differences in mobility between the two groups. Most fishes and invertebrates have pelagic larval stages with durations that may or may not be related to range size [103] but fishes are typically more mobile as adults than macroinvertebrates, which include many fixed or slow-moving benthic species as adults. The nearly complete set of expert-based range maps for the coastal fishes, the corroboration of peaks in species richness among different taxonomic sets (Figure 1), and the radiating pattern from the epicenter (Figure 1B) strongly supports an epicenter of species richness within the Coral Triangle (Figure 1A). The often-posed question of what factors contribute to the epicenter of marine species richness of the Coral Triangle, therefore, can be focused toward identification of predictors of



VISIT THE SCIENTIFIC PUBLICATIONS REPORT ARCHIVE

**Table 1.** Pearson correlation coefficients between all predictor variables within the same grid size.

| | SW | CL | HDIa | HDIn | SST |
|---|---|---|---|---|---|
| **CL Small Grid** | 0.382*** | 1 | | | |
| **CL Medium Grid** | 0.665*** | 1 | | | |
| **CL Large Grid** | 0.794*** | 1 | | | |
| **CL UTM Grid** | 0.794*** | 1 | | | |
| **CL X Large Grid** | 0.823*** | 1 | | | |
| **CL Largest Grid** | 0.909*** | 1 | | | |
| **HDIa Small Grid** | −0.365*** | 0.164*** | 1 | | |
| **HDIa Medium Grid** | −0.241*** | 0.130** | 1 | | |
| **HDIa Large Grid** | −0.426*** | −0.135* | 1 | | |
| **HDIa UTM Grid** | −0.357** | −0.102 ns | 1 | | |
| **HDIa X Large Grid** | −0.392*** | −0.081 ns | 1 | | |
| **HDIa Largest Grid** | 0.217 ns | 0.218 ns | 1 | | |
| **HDIn Small Grid** | 0.046 ns | 0.456*** | 0.488*** | 1 | |
| **HDIn Medium Grid** | 0.247*** | 0.445*** | 0.447*** | 1 | |
| **HDIn Large Grid** | 0.292*** | 0.366*** | 0.281*** | 1 | |
| **HDIn UTM Grid** | 0.377*** | 0.449*** | 0.301*** | 1 | |
| **HDIn X Large Grid** | 0.358*** | 0.399*** | 0.263* | 1 | |
| **HDIn Largest Grid** | 0.578*** | 0.584*** | 0.457** | 1 | |
| **SST Small Grid** | −0.086** | −0.116*** | 0.129*** | 0.015 ns | 1 |
| **SST Medium Grid** | −0.033 ns | −0.026 ns | 0.154*** | 0.096* | 1 |
| **SST Large Grid** | −0.087 ns | −0.060 ns | 0.395*** | 0.234*** | 1 |
| **SST UTM Grid** | 0.005 ns | 0.068 ns | 0.464*** | 0.233** | 1 |
| **SST X Large Grid** | 0.106 ns | 0.221* | 0.402*** | 0.357*** | 1 |
| **SST Largest Grid** | 0.279 ns | 0.294 ns | 0.246 ns | 0.429* | 1 |
| **NPP Small Grid** | 0.522*** | 0.107*** | −0.426*** | −0.121*** | 0.003 ns |
| **NPP Medium Grid** | 0.511*** | 0.269*** | −0.364*** | 0.011 ns | 0.142** |
| **NPP Large Grid** | 0.468*** | 0.337*** | −0.415*** | −0.033 ns | −0.211** |
| **NPP UTM Grid** | 0.400*** | 0.254** | −0.437*** | −0.075 ns | −0.257** |
| **NPP X Large Grid** | 0.647*** | 0.545*** | 0.581*** | 0.001 ns | −0.213* |
| **NPP Largest Grid** | 0.563** | 0.625*** | −0.109 ns | 0.140 ns | −0.007 ns |

The predictors are shallow water area (SW), coastline length (CL), habitat diversity based on area (HDIa), habitat diversity based on number of patches (HDIn), sea surface temperature (SST), and net primary productivity (NPP). Asterisks indicate significance value of P:
*(<0.05),
**(<0.01);
***(<0.001); ns (not significant).
Grid sizes are as follows: Small = 23,000 $km^2$; Medium = 92,000 $km^2$; Large = 368,000 $km^2$; UTM = 617,000 $km^2$; Extra large = 1,470,000 $km^2$; Largest = 5,100,000 $km^2$.
doi:10.1371/journal.pone.0056245.t001

species richness in the northern apex and central region of the Coral Triangle.

The high correlation among our predictor variables (Table 1) and the very high frequency of single predictor significant models (Table 2) makes it challenging to identify any one predictor of species richness. Fortunately, NPP is significant in single predictor models, but is infrequently retained in multiple predictor models (Table 3) and when retained, mostly negative. NPP is highly correlated with SW and CL because of elevated productivity in shallow sunlit coastal areas. NPP is highly negatively correlated with HDIa because habitat complexity is high around oceanic islands where NPP is low. SST and NPP are not highly correlated as the Indo-Pacific Warm Pool is largely oligotrophic [30]. The reduced importance of NPP as a factor in species richness is similar to what was observed on a global scale [57]. The negatively significant retention of NPP in multiple predictor models may be because higher NPP is typically associated with more turbid coastal waters or cooler upwelling waters, both of which are inconsistent with nutrient limited, highly diverse coral reef ecosystems. Therefore, the idea that more available energy promotes more species because of reduced partitioning of available food resources [48] is not supported in our models. SST also gives a clear signal in that it is insignificantly or negatively correlated with SW and CL and significantly correlated with HDIa also because of the oceanic coverage of the Indo-Pacific Warm Pool. However, the retention of SST and the habitat availability predictors in multiple-predictor models (Table 3) is variable and often depends on scale and autocorrelation.

The choice of best predictors for species richness (Table 3) is influenced by resolution, scale, and autocorrelation. The correction for autocorrelation and for that matter, the use of regression models in spatial analyses of species richness is somewhat



VISIT THE SCIENTIFIC PUBLICATIONS REPORT ARCHIVE

**Table 2.** Significant single-predictor Generalized Linear Model (GLM) and Spatial Linear Model (SLM) for species richness.

| Subgroups | Grid Size | Single Predictor Generalized Linear Model | | | | | | Single Predictor Spatial Linear Model | | | | | |
|---|---|---|---|---|---|---|---|---|---|---|---|---|---|
| | | SW | CL | HDIa | HDIn | SST | NPP | SW | CL | HDIa | HDIn | SST | NPP |
| **All Species** | Small | *** | *** | *** | *** | ns | *** | *** | *** | *** | *** | ns | * |
| | Medium | *** | *** | *** | *** | * | * | *** | *** | *** | *** | ns | ns |
| | Large | *** | *** | ** | *** | *** | ns | *** | *** | *** | *** | *** | ns |
| | UTM | *** | *** | ** | *** | *** | ns | *** | *** | * | *** | *** | ns |
| | X Large | *** | *** | ** | *** | *** | ns | *** | *** | ns | *** | ** | ns |
| | Largest | *** | *** | ** | *** | *** | ns | *** | *** | ns | ** | * | ns |
| **All Fish Species** | Small | *** | *** | *** | *** | ns | *** | *** | *** | *** | *** | ns | * |
| | Medium | *** | *** | ** | *** | ns | ** | *** | *** | ** | *** | ns | ns |
| | Large | *** | *** | ns | *** | *** | ** | *** | *** | *** | *** | *** | ns |
| | UTM | *** | *** | * | *** | *** | ns | *** | *** | ** | *** | *** | ns |
| | X Large | *** | *** | ns | *** | *** | ns | *** | *** | ns | *** | ** | ns |
| | Largest | *** | *** | * | *** | *** | ns | *** | *** | ns | *** | * | ns |
| **All invertebrates** | Small | *** | *** | *** | *** | ns | ns | *** | *** | *** | *** | ns | ns |
| | Medium | *** | *** | *** | *** | ns | ns | *** | *** | *** | *** | ns | ns |
| | Large | *** | *** | *** | *** | *** | ns | *** | *** | *** | *** | ** | ns |
| | UTM | *** | *** | *** | *** | *** | ns | *** | *** | ** | *** | *** | ns |
| | X Large | *** | *** | *** | *** | *** | ns | * | ** | * | *** | * | ns |
| | Largest | *** | * | * | *** | *** | ns | ns | ns | ns | ** | *** | ns |
| **All habitat-forming species** | Small | *** | *** | *** | *** | ** | ns | *** | *** | *** | *** | ns | ns |
| | Medium | *** | *** | *** | *** | ** | ns | *** | *** | ** | *** | ns | ns |
| | Large | *** | *** | *** | *** | *** | ns | *** | *** | *** | *** | *** | ns |
| | UTM | *** | *** | *** | *** | *** | ns | *** | *** | ** | *** | *** | ns |
| | X Large | *** | *** | *** | *** | *** | ns | ** | *** | ns | ** | *** | ns |
| | Largest | ** | * | * | *** | *** | ns | ns | ns | ns | * | *** | ns |

Actual $R^2$ and pseudo-$R^2$ values can be found in Table S4. The predictors are shallow water area (SW), coastline length (CL), habitat diversity based on area (HDIa), habitat diversity based on number of patches (HDIn), sea surface temperature (SST), and net primary productivity (NPP). Asterisks indicate significance value of P:
*(<0.05),
**(<0.01);
***(<0.001); ns (not significant).
Grid sizes are as follows: Small = 23,000 km$^2$; Medium = 92,000 km$^2$; Large = 368,000 km$^2$; UTM = 617,000 km$^2$; Extra large = 1,470,000 km$^2$; Largest = 5,100,000 km$^2$. The significance value with the highest adjusted $R^2$ and pseudo-$R^2$ is highlighted in boldface.
doi:10.1371/journal.pone.0056245.t002

controversial [104,105]. Moran's $I$ test shows significant effects of autocorrelation in our data (Table 3) similar to what was observed by Bellwood et al. (2005) [53] and Tittensor et al. (2010) [57]. The rank of predictor variables without correction for autocorrelation was similar to the rank with correction except that fewer predictors were retained in SLM. However, it is clear that correction of autocorrelation in SLM (Table 3) consistently resulted in more variation explained (higher pseudo-$R^2$ than $R^2$) and more entropy removed from the model (lower AIC). When comparing models based on the same grid size, correction for autocorrelation resulted in a lower AIC, and therefore, SLM is the preferred model [106,107] in all cases for all species groups except for the largest grain where tests for autocorrelations were insignificant or not highly significant (Table 3). Therefore, the SLM model is preferred in all cases except the largest grid size for all species and habitat-forming species taxonomic subsets, where GLM is preferred.

The choice of an optimal grid or grain size is not straightforward because model choice using different data sets (e.g., with different sample sizes) is not statistically defensible [106], cf. [57]. As expected, $R^2$ values increase with increasing grid size over the same area since there is less variation to explain with smaller sample sizes (Table 3). Similarly, AIC values decrease with larger grid sizes because there is less entropy to account for in smaller sample sizes. In fact, there may not be an optimal grain size in analyses that attempt to explain spatial variation in species richness [79]. The choice of grid size will ultimately depend on practical and ecological considerations such as the presence or absence of a predictor variable at different grain sizes. For example, a value for coastline length may not be found in a grid over a continental shelf at small grain sizes. Therefore, optimal grid size will mostly depend on the predictor variables chosen to explain variation in species richness.

Habitat availability predictor variables (SW, CL, HDIa, HDIn) and the available kinetic energy predictor variable (SST) are consistently retained as positive significant predicator variables across species groups and grid sizes, accounting for autocorrelation (Table 3). Coastline length (CL) is most consistently retained for all grid sizes except the largest grid size and CL most consistently explained the highest amount of variation in species richness in single predictor spatial models (Table 2). Our identification of CL as a powerful proxy for habitat availability is consistent with the



VISIT THE SCIENTIFIC PUBLICATIONS REPORT ARCHIVE

**Table 3.** Minimal adequate multiple-predictor Generalized Linear Model (GLM) and Spatial Linear Model (SLM) results for all grid sizes.

| Models | Grid Size | SW | CL | HDIa | HDIn | SST | NPP | Moran's I | $R^2$/p-$R^2$ | AIC |
|---|---|---|---|---|---|---|---|---|---|---|
| **GLM (t-values) for all species** | Small | 11.138*** | 7.520*** | 4.888*** | 2.570* | 2.262* | | 0.4468*** | 0.236 | 3719.64 |
| | Medium | 4.551*** | 8.167*** | | 3.552*** | 3.281** | −3.654*** | 0.2847*** | 0.369 | 1354.75 |
| | Large | 3.416*** | 4.509*** | 3.667*** | 3.160** | 5.077*** | | 0.1914*** | 0.573 | 411.74 |
| | UTM | | 10.087*** | | 3.456*** | 7.440*** | | 0.2314*** | 0.604 | 328.53 |
| | X Large | | 10.089*** | | 6.240*** | 4.686*** | −3.552*** | 0.1888*** | 0.804 | 100.27 |
| | Largest | 6.864*** | | | 2.918** | 4.005*** | −4.084*** | −0.0443 ns | 0.871 | **23.17** |
| **SLM (z-values) for all species** | Small | 8.192*** | 4.267*** | 2.839** | | | | −0.0110 | 0.508 | **3109.00** |
| | Medium | 3.643*** | 6.932*** | | | | | −0.0140 | 0.486 | **1238.30** |
| | Large | | 10.873*** | 2.490* | 2.218* | 4.885*** | | −0.0214 | 0.618 | **392.04** |
| | UTM | | 9.885*** | | 2.346* | 5.421*** | | −0.0161 | 0.656 | **308.67** |
| | X Large | | 10.640*** | | 4.567*** | 3.282** | −2.243* | −0.0119 | 0.837 | **88.74** |
| | Largest | 9.699*** | | | 3.642*** | 3.727*** | −7.754*** | 0.0383 | 0.878 | 23.22 |
| **GLM (t-values) for all fish species** | Small | 11.621*** | 8.375*** | 4.869*** | 2.481* | | | 0.4488*** | 0.257 | 3384.89 |
| | Medium | 5.291*** | 8.708*** | | 3.380*** | 3.027** | −3.220** | 0.2740*** | 0.407 | 1209.05 |
| | Large | 3.503*** | 5.351*** | 2.712** | 3.304** | 5.009*** | | 0.2085*** | 0.606 | 348.05 |
| | UTM | | 12.679*** | | 3.411*** | 7.009*** | | 0.1890*** | 0.664 | 275.83 |
| | X Large | 3.279** | 7.003*** | | 5.858*** | 4.960*** | −3.572*** | 0.1096* | 0.847 | 51.58 |
| | Largest | 7.520*** | | | 2.863** | 3.318** | −3.647** | −0.1213 ns | 0.859 | 19.12 |
| **SLM (z-values) for all fish species** | Small | 8.817*** | 4.228*** | 2.649** | | | | −0.0072 | 0.529 | **2756.30** |
| | Medium | 4.539*** | 6.860*** | | | | | −0.0159 | 0.510 | **1101.30** |
| | Large | 2.023* | 5.439*** | 2.363* | 2.310* | 4.868*** | | −0.0121 | 0.657 | **324.40** |
| | UTM | | 11.934*** | | 2.585** | 5.466*** | | −0.0110 | 0.696 | **262.84** |
| | X Large | | 11.697*** | | 4.915*** | 3.769*** | | −0.0150 | 0.861 | **45.58** |
| | Largest | 12.855*** | | | 3.973*** | 2.558* | −9.571*** | 0.0246 | 0.901 | **13.35** |
| **GLM (t-values) for invertebrates** | Small | 8.797*** | 6.980*** | 5.662*** | | 2.093* | −2.028* | 0.4593*** | 0.160 | 4935.93 |
| | Medium | | 10.655*** | | 2.768** | 1.990* | −3.136** | 0.2608*** | 0.250 | 2011.48 |
| | Large | 7.800*** | | 4.381*** | 3.191** | 2.786** | | 0.2284*** | 0.414 | 690.23 |
| | UTM | | 4.746*** | | 3.155** | 6.161*** | | 0.2481*** | 0.390 | 522.40 |
| | X Large | | 5.304*** | 1.995* | 5.186*** | 2.574* | −2.498* | 0.3689*** | 0.657 | 227.71 |
| | Largest | 3.060** | | | 3.270** | 3.391** | −4.541*** | 0.2722** | 0.743 | 60.89 |
| **SLM (z-values) for invertebrates** | Small | 6.527*** | 4.116*** | 2.825** | | | | −0.0153 | 0.450 | **4347.70** |
| | Medium | | 10.755*** | | | | | −0.0166 | 0.358 | **1922.20** |
| | Large | | 9.430*** | 4.765*** | | 2.787** | | −0.0249 | 0.485 | **665.64** |
| | UTM | | 7.003*** | | | 4.218*** | | −0.0242 | 0.480 | **497.54** |
| | X Large | −3.918*** | 8.575*** | | 3.910*** | | | −0.0310 | 0.814 | **172.55** |
| | Largest | | | | 3.110** | 3.883*** | | −0.0008 | 0.885 | **35.79** |
| **GLM (t-values) for habitat-forming species** | Small | 11.103*** | 4.753*** | 4.130*** | 4.727*** | 4.027*** | −3.908*** | 0.5059*** | 0.219 | 5342.45 |
| | Medium | 4.682*** | 6.195*** | | 4.724*** | 4.316*** | −5.316*** | 0.2778*** | 0.328 | 2121.49 |
| | Large | 3.206** | 2.475* | 4.325*** | 3.565*** | 5.298*** | | 0.1602*** | 0.505 | 762.75 |
| | UTM | 6.337*** | | 1.988* | 3.925*** | 7.047*** | | 0.2102*** | 0.562 | 548.46 |
| | X Large | | 5.071*** | | 5.419*** | 5.113*** | −2.889** | 0.3229*** | 0.677 | 264.06 |
| | Largest | | | | 4.476*** | 5.266*** | | 0.0716 ns | 0.711 | **81.14** |
| **SLM (z-values) for habitat-forming species** | Small | 7.648*** | 3.840*** | 2.807** | | | | −0.0203 | 0.559 | **4548.50** |
| | Medium | 3.552*** | 5.311*** | | 2.015* | | −2.026* | −0.0100 | 0.456 | **2006.30** |



VISIT THE SCIENTIFIC PUBLICATIONS REPORT ARCHIVE

**Table 3.** Cont.

| Models | Grid Size | SW | CL | HDIa | HDIn | SST | NPP | Moran's I | $R^2$/p-$R^2$ | AIC |
|---|---|---|---|---|---|---|---|---|---|---|
| | Large | 9.606*** | 4.202*** | | | 4.367*** | | −0.0220 | 0.545 | **746.99** |
| | UTM | | 6.710*** | | 3.300*** | 4.983*** | | −0.0236 | 0.628 | **524.21** |
| | X Large | | 5.761*** | | 2.663** | 3.724*** | −2.517* | −0.0211 | 0.787 | **230.56** |
| | Largest | 2.496* | | | 3.510*** | 5.445*** | −2.800** | 0.0040 | 0.770 | 81.54 |

The predictors are shallow water area (SW), coastline length (CL), habitat diversity based on area (HDIa), habitat diversity based on number of patches (HDIn), sea surface temperature (SST), and net primary productivity (NPP). Values under predictor variables are t-values for GLM and z-values for SLM. Asterisks indicate significance value of P:
*(<0.05),
**(<0.01);
***(<0.001); ns (not significant). Grid sizes are as follows: Small = 23,000 km$^2$; Medium = 92,000 km$^2$; Large = 368,000 km$^2$; UTM = 617,000 km$^2$; Extra large = 1,470,000 km$^2$; Largest = 5,100,000 km$^2$. $R^2$ values are for GLM results, while pseudo-$R^2$ (p-$R^2$) values are for SLM results. The lower AIC values between SLM and GLM of the same grid size per group are highlighted in boldface. Lower AIC values suggest that SLM models are preferred in most cases than its GLM counterparts.
doi:10.1371/journal.pone.0056245.t003

results of Etnoyer (2001) [36] and Tittensor et al. (2010) [57]. However, CL does not capture all aspects of habitat availability (or some other factor) because at least one other habitat availability variable is retained in SLM at all grid sizes that CL is retained. This suggests that both habitat area and habitat complexity components may be needed to best test the 'area of refuge' hypothesis [32] for the Coral Triangle epicenter of species richness. Our results may help to guide selection of habitat availability variables that can predict variation in marine species richness at different grid sizes, since different habitat predictors operate at different spatial grains [79]. For example, in the shore fishes, shallow water area and heterogeneity (HDIa) should be considered at grain sizes equivalent to our small and medium grid sizes. At the large equivalent grain size all habitat availability variables should be considered. For UTM and grain sizes around 5 million km$^2$ a habitat heterogeneity index similar to HDIn may suffice in addition to CL as a proxy for habitat availability. Differences in how the different habitat complexity indices behave in models are a result of the form of complexity they emphasize. Our HDIa index is based on the relative proportion of area for our different habitat types (soft bottom, coral reef, seagrass, and mangrove) in a grid. Heterogeneity is negatively correlated with shallow water area (Table 1) because soft sediment habitats will have proportionally larger area in grids with extensive continental shelf area. This keystone habitat type will dominate (reducing diversity of habitats) in these grids while oceanic island grids without extensive shelf area will score highly (Figure 3D). HDIn is calculated based on the number of polygons of the different habitat types found in each grid, and therefore, dominance of any one habitat type is minimized. This habitat complexity index is more concentrated in coastal areas and it consistently explains variation in species richness at larger grid sizes when proximity to other coastal areas is reduced by autocorrelation correction (Table 3). Further development of these types of habitat complexity indices may be possible as GIS layers that map the different nearshore habitats become more available and more refined. More refined GIS layers may also help address habitat complexity in terms of habitat or environmental gradients that may also influence species richness patterns [68,69,108]. Heterogeneity indices like these may help more clearly identify keystone structures as indicators of species richness [64–66].

The position of the Indo-Pacific Warm Pool appears to be a primary reason that available kinetic energy, as exemplified by SST, is most consistently retained in models with autocorrelation considered (Table 3). Latitudinal variations in SST will account for some variation in species richness although the epicenter of species richness at the apex of the Coral Triangle (Figure 1) occurs north of peaks in SST (Figure 4A, 4B). This epicenter of species richness corresponds more closely with peaks in CL (Figure 3A) than SST (Figure 3D), and CL is consistently and strongly retained in models (Table 3). The longitudinal peaks in SST correlate significantly with species richness. They spatially corresponded with the secondary 10–30% area of species richness (Figures 3B, 4C, 4D). The primary longitudinal peak in species richness is best explained by the area of highest concentration of CL while the secondary 10–30% area of species richness is best explained by the longitudinal peak in SST corresponding to the Indo-Pacific Warm Pool. Bellwood et al. (2005) [53] dismissed the importance of SST in their analysis of Indo-Pacific species richness patterns of fishes in favor of a mid-domain effect. Their peak in species richness from a limited subset of fishes was far to the east of the epicenter shown from the more complete data set we introduce here (Figure 1). Their epicenter corresponded a little more closely with their choice of the mid-domain which also corresponded with the center of the Indo-Pacific Warm Pool. In contrast, the main conclusion of Tittensor et al. (2010) [57] was that SST is the primary factor in shaping global marine biodiversity (having dismissed the choice of a mid-domain as indefensible) and that available kinetic energy promotes higher rates of speciation in the tropics. However, their conclusion was based on strong latitudinal effects reinforced by long-held observations that fewer species are found at higher latitudes. Tittensor et al. (2010) [57] did not specifically address the fact that the peak in species richness of the bulk of their dataset, the tropical coastal fishes, may have coincided with the position of the Indo-Pacific Warm Pool. The position of the Indo-Pacific Warm Pool correlates with a portion of the peak in species richness in our data set and this also could have been a factor in the dataset of Tittensor et al. (2010) [57].

Our results suggest that kinetic energy, habitat availability, and habitat complexity are all important in shaping species richness patterns across the Indo-Pacific but the relationship of these variables to area of refuge, area of accumulation, and center of origin hypotheses is not straightforward. The striking pattern of diminishing species richness away from the epicenter in the Coral Triangle was a factor in formation of both the center of origin and area of accumulation hypotheses, both mediated primarily by dispersal out of or into the Coral Triangle [1]. The center of origin hypothesis relies on speciation within the Coral Triangle and dispersal away from the speciation center while the area of accumulation hypothesis relies on speciation outside the Coral



VISIT THE SCIENTIFIC PUBLICATIONS REPORT ARCHIVE

Triangle and dispersal into the Coral Triangle. The latter hypothesis relies on the observation that prevailing currents that could dominate dispersal are mostly toward the Coral Triangle from Oceania where numerous isolated islands could promote allopatric speciation [45,46]. The position of the Indo-Pacific Warm Pool over a great many of these isolated islands outside the Coral Triangle could also promote speciation as warmer temperatures are thought to hasten population turnover times and, therefore, hasten rates of evolution [70]. There is some evidence for speciation on these peripheral islands [109] but this is only one example out of the highly diverse Indo-Pacific biota. However, if the Indo-Pacific Warm Pool does hasten speciation and extinction over these numerous isolated islands, the pattern of increasing species richness into the Coral Triangle from the east (Figure 1B) corresponds closely to this hypothesis. Ample available habitat may provide refuge for peripherally-derived species and the cooler temperature within the Coral Triangle may also depress population turnover times and therefore, rates of extinction.

An alternative explanation for the pattern of increasing species richness into the Coral Triangle from the east and the correlation of SST with species richness is that the position of the Indo-Pacific Warm Pool is only a coincidence and does not influence speciation and extinction rates. If speciation within the Coral Triangle is the dominant factor then dispersal out of the Coral Triangle would rely on stepping stones of available habitat counter to prevailing currents over geologic time periods. There is some evidence for gene direction out of the Coral Triangle [110] and a preponderance of Indo-Pacific species originating from the Miocene [42], so there would be sufficient geological time to disperse out of the Coral Triangle against prevailing currents. Teasing apart whether area of accumulation or center of origin is most important may hinge on our ability to demonstrate whether diversification of a lineage is most common within the Coral Triangle [4] or outside the Coral Triangle within the Indo-Pacific Warm Pool. Both of these hypotheses rely on the existence of available habitat to serve as refuge or as a means to promote speciation.

Habitat availability is central to both the center of origin and area of accumulation hypotheses but also to the neutral and eclectic hypotheses as well. The observed correlations among species richness, habitat availability, and habitat heterogeneity may simply be a function of the well-known species-area relationship [32]. This relationship could be interpreted as a neutral, probabilistic process wherein greater area provides higher probability of finding more species, or, more area provides a greater variety of habitats that provide more niches for species to fill [1]. Coastline length is a strong predictor for species richness in models and should be considered as a proxy for greater area or more available niches. Alternatively or additionally, more habitat may provide more refuge from extinction [32,63] which is the same as enhanced survival in eclectic hypotheses that prefer multiple hypotheses as an explanation for the epicenter of diversity in the Coral Triangle [6,8,9,20,35,42,49–51]. To complicate these hypotheses further, habitat complexity may alternatively or additionally provide favorable conditions for either sympatric or allopatric speciation [111]. The presence of extensive and complex habitat potentially creates barriers to gene flow promoting speciation at both close range and wide range spatial scales. Both forms of speciation could be mediated by fluctuations in sea level [111,112] and dramatic changes in ocean circulation that took place during the geological formation of the Coral Triangle [26].

This complex view of the area of refuge hypothesis supports the concept that both area of available habitat and complexity of available habitat are potentially important in models seeking to predict and conserve tropical marine species diversity. Shallow water area, as a measure of available habitat, is a significant component in shaping species richness in the region across different taxonomic groups. However, the largest shallow water area (the Sunda and Arafura shelves), does not coincide with the location of highest species richness (the Philippines, eastern Sabah, and eastern Indonesia). Available habitat in terms of shallow water area alone is not the optimal explanation for variation in species richness because coastline length and habitat heterogeneity are significant explanations for variation in species richness (Table 3). Bellwood and Hughes (2001) [10] used shallow water area alone to represent area of refuge and found that it explained a significant amount of variation in species richness. Their observed conclusions may have been stronger if they had also included a component of habitat complexity such as coastline length and a habitat diversity index. Spatial distribution and statistical analyses both show that coastline length is a better predictor for species richness than shallow water area. The longest coastline per unit area is most consistently found in the Philippines and eastern Indonesia at all grids (Figure S9) – the same locations where the highest 10% of species richness is found (Figure 1). The amount of variation in species richness explained by coastline concentration is consistently higher than that explained by shallow water area.

Another factor that may profoundly influence the role that available shallow water area plays in shaping biodiversity in the Coral Triangle is local extinction from glacial maxima and concomitant sea level lows. Marine life was extirpated on the extensive tropical sea floor represented by the Sunda and Arafura shelves several times during the Pleistocene [1]. A comparison of Figures 1B and 2A shows a surprising complementarity in the highest 30% range overlap of species richness with these extensive shelf areas that suggests that there may still be a limitation to marine species richness remaining from recent ice ages. This is a hypothesis that warrants further testing and could have implications for our understanding of marine connectivity beyond calibrating molecular clocks [113].

Tittensor et al. (2010) [57] showed that coastline length, as originally demonstrated by Etnoyer (2001) [36], is significant in explaining variation in species richness. Their conclusions may also have been strengthened by inclusion of an index of available area and habitat complexity and the use of expert-derived range maps [86]. The Coral Triangle has the most concentrated coastline (km of coastline per grid) in the Indo-Pacific region, contributed by the numerous islands in the archipelagos of the Philippines and Indonesia. Although the availability of shallow water habitat is important, a more complex shoreline is also important for many fishes and invertebrates during their early life history stages [114]. The complexity of shoreline in the Coral Triangle also resulted in an increase in habitat complexity, along with the concurrent increase in coral-carbonate platforms that contributes to species diversification [25].

Our findings further support previous studies based largely on different distribution databases [9,67,74,115] that indicate that the global peak in species richness of shallow nearshore marine biota is in the central Philippines between southern Luzon and northern Mindanao (Figure 1). This is in spite of a more intense sampling of shore fishes that make up the bulk of our data in Indonesia than the Philippines both recently [51] and historically. Indonesia is listed as the type locality for more marine fishes than any other country because of intense periods of collections in Indonesia by Pieter Bleeker and earlier ichthyologists [116,117] while the Philippines has relatively meager colonial natural history collections prior to the 20$^{th}$ century [118]. In addition to habitat availability correlates with this species richness peak in the Philippines and the potential for cooler temperatures in the



VISIT THE SCIENTIFIC PUBLICATIONS REPORT ARCHIVE

northern Coral Triangle moderating extinction rates, the temperature-latitudinal range in this area may also contribute to species richness. This region includes warm temperate species (e.g. [119]) that are not likely to be found in the more equatorial portion of the Coral Triangle. The Philippines also has more extensive shallow soft bottom shelf area than eastern Indonesia where species richness is marginally lower than the Philippines. This additional available habitat in the Philippines would allow the addition of many soft bottom species that will not be present in eastern Indonesia. In contrast to the finding in this study that shows a peak in shore fish species richness in the Visayan region of the Philippines (Figure 1C), one study indicates that eastern Indonesia may eventually overtake the central Philippines in terms of species richness of coral reef fishes [51]. However, Allen's (2007) [67] comprehensive analysis supported higher species richness in the Philippines and Allen and Adrim (2003) [51] based their prediction on new species recently described and a very high level of sampling in eastern Indonesia, compared to the Philippines. It is likely that new species discovered in eastern Indonesia will eventually be found in the Philippines, particularly if a similar level of sampling effort were to take place in the Philippines. However, it should be emphasized that the peak in species richness delineated in this study is based on historical distribution records and there is evidence of exploitation-related biodiversity loss in the central Philippines [115]. Clearly, the central Philippines needs to redouble efforts in marine conservation to recover from and prevent further biodiversity loss in this unique global marine biodiversity epicenter. However, the pristine nature of many areas of the Bird's Head region of Indonesia should also be the focus of intense marine conservation efforts to preserve the rich diversity there.

Available habitat and habitat complexity both significantly explain variation in species richness, and therefore, the loss of these attributes may reduce diversity. Advances in our understanding of the different components of area of refuge may help more clearly define distinctions between available habitat and complexity of habitat. For example, more accurate mapping of presumptive keystone structures such as seagrass beds, mangrove areas, and coral reefs may improve the accuracy of habitat diversity indices. Testing additional types of habitat indices may also improve our understanding. Finding a practical alternative to grid-based spatial analyses may also improve resolution of the degree to which habitat availability components and factors such as SST explain variation in species richness. It is clear that habitat-based conservation efforts targeted at preserving biodiversity should aim to preserve both area and complexity of habitats. This effort is most crucial in the Coral Triangle where species richness is at its peak but it may also be very important in preserving the evolutionary potential of isolated islands, particularly those in the Indo-Pacific Warm Pool. Habitat destruction is a key factor linked to species threats in the Coral Triangle but fortunately, destruction is less intense at present in the islands of Oceania [2]. Continued habitat loss and unrestrained exploitation [115] has the potential for a maximal threat in the Coral Triangle epicenter of species richness.

## Supporting Information

**Figure S1 Distribution pattern of shallow water extent in the Indo-Pacific at UTM grids shifted into different orientations.** The grids were classified (equal interval) into 10 classes based on the amount of shallow water area recorded in each cell such that cells in red have the largest amount of shallow water area, and cells in blue have the lowest amount of shallow water area. (A) UTM shifted north/south, (B) UTM shifted east/west, (C) UTM shifted northeast/southwest.
(PDF)

**Figure S2 Distribution pattern of coastal length extent in the Indo-Pacific at UTM grids shifted into different orientations.** The grids were classified (equal interval) into 10 classes based on the amount of coastal length recorded in each cell such that cells in red have the largest amount of coastal length, and cells in blue have the lowest amount of coastal length. (A) UTM shifted north/south, (B) UTM shifted east/west, (C) UTM shifted northeast/southwest.
(PDF)

**Figure S3 Distribution pattern of the habitat heterogeneity index using area in the Indo-Pacific at UTM grids shifted into different orientations.** The grids were classified (equal interval) into 10 classes based on the index values recorded in each cell such that cells in red have the largest index values, and cells in blue have the lowest index values. (A) UTM shifted north/south, (B) UTM shifted east/west, (C) UTM shifted northeast/southwest.
(PDF)

**Figure S4 Distribution pattern of the habitat heterogeneity index using number in the Indo-Pacific at UTM grids shifted into different orientations.** The grids were classified (equal interval) into 10 classes based on the index values recorded in each cell such that cells in red have the largest index values, and cells in blue have the lowest index values. (A) UTM shifted north/south, (B) UTM shifted east/west, (C) UTM shifted northeast/southwest.
(PDF)

**Figure S5 Distribution pattern of the mean sea surface temperature in the Indo-Pacific at UTM grids shifted into different orientations.** The grids were classified (equal interval) into 10 classes based on the index values recorded in each cell such that cells in red have the highest temperature, and cells in blue have the lowest temperature. (A) UTM shifted north/south, (B) UTM shifted east/west, (C) UTM shifted northeast/southwest.
(PDF)

**Figure S6 Distribution pattern of the mean net primary productivity in the Indo-Pacific at UTM grids shifted into different orientations.** The grids were classified (equal interval) into 10 classes based on the index values recorded in each cell such that cells in red have the highest productivity, and cells in blue have the lowest productivity. (A) UTM shifted north/south, (B) UTM shifted east/west, (C) UTM shifted northeast/southwest.
(PDF)

**Figure S7 Combined adjacent cells (red color) against the regular sized cells (yellow color).** (A) Small grid, (B) Medium grid, (C) Large grid, (D) UTM, (E) UTM shifted north/south, (F) UTM shifted east/west, (G) UTM shifted northeast/southwest. There are no adjacent cells that were combined in extra large and largest grids.
(PDF)

**Figure S8 The two types of basemaps used in this study.** (A) Visualization basemap consisting of 200 m depth and 100 km buffer, (B) Bathymetry basemap showing the 200 m depth used in analyses of species richness versus independent variables.
(PDF)

**Figure S9 Distribution pattern of coastal length extent in the Indo-Pacific at different grid scales.** The grids were



VISIT THE SCIENTIFIC PUBLICATIONS REPORT ARCHIVE

classified (equal interval) into 10 classes based on the amount of coastal length recorded in each cell such that cells in red have the largest amount of coastal length, and cells in blue have the lowest amount of coastal length. (A) Small grid, (B) Medium grid, (C) Large grid, (D) Extra large grid, (E) Largest grid.
(PDF)

**Figure S10 Distribution pattern of the habitat heterogeneity index using area in the Indo-Pacific at different grid scales.** The grids were classified (equal interval) into 10 classes based on the index values recorded in each cell such that cells in red have the largest index values, and cells in blue have the lowest index values. (A) Small grid, (B) Medium grid, (C) Large grid, (D) Extra large grid, (E) Largest grid.
(PDF)

**Figure S11 Distribution pattern of the habitat heterogeneity index using number in the Indo-Pacific at different grid scales.** The grids were classified (equal interval) into 10 classes based on the index values recorded in each cell such that cells in red have the largest index values, and cells in blue have the lowest index values. (A) Small grid, (B) Medium grid, (C) Large grid, (D) Extra large grid, (E) Largest grid.
(PDF)

**Figure S12 Distribution pattern of the mean sea surface temperature in the Indo-Pacific at different grid scales.** The grids were classified (equal interval) into 10 classes based on the index values recorded in each cell such that cells in red have the highest temperature, and cells in blue have the lowest temperature. (A) Small grid, (B) Medium grid, (C) Large grid, (D) Extra large grid, (E) Largest grid.
(PDF)

**Figure S13 Distribution pattern of the mean net primary productivity in the Indo-Pacific at different grid scales.** The grids were classified (equal interval) into 10 classes based on the index values recorded in each cell such that cells in red have the highest productivity, and cells in blue have the lowest productivity. (A) Small grid, (B) Medium grid, (C) Large grid, (D) Extra large grid, (E) Largest grid.
(PDF)

**Table S1 Single predictor Generalized Linear Model (GLM) and Spatial Linear Model (SLM) results at different UTM grid orientations.** The predictors are shallow water area (SW), coastline length (CL), habitat diversity based on area (HDIa), habitat diversity based on number of patches (HDIn), sea surface temperature (SST), and net primary productivity (NPP). Values under predictor variables are t-values for GLM and z-values for SLM. Asterisks indicate significance value of P: *(<0.05), **(<0.01); ***(<0.001); ns (not significant). UTM NS = centroid shifted on a North-South plane, UTM EW = centroid shifted on an East-West plane and UTM NE = centroid shifted along a Northeast-Southwest plane. Sample size for each grid (n) is shown. The highest adjusted $R^2$ (GLM) and pseudo-$R^2$ (p–$R^2$; SLM) value within each grid size are highlighted in boldface.
(PDF)

**Table S2 Multiple predictor Generalized Linear Model (GLM) and Spatial Linear Model (SLM) results at different UTM grid orientations.** The predictors are shallow water area (SW), coastline length (CL), habitat diversity based on area (HDIa), habitat diversity based on number of patches (HDIn), sea surface temperature (SST), and net primary productivity (NPP). Values under predictor variables are t-values for GLM and z-values for SLM. Asterisks indicate significance value of P: *(<0.05), **(<0.01); ***(<0.001). UTM NS = centroid shifted on a North-South plane, UTM EW = centroid shifted on an East-West plane and UTM NE = centroid shifted along a Northeast-Southwest plane. Sample size for each grid (n) is shown. $R^2$ values are for GLM results, while pseudo-$R^2$ (p–$R^2$) values are for SLM results.
(PDF)

**Table S3 List of families with the number of species distribution maps used in this study.**
(PDF)

**Table S4 Single predictor Generalized Linear Model (GLM) and Spatial Linear Model (SLM) complete results at different grid sizes.** The predictors are shallow water area (SW), coastline length (CL), habitat diversity based on area (HDIa), habitat diversity based on number of patches (HDIn), sea surface temperature (SST), and net primary productivity (NPP). Values under predictor variables are t-values for GLM and z-values for SLM. Asterisks indicate significance value of P: *(<0.05), **(<0.01); ***(<0.001); ns (not significant). Sample size for each grid (n) is shown. The highest adjusted $R^2$ (GLM) and pseudo-$R^2$ (p–$R^2$; SLM) value within each grid size are highlighted in boldface.
(PDF)

**Text S1 Methods and results for UTM grids shifted to different centroid orientation.**
(PDF)

**Text S2 Sources for species range used in producing the distribution maps.**
(PDF)

## Acknowledgments

This study was made possible by the International Union for Conservation of Nature and Conservation International Global Marine Species Assessment (GMSA) project, which is a part of the IUCN Species Programme Marine Biodiversity Unit. We are very thankful to Roger McManus, David Knight, Simon Stuart, Jean-Christophe Vie, and Jane Smart for their ardent support of the GMSA. GMSA professionals Suzanne Livingstone, Beth Polidoro, Heather Harwell, Mia Comeros-Raynal, Cristiane Elfes, and Andrew Hines all worked hard to ensure expert review of distribution maps in GMSA workshops, as did IUCN staff Caroline Pollock and Mike Hoffman. We thank Conservation International for making available to the GMSA the distribution map databases of Gerry Allen and John E. N. Veron. We are very grateful to Jon Hutton and the UNEP World Conservation Monitoring Centre for allowing us to use their GIS habitat layers of mangroves, seagrasses, and coral reefs. John McEachran produced distribution maps of all batoid fishes used in this study. We thank the MacArthur Foundation who provided support for production of most of the invertebrate distribution maps used in this study and to Myra McShane who provided valuable research assistance in the course of this work. We are very grateful for Manasi Sheth, Mark Butler, N. Rao Chaganty, Dayanand N. Naik, and Holly Gaff for statistical advice and to Vineet Katariya, George McLeod, and Hua Liu for their GIS support. We also thank Dana Zebrowski, Samantha Hoover, Joyce Strain, Benjamin Lawson, and Andrew Calhoun for their help in digitizing the distribution maps. John Holsinger provided valuable advice in biogeography. We also thank Scott Cross, Len Balthis, and Brian Kinlan of NOAA for reviewing an early version of this manuscript. Bert Hoeksema and an anonymous reviewer provided useful suggestions for improvement that are very much appreciated. This study was completed as partial fulfillment of a Master's thesis of Jonnell C. Sanciangco in the Department of Biological Sciences, Old Dominion University.



VISIT THE SCIENTIFIC PUBLICATIONS REPORT ARCHIVE

## Author Contributions

Conceived and designed the experiments: KEC JCS. Performed the experiments: JCS. Analyzed the data: JCS. Contributed reagents/materials/analysis tools: JCS KEC PJE FM. Wrote the paper: KEC JCS.

## References


1. Hoeksema BW (2007) Delineation of the Indo-Malayan centre of maximum marine biodiversity: The Coral Triangle. In: Renema W, editor. Biogeography, time, and place: Distributions, barriers, and islands. The Netherlands: Springer. 416.
2. Carpenter KE, Abrar M, Aeby G, Aronson RB, Banks S, et al. (2008) One-third of reef-building corals face elevated extinction risk from climate change and local impacts. Science 321: 560–563.
3. Veron JEN, Devantier LM, Turak E, Green AL, Kininmonth S, et al. (2009) Delineating the Coral Triangle. Galaxea 11: 91–100.
4. Carpenter KE, Barber PH, Crandall ED, Ablan-Lagman MCA, Ambariyanto, etal. (2011) Comparative phylogeography of the Coral Triangle and implications for marine management. J Mar Biol 2011: 1–14.
5. Briggs JC (1992) The marine East Indies: Centre of origin? Glob Ecol Biogeogr Lett 2: 149–156.
6. Randall JE (1998) Zoogeography of shore fishes of the Indo-Pacific region. Zool Stud 37: 227–268.
7. Santini F, Winterbottom R (2002) Historical biogeography of Indo-Western Pacific coral reef biota: Is the Indonesian region a centre of origin? J Biogeogr 29: 189–205.
8. Bellwood DR, Wainwright PC (2002) The history and biogeography of fishes on coral reefs. In: Sale PF, ed. Coral reef fishes. New York: Academic Press. 5–32.
9. Carpenter KE, Springer VG (2005) The center of the center of marine shore fish biodiversity: The Philippine Islands. Environ Biol Fishes 72: 467–480.
10. Bellwood DR, Hughes TP (2001) Regional-scale assembly rules and biodiversity of coral reefs. Science 292: 1532–1534.
11. Bellwood DR, Meyer CP (2009) Searching for heat in a marine biodiversity hotspot. J Biogeogr 36: 569–576.
12. Hall R (2002) Cenozoic geological and plate tectonic evolution of SE Asia and the SW Pacific: Computer-based reconstructions, model and animations. J Asian Earth Sci 20: 353–431.
13. Briggs JC (1974) Marine zoogeography. New York: McGraw-Hill. 475 p.
14. Briggs JC, Bowen BW (2012) A realignment of marine biogeographic provinces with particular reference to fish distributions. J Biogeogr 39: 12–30.
15. Ekman S (1953) Zoogeography of the sea. London: Sidgwick & Jackson. 440 p.
16. Fukami H, Budd AF, Paulay G, Solé-Cava A, Chen CA, et al. (2004) Conventional taxonomy obscures deep divergence between Pacific and Atlantic corals. Nature 427: 832–835.
17. Briggs JC (1999) Coincident biogeographic patterns: Indo-West Pacific ocean. Evolution 53: 326–335.
18. Spalding MD, Fox HE, Allen GR, Davidson N, Ferdaña ZA, et al. (2007) Marine ecoregions of the world: A bioregionalization of coastal and shelf areas. Bioscience 57: 573–583.
19. Lomolino MV, Riddle BR, Brown JH (2006) Biogeography. Sunderland: Sinauer Associates, Inc. 691 p.
20. Wilson MEJ, Rosen BR (1998) Implications of paucity of corals in the Paleogene of SE Asia: Plate tectonics or Centre of Origin? In: Hall R, Holloway JD, eds. Biogeography and geological evolution of SE Asia. Leiden, The Netherlands: Backbuys Publishers. 165–195.
21. Briggs JC (2000) Centrifugal speciation and centres of origin. J Biogeogr 27: 1183–1188.
22. Briggs JC (2003) Marine centres of origin as evolutionary engines. J Biogeogr 30: 1–18.
23. Vermeij GJ (2001) Community assembly in the sea: Geologic history of the living shore biota. In: Bertness MD, Gaines SD, Hay ME, editors. Marine community ecology. Massachusetts: Sinauer Associates. 39–60.
24. Renema W, Bellwood DR, Braga JC, Bromfield K, Hall R, et al. (2008) Hopping hotspots: Global shifts in marine biodiversity. Science 321: 654–657.
25. Williams ST, Duda TF Jr (2008) Did tectonic activity stimulate Oligo-Miocene speciation in the Indo-West Pacific? Evolution 62: 1618–1634.
26. Holloway JD, Hall R (1998) SE Asian geology and biogeography: An introduction. In: Hall R, Holloway JD, editors. Biogeography and geological evolution of SE Asia. Leiden, The Netherlands: Backhuys Publishers. 419.
27. Nathan SA, Leckie RM (2009) Early history of the western Pacific Warm Pool during the middle to late Miocene (~13.2–5.8 Ma): Role of sea-level change and implications for equatorial circulation. Palaeogeogr, Palaeoclimatol, Palaeoecol 274: 140–159.
28. Yan X-H, Ho C-R, Zheng Q, Klemas V (1992) Temperature and size variability of the eastern Pacific Warm Pool. Science 258: 1643–1645.
29. de Garidel-Thoron T, Rosenthal Y, Bassinot F, Beaufort L (2005) Stable sea surface temperatures in the western Pacific Warm Pool over the past 1.75million years. Nature 433: 294–298.
30. Abram NJ, McGregor HV, Gagan MK, Hantoro WS, Suwargadi BW (2009) Oscillations in the southern extent of the Indo-Pacific Warm Pool during the mid-Holocene. Quat Sci Rev 28: 2794–2803.
31. Rosen BR (1988) Progress, problems and patterns in the biogeography of reef corals and other tropical marine organisms. Helgoländer Meeresuntersuchungen 42: 269–301.
32. McCoy ED, Heck KL Jr (1976) Biogeography of corals, seagrasses, and mangroves: An alternative to the center of origin concept. Syst Zool 25: 201–210.
33. Rosenzweig ML (1995) Species diversity in space and time. Cambridge: Cambridge University Press. 460 p.
34. Woodland DJ (1990) Revision of the fish family Siganidae with descriptions of two new species and comments on distribution and ecology. Indo-Pacific Fishes 19: 1–136.
35. Carpenter KE (1998) An introduction to the oceanography, geology, biogeography, and fisheries of the tropical and subtropical western and central Pacific. In: Carpenter KE, Niem VH, editors. FAO species identification guide for fishery purposes: The living marine resources of the western central Pacific. Rome: FAO. 1–19.
36. Etnoyer PJ (2001) Marine protected area siting for coral reefs in a large marine ecosystem (MS Thesis). Durham, North Carolina: Duke University.
37. Stehli F, Wells JW (1971) Diversity and age patterns in hermatypic corals. Syst Zool 20: 115–126.
38. Potts DC (1985) Sea-level fluctuations and speciation in Scleractinia. Proc 5th Int Coral Reef Congr 4: 127–132.
39. Paulay G (1990) Effects of late Cenozoic sea-level fluctuations on the bivalve faunas of tropical oceanic islands. Paleobiology 16: 415–134.
40. Briggs JC (1995) Global biogeography. Amsterdam: Elsevier. 452 p.
41. Briggs JC (2007) Marine biogeography and ecology: Invasions and introductions. J Biogeogr 34: 193–198.
42. Barber PH, Bellwood DR (2005) Biodiversity hotspots: Evolutionary origins of biodiversity in wrasses (Halichoeres: Labridae) in the Indo-Pacific and new world tropics. Mol Phylogen Evol 35: 235–253.
43. Barber PH, Erdmann MV, Palumbi SR (2006) Comparative phylogeography of three co-distributed stomatopods: Origins and timing of regional lineage diversification in the Coral Triangle. Evolution 60: 1825–1839.
44. Woodland DJ (1983) Zoogeography of the Siganidae (Pisces): An interpretation of distribution and richness patterns. Bull Mar Sci 33: 713–717.
45. Ladd HS (1960) Origin of the Pacific Island molluscan fauna. Am J Sci 258–A: 137–150.
46. Jokiel P, Martinelli FJ (1992) The vortex model of coral reef biogeography. J Biogeogr 19: 449–458.
47. Rosen BR, Smith AB (1988) Tectonics from fossils?: Analysis of reef-coral and sea-urchin distributions from late Cretaceous to Recent, using a new method. In: Audley-Charles MG, Hallam A, editors. Gondwana and Tethys. London: Geological Society Special Publication No. 17. 275–306.
48. Fraser RH, Currie DJ (1996) The species richness-energy hypothesis in a system where historical factors are thought to prevail: Coral reefs. Am Nat 148: 138–159.
49. Palumbi SR (1996) What can molecular genetics contribute to marine biogeography?: An urchin's tale. J Exp Mar Biol Ecol 203: 75–92.
50. Wallace CC (1997) The Indo-Pacific centre of coral diversity re-examined at species level. Proc 8th Int Coral Reef Congr 1: 365–370.
51. Allen GR, Adrim M (2003) Coral reef fishes of Indonesia. Zool Stud 42: 1–72.
52. Connolly SR, Bellwood DR, Hughes TP (2003) Indo-Pacific biodiversity of coral reefs: Deviations from a mid-domain model. Ecology 84: 2178–2190.
53. Bellwood DR, Hughes TP, Connolly SR, Tanner J (2005) Environmental and geometric constraints on Indo-Pacific coral reef biodiversity. Ecol Lett 8: 643–651.
54. Currie DJ, Kerr JT (2008) Tests of mid-domain hypothesis: A review of the evidence. Ecol Monogr 78: 3–18.
55. McClain CR, White EP, Hurlbert AH (2007) Challenges in the application of geometric constraint models. Glob Ecol Biogeogr 16: 257–264.
56. Colwell RK, Gotelli NJ, Rahbek C, Entsminger GL, Farrell C, et al. (2009) Peaks, plateaus, canyons, and craters: The complex geometry of simple mid-domain effect models. Evol Ecol Res 11: 335–370.
57. Tittensor DP, Mora C, Jetz W, Lotze HK, Ricard D, et al. (2010) Global patterns and predictors of marine biodiversity across taxa. Nature 466: 1098–1101.
58. Cowman PF, Bellwood DR (2011) Coral reefs as drivers of cladogenesis: Expanding coral reefs, cryptic extinction events, and the development of biodiversity hotspots. J Evol Biol. 10.1111/j.1420-9101.2011.02391.x.
59. Williams ST, Reid DG (2004) Speciation and diversity on tropical rocky shores: A global phylogeny of snails of the genus *Echinolittorina*. Evolution 58: 2227–2251.
60. Read CI, Bellwood DR, van Herwerden L (2006) Ancient origins of Indo-Pacific coral reef fish biodiversity: A case study of the leopard wrasses (Labridae: *Macropharyngodon*). Mol Phylogenet Evol 38: 808–819.




VISIT THE SCIENTIFIC PUBLICATIONS REPORT ARCHIVE

61. Pianka ER (1966) Latitudinal gradients in species diversity: A review of concepts. Am Nat 100: 33–46.
62. Ricklefs RE, Schluter D (1993) Regional and historical influences In: Ricklefs RE, Schluter D, eds. Species diversity in ecological communities. Chicago: University of Chicago Press. 350–363.
63. Best MB, Hoeksema BW, Moka W, Moll H, Suharsono, etal. (1989) Recent scleractinian coral species collected during the Snellius-II expedition in eastern Indonesia. Neth J Sea Res 23: 107–115.
64. Whittaker RJ, Willis KJ, Field R (2001) Scale and species richness: Towards a general, hierarchical theory of species diversity. J Biogeogr 28: 453–470.
65. Tews J, Brose U, Grimm V, Tielbörger K, Wichmann MC, et al. (2004) Animal species diversity driven by habitat heterogeneity/diversity: The importance of keystone structures. J Biogeogr 31: 79–92.
66. Field R, Hawkins BA, Cornell HV, Currie DJ, Diniz-Filho JAF, et al. (2009) Spatial species-richness gradients across scales: A meta-analysis. J Biogeogr 36: 132–147.
67. Allen GR (2007) Conservation hotspots of biodiversity and endemism for Indo-Pacific coral reef fishes. Aquat Conserv: Mar Freshwat Ecosyst 17: 1–16.
68. Cleary D, Becking L, Devoogd N, Renema W, Debeer M, et al. (2005) Variation in the diversity and composition of benthic taxa as a function of distance offshore, depth and exposure in the Spermonde Archipelago, Indonesia. Estuar Coast Shelf Sci 65: 557–570.
69. Hoeksema BW (2012) Distribution patterns of mushroom corals (Scleractinia: Fungiidae) across the Spermonde Shelf, South Sulawesi. Raffles B Zool 60: 182–212.
70. Rohde K (1992) Latitudinal gradients in species diversity: The search for the primary cause. Oikos 65: 514–527.
71. Roy K, Jablonski D, Valentine JW, Rosenberg G (1998) Marine latitudinal diversity gradients: Tests of causal hypotheses. Proc Natl Acad Sci USA 95: 3699–3702.
72. Jetz W, Kreft H, Ceballos G, Mutke J (2009) Global associations between terrestrial producer and vertebrate consumer diversity. Proc R Soc Lond B Biol Sci 276: 269–278.
73. Halas D, Winterbottom R (2009) A phylogenetic test of multiple proposals for the origins of the East Indies coral reef biota. J Biogeogr 36: 1847–1860.
74. Moretzsohn F, McShane MKK (2004) Mapping marine invertebrate biodiversity hotspots in the Indo-Pacific ocean using GIS. Bishop Museum Technical Report No 30. Honolulu, Hawai'i: The John D. and Catherine T. MacArthur Foundation. 93 p.
75. Kerswell AP (2006) Global biodiversity patterns of benthic marine algae. Ecology 87: 2479–2488.
76. Reaka ML, Rodgers PJ, Kudla AU (2008a) Speciation extinction dynamics and the topography of diversity on Indo-West Pacific coral reefs. Proc 11th Int Coral Reef Congr 2: 1384–1388.
77. Reaka ML, Rodgers PJ, Kudla AU (2008b) Patterns of biodiversity and endemism on Indo-West Pacific coral reefs. Proc Natl Acad Sci USA105: 11474–11481.
78. Dormann CF, McPherson JM, Araújo MB, Bivand R, Bolliger J, et al. (2007) Methods to account for spatial autocorrelation in the analysis of species distributional data: A review. Ecography 30: 609–628.
79. Hawkins BA (2012a) Eight (and a half) deadly sins of spatial analysis. J Biogeogr 39: 1–9.
80. Currie DJ (1991) Energy and large-scale patterns of animal- and plant-species richness. Am Nat 137: 27–49.
81. Badgley C, Fox DL (2000) Ecological biogeography of North American mammals: Species density and ecological structure in relation to environmental gradients. J Biogeogr 27: 1437–1467.
82. Hawkins BA, Porter EE, Diniz-Filho JAF (2003) Productivity and history as predictors of the latitudinal diversity gradient of terrestrial birds. Ecology 84: 1608–1623.
83. Diniz-Filho JAF, Rangel TFLVB, Hawkins BA (2004) A test of multiple hypotheses of South American owls. Oecologia 140: 633–638.
84. Nogués-Bravo D, Araújo MB (2006) Species richness, area and climate correlates. Glob Ecol Biogeogr 15: 452–460.
85. Bini LM, Diniz-Filho JAF, Hawkins BA (2004) Macroecological explanations for differences in species richness gradients: A canonical analysis of South American birds. J Biogeogr 31: 1819–1827.
86. Robertson DR (2008) Global biogeographical data bases on marine fishes: Caveat emptor. Divers Distrib 14: 891–892.
87. Nichols G (2009) The marine realm: Morphology and processes. In: Nichols G, ed. Sedimentology and stratigraphy, 2nd ed. West Sussex, U.K.: Wiley-Blackwell. 163–178.
88. Amante C, Eakins BW (2008) ETOPO1 1 arc-minute global relief model: Procedures, data sources and analysis. NOAA Technical Memorandum NESDIS NGDC-24. Boulder, CO: NESDIS-NGDC.
89. Soluri EA, Woodson VA (1990) World Vector Shoreline. Int Hydrogr Rev 67: 27–36.
90. Spalding MD, Blasco F, Field C (1997) World mangrove atlas. Okinawa, Japan: The International Society for Mangrove Ecosystems. 304 p.
91. Spalding MD, Ravilious C, Green EP (2001) World atlas of coral reefs. Berkeley: University of California Press. 416 p.
92. Green EP, Short FT (2003) World atlas of seagrasses. Berkeley: University of California Press. 310 p.
93. Shannon CE, Weaver W (1963) The mathematical theory of communication. Urbana: University of Illinois Press. 144 p.
94. McGarigal K, Marks BJ (1995) FRAGSTATS: Spatial pattern analysis program for quantifying landscape structure. Portland, OR: U.S. Department of Agriculture, Forest Service, Pacific Northwest Research Station. 122 p.
95. Smith TM, Reynolds RW (1998) A high-resolution global sea surface temperature climatology for the 1961–90 base period. J Clim 11: 3320–3323.
96. Behrenfeld MJ, Falkowski PG (1997) Photosynthetic rates derived from satellite-based chlorophyll concentration. Limnol Oceanogr 42: 1–20.
97. Nagelkerke NJD (1991) A note on a general definition of the coefficient of determination. Biometrika 78: 691–692.
98. Moran PAP (1950) Notes on continuous stochastic phenomena. Biometrika 37: 17–23.
99. Bivand R (2009) spdep: Spatial dependence: Weighting schemes, statistics, and model. R Package Version 0.5–46. Available: http://cran.r-project.org/web/packages/s?pdep. Accessed 2012 May 10.
100. Polidoro BA, Carpenter KE, Collins L, Duke NC, Ellison AM, et al. (2010) The loss of species: Mangrove extinction risk and geographic areas of global concern. PLoS ONE 5: e10095.
101. Short FT, Polidoro B, Livingstone SR, Carpenter KE, Bandeira S, et al. (2011) Extinction risk assessment of the world's seagrass species. Biol Conserv 144: 1961–1971.
102. Dorenbosch M, Grol MGG, Christianen MJA, Nagelkerken I, van der Velde G (2005) Indo-Pacific seagrass beds and mangroves contribute to fish density and diversity on adjacent coral reefs. Mar Ecol Prog Ser 302: 63–76.
103. Mora C, Treml EA, Roberts J, Crosby K, Roy D, et al. (2012) High connectivity among habitats precludes the relationship between dispersal and range size in tropical reef fishes. Ecography 35: 89–96.
104. Kühn I, Dormann CF (2012) Less than eight (and a half) misconceptions of spatial analysis. J Biogeogr 39: 995–998.
105. Hawkins BA (2012b) Are multiple regression models of spatially structured data to be trusted? J Biogeogr 39: 998.
106. Anderson DR, Burnham KP (2002) Avoiding pitfalls when using information-theoretic methods. J Wildl Manage 66: 912–918.
107. Johnson JB, Omland KS (2004) Model selection in ecology and evolution. Trends Ecol Evol 19: 101–108.
108. Cleary DFR, Suharsono, Hoeksema BW (2006) Coral diversity across a disturbance gradient in the Pulau Seribu reef complex off Jakarta, Indonesia. Biodivers Conserv 15: 3653–3674.
109. Malay MC, Paulay G (2010) Peripatric speciation drives diversification and distributional pattern of reef hermit crabs (Decapoda: Diogenidae: *Calcinus*). Evolution 64: 634–662.
110. Benzie JAH, Williams ST (1997) Genetic structure of Giant Clam (*Tridacna maxima*) populations in the west Pacific is not consistent with dispersal by present-day ocean currents. Evolution 51: 768–783.
111. Rocha LA, Bowen BW (2008) Speciation in coral-reef fishes. J Fish Biol 72: 1101–1121.
112. McMannus JP (1985) Marine speciation, tectonics and sea-level changes in Southeast Asia. Proc 5th Int Coral Reef Congr 4: 133–138.
113. Crandall ED, Sbrocco EJ, Deboer TS, Barber PH, Carpenter KE (2012) Expansion dating: Calibrating molecular clocks in marine species from expansions onto the Sunda Shelf following the last glacial maximum. Mol Biol Evol 29: 707–719.
114. Peterson MS, Comyns BH, Hendon JR, Bond PJ, Duff GA (2000) Habitat use by early life-history stages of fishes and crustaceans along a changing estuarine landscape: Differences between natural and altered shoreline sites. Wetlands Ecol Manage 8: 209–219.
115. Nañola CL, Aliño PM, Carpenter KE (2011) Exploitation-related reef fish species richness depletion in the epicenter of marine biodiversity. Environ Biol Fishes 90: 405–420.
116. Eschmeyer WN, Fricke R, Fong JD, Polack DA (2010) Marine fish diversity: History of knowledge and discovery (Pisces). Zootaxa 2525: 19–50.
117. Eschmeyer WN (2012) Catalog of Fishes on-line. California Academy of Sciences. Available: http://research.calacademy.org/ichthyology/catalog. Accessed 2012 Dec 18.
118. Herre AW (1953) Checklist of Philippine fishes. Research Report 20. Washington, DC: U.S. Printing Office.
119. Willette DA, Santos MD, Aragon MA (2011) First report of the Taiwan sardinella *Sardinella hualiensis* (Clupeiformes: Clupeidae) in the Philippines. J Fish Biol 79: 2087–2094.




VISIT THE SCIENTIFIC PUBLICATIONS REPORT ARCHIVE